Characterization of LINA a new RING-Finger protein with axon growth promoting activity

Dissertation

zur Erlangung des Doktorgrades *Dr. rer. nat.*
der Fakultät für Naturwissenschaften der Universität Ulm

vorgelegt von

Jieun Lee

aus Samchok, Südkorea

2009

Amtierender Dekan:	Prof. Dr. Peter Bäuerle
Erster Gutachter:	Prof. Dr. Harald Wolf
Zweiter Gutachter:	Dr. Wolfgang Stein
Tag der mündlichen Prüfung:	15.06.2009

Contents

Contents **3**

Figures **6**

Abstract **7**

Zusammenfassung **8**

Abbreviations **9**

1 Introduction **13**

1.1 The visual system 13

1.2 Difference of glial environment between CNS and PNS 15

1.2.1 Myelin inhibitory proteins 16

1.2.2 The glial scar 18

1.2.3 Schwann cells 19

1.3 Changes of intrinsic capabilities for axonal regeneration 20

1.4 LINA, a new RING finger protein promoting neurite outgrowth 21

2 Material **25**

2.1 Technical equipments 25

2.2 Consumable Materials 26

2.3 Plasmids 26

2.4 Enzymes 27

2.5 Antibodies 27

2.6 Reagent kits 28

2.7 Chemicals and reagents 28

2.8 Buffers 30

2.9 Cell and Bacterial culture and medium 31

2.9.1 PC12 cells and medium 31

2.9.2 HEK293 cells and medium 32

2.9.3 RGCs and medium 32

2.9.4 Hippocampus cells and medium 32

2.9.5 Escherichia coli (*E. coli*) DH 5α ™ and medium 32

2.10 Rat animal material 32

2.11 Oligonucleotide 33

2.11.1 Cloning primer for LINA and LINA variants 33

3 Experimental Methods **36**

3.1 Cell culture 36
3.1.1 Cell freezing and defreezing 36
3.1.2 PDL and laminin coating 36
3.1.3 Transfection of PC12 cells 36
3.1.4 Transfection of HEK293 cells by calcium phosphate method 37
3.1.5 Dissociated RGCs cell culture 37
3.1.6 Hippocampal cell culture 37
3.1.7 Myelin isolation and preparation 38
3.2 Surgical methods 39
3.2.1 Optic nerve crush (ONC) 39
3.2.2 Lens Injury (LI) 39
3.3 Molecular biological methods 39
3.3.1 Cloning of LINA 39
3.3.2 Cloning of LINA-GFP (Green fluorescence protein) and LINA-RFP (Red fluorescence protein) fusion protein 41
3.3.3 Phenol/Chloroform DNA purification 41
3.3.4 Site-directed Mutagenesis 42
3.3.5 *In vitro* Mutagenesis by Overlap Extension and Splicing PCR 42
3.4 Protein biochemical methods 43
3.4.1 Protein Isolation 43
3.4.2 Bradford test 44
3.4.3 Western Blot Analysis 44
3.4.4 Coomasie brilliant blue staining 46
3.4.5 Cross Linking 46
3.4.6 Co-immunoprecipitation 46
3.4.7 Membrane fragmentation 47
3.4.8 GST-fusion protein 47
3.4.9 Affinity Chromatography for purification of anti-LINA Antibody 49
3.5 Immunocytochemistry and Immunohistochemistry 49
3.5.1 Immunocytochemistry 49
3.5.2 Immunohistochemistry 50
3.5.3 Haematoxylin and eosin staining (HE staining) 50
3.6 Whole Mount *In situ* Hybridization on post-implantation mouse embryos 50
3.6.1 RNA probes 51
3.6.2 Materials for hybridization 51
3.6.3 Mouse whole mount *in situ* Hybridization 52
4 Results 55
4.1 Cloning and sequence analysis of LINA 55
4.2 Functional characterization of LINA 58
4.2.1 LINA promotes NGF-induced neurite outgrowth of PC12 cells 58
4.2.2 $LINA^{C93A}$ abrogates the neurite outgrowth effect of LINA in PC12 cells 60
4.3 Biochemical characterization of LINA 62

4.3.1 LINA is a membrane associated protein 62
4.3.2 LINA has a glycosylation site at N20 63
4.3.3 LINA forms a ternary complex 64
4.3.4 LINA forms a ternary complex with its RING finger domain 70
4.4 Subcellular localization of exogenous LINA 72
4.5 Investigation of endogenous LINA expression 76
4.5.1 Verification of anti-LINA antibody 76
4.5.2 Endogenous LINA expression in cultured primary RGCs and hippocampal neurons 79
4.5.3 Subcellular localization of endogenous LINA in Hippocampal neurons 81
4.5.4 Investigation of endogenous LINA expression in the rat brain 82
4.5.5 Upregulation of LINA expression in PC 12 cells after NGF treatment 86
4.5.6 Upregulation of LINA expression after optic nerve crush (ONC) and lens injury (LI) in retina 87
4.6 Investigation of LINA expression on mRNA level 90

5 Discussion 92

5.1 LINA ([redacted]a new RING finger protein 92
5.2 What could be the signaling mechanism underlying the neurite outgrowth promoting effects of LINA? 95

6 References 102

7 Appendices 119

Acknowledgement 123

List of Publications 124

Erklärung 125

Figures

Figure 1-1: Anatomy of the human eye (from http://thalamus.wustl.edu/course/eyeret.html) 14
Figure 1-2: Structure of the retina (from http://instruct.uwo.ca/anatomy/530/retina.jpg) 15
Figure 1-3: Myelin inhibitory proteins and intracellular signaling mechanisms. 17
Figure 3-1: Principle of *in vitro* mutagenesis by overlap extension and splicing PCR (modified from Lottspeich et al. (1998)) 43
Figure 4-1: The alignment of the human, rat and mouse LINA proteins with PRALINE multiple alignment program 56
Figure 4-2: The alignment of the human, rat and mouse LINA RNA sequence with CLUSTAL W multiple sequence alignment program. 57
Figure 4-3: Schematic drawing of the LINA protein with functional domains, potential glycosylation and phosphorylation site as predicted by the analysis tool “PROSITE” in ExPASy (**Ex**pert **P**rotein **A**nalysis **Sy**stem). 58
Figure 4-4: LINA promotes neurite outgrowth in PC12 cells with NGF 59
Figure 4-5: LINA does not desensitize the growth cones towards myelin 60
Figure 4-6: Functional phenotype of PC12 cells expressing control (con), LINA and LINA^{C93A}. 61
Figure 4-7: Membrane fragmentation of LINA and LINA$^{60-155}$ 63
Figure 4-8: *N*-Glycosylation of LINA at N20 64
Figure 4-9: Co-immunoprecipitation showing the self assembling of LINA protein. 66
Figure 4-10: The amino acids spanning position 60 to 155 are responsible for the self assembling of LINA. 68
Figure 4-11: Cross linking experiment confirms that LINA forms a ternary complex 69
Figure 4-12: Schematic drawing of different LINA variants 70
Figure 4-13: The RING finger domain is required for a ternary complex formation. 72
Figure 4-14: Characterization of subcellular localization of LINA with different cellular markers 75
Figure 4-15: Specificity of the affinity purified rabbit anti-LINA antibody by immunocytochemistry in HEK293 cell system 77
Figure 4-16: Verification of the polyclonal rabbit serum anti-LINA antibody by western blot analysis 79
Figure 4-17: Endogenously expressed LINA in cultured primary RGCs and hippocampal neurons 80
Figure 4-18: LINA and ProSAP2 are partially co-localized in primary hippocampal neurons 82
Figure 4-19: LINA is expressed in Purkinje cells in the cerebellum of the rat brain 83
Figure 4-20: LINA is expressed in the cortex of the rat brain 84
Figure 4-21: Investigation of endogenous LINA expression in the dentate gyrus of the rat brain 85
Figure 4-22: Upregulation of endogenous LINA expression with NGF treatment in PC12 cells 87
Figure 4-23: Upregulation of LINA in retina after ONC+LI and LI 88
Figure 4-24: Upregulation of LINA in retina after ONC+LI 89
Figure 4-25: Whole mount mouse embryo stained by *in situ* hybridization (ISH) 91

Abstract

Axons in the adult central nervous system (CNS) fail to regenerate after injury, while axons in the peripheral nervous system can regrow and succeed in reinnervating their target. This difference results from the non-permissive growth environment in the CNS. The CNS glial environment contains myelin-associated growth inhibitory proteins that cause the growth cone collapse of axons. The formation of the glial scar at the lesion site is another barrier for axonal regeneration. Another major obstacle is the absence of or limited intrinsic capability for axonal regeneration in injured CNS neurons. Retinal ganglion cells (RGCs) represent typical projection neurons of the CNS. RGCs exhibit little or no spontaneous regeneration after injury. However, RGCs can survive an injury and reactivate their intrinsic axonal growth program 4 days after a lens injury (LI), which transforms RGCs to a robust regeneration state. The switch to this regenerative state is associated with a dramatic change in gene expression. Among those genes which were specifically upregulated in the regenerative state, I focused on a gene encoding a so far uncharacterized, but identified protein, known as [redacted]([redacted]) in mice. The sequence of this protein in the rat has not been identified yet and after cloning, the protein sequence of the rat showed 100% identity to that of the mouse. In our lab we named this protein Lens Injury induced factor with Neurite outgrowth promoting Activity (LINA). The main focus of my work was to characterize this protein and its possible role for the neurite outgrowth. LINA consists of 155 amino acids containing a highly conserved motif consistent with a RING finger ($C_3H_2C_3$ type zinc finger) and a hydrophobic transmembrane domain. LINA was expressed in retina and rat brain, such as the cortex, cerebellum, and hippocampus. LINA was partially co-localized with the trans-Golgi network and Beta-site APP cleavage enzyme 1, suggesting that LINA is involved in a secretory pathway. LINA showed a ternary complex formation as a biochemical characteristic. LINA overexpression increased neurite outgrowth 2.5 fold compared with controls in PC12 cells, when cells were differentiated by nerve growth factor (NGF), whereas expression of the dominant negative form of LINA significantly reduced outgrowth. My results thus show that LINA contributes to the neurite outgrowth. Understanding the molecular mechanisms underlying its axon growth promoting effects may open new strategies to improve recovery after CNS injuries.

Zusammenfassung

Axone des adulten Zentralen Nervensystems (ZNS) können sich nach einer Verletzung nicht regenerieren, während Axone des Peripheren Nervensystems über lange Distanzen wachsen und ihr Ziel wieder innervieren können. Dieser Unterschied resultiert u.a. aus der beschränkten intrinsischen Fähigkeit für axonales Wachstum adulter ZNS Neurone. Retinale Ganglienzellen (RGZ) sind typische Projektionsneuronen des ZNS und zeigen nach einer Verletzung des Sehnervens kaum regenerative Reaktionen. Sie reaktivieren jedoch ihr intrinsisches, axonales Wachstumsprogramm, wenn die Axotomie mit einer Linsenverletzung einhergeht. Während dieser Reaktivierung ändert sich das genetische Expressionsmuster der RGZ.

In meiner Arbeit habe ich die Eigenschaften und Wirkungen des bis dahin in der Ratte nicht charakterisierten Proteins LINA (Lens Injury induced factor with Neurite outgrowth promoting Activity) untersucht. Die Sequenzierung zeigte eine 100%ige Übereinstimmung mit dem entsprechenden Mausprotein [redacted]LINA besteht aus 155 Aminosäuren und beinhaltet hochkonservierte Motive, wie die RING-Finger-Domäne ($C_3H_2C_3$ Typ Zinkfinger) und eine transmembrane Domäne. LINA kommt hauptsächlich in Retina und Gehirn von Ratte wie im Kortex, Zerebellum, Hippocampus vor. LINA kolokalisiert partiell mit dem Trans-Golgi-Netzwerk und dem Beta-site cleavage enzyme 1, was darauf schließen lässt, dass LINA in den sekretorischen Signalwegen involviert ist. Als biochemische Charakterizierung zeigte LINA eine homotrimere Komplexebildung. Anschließend untersuchte ich den funktionellen Effekt des LINA-Proteins in PC12-Zellen. Die LINA überexprimierenden und mit NGF differenzierten PC12-Zellen zeigen ein 2.5-fach gesteigertes Neuritenwachstum, was darauf schließen lässt, dass LINA in Kombination mit NGF das Neuritenwachstum in PC12-Zellen fördert. Durch eine Punktmutation des ersten Cysteins im Zinkfinger wurde $LINA^{C93A}$ hergestellt und fungiert als dominant negative Variante von LINA. Die Ergebnisse meiner Arbeit zeigten, dass LINA für das neuriten Wachstum eine Rolle spielt und das Verständnis der molekularen Mechanismen über LINA neue Aspekte für die Heilung des ZNS eröffnen könnte.

Abbreviations

A	Adenosine
AAV	Adeno associated virus
ADF	Actin depolymerising factors
APP	Amyloid precursor protein
APS	Ammoniumpersulphate
ATP	Adenosine-5`-triphosphate
BACE1	Beta-site APP cleavage enzyme 1
BCIP	5-Bromo-4-chloro-3-idolyl-phosphate
BDNF	Brain derived neurotrophic factor
BLAST	Basic local alignment search tool
bp	Base pair
BSA	Bovine serum albumin
C	Cysteine
cAMP	Cyclic adenosine monophosphate
CNTF	Ciliary neurotrophic factor
CNS	Central nervous system
CREB	cAMP response element-binding protein
CSPGs	Chondroitin sulphate proteoglycan
dNTP	Deoxyribonucleosid-5`-triphosphate
DEPC	Diethylene pyrocarbonate
DMEM	Dulbecco`s modified eagle medium
DMSO	Dimethylsulfoxid
DNA	Desoxy ribonucleic acid
dpc	day post coitum
DTT	Dithiothreitol
E	Embryo

ECL	Enhanced chemiluminescent
EGS	Ethylene glycolbis
EST	Expressed sequence tag
EtBr	Ethidiumbromid
EDTA	Ethylen-diamin-tetra-acetic acid
ER	Endoplasmic reticulum
FCS	Fetal calf serum
FCSi	Fetal calf serum inactivated
Gap 43	Growth associated protein 43
GCL	RGCs layer
GDNF	Glial cell line-derived neurotrophic factor
GFAP	Glial fibrillary acidic protein
GFP	Green fluorescence protein
GDP	Guanosine diphosphate
GPI	Glycosylphophatidyl-inositol
GTP	Guanosine-5'-triphosphate
GST	Glutathione-S-transferase
g/v	Gram per volume
h	hour
H	Histidine
HA	Human influenza hemagglutinin
HBS	HEPES buffered saline
HBSS	Hank´s buffered salt solution
HE	Haematoxylin and eosin
HEK293	Human embryonic kidney cell line
HEPES	4-(2-hydroxyethyl)-1-piperazineethanesulfonic acid
i.p.	Intraperitoneal
IRES	Internal ribosomal entry site
IGF	Insulin-like growth factors

IPL	Inner plexiform layer
IPTG	Isopropylthiogalactoside
LI	Lens injury
LINA	Lens injury induced neurite outgrowth promoting activity
MAG	Myelin associated glycoprotein
min	minute
N	Asparagine
NBT	Nitro-blue tetrazolium chloride
NGF	Nerve growth factor
NgR	Nogo receptor
NT-3	Neurotrophin 3
NTMT	NaCl, Tris, $MgCl_2$, Tween
OD	Optic density
ONC	Optic nerve crush
OMgp	Oligodendrocyte myelin glycoprotein
PBS	Phosphate buffered saline
PC12	Pheochromocytoma cell line
PCR	Polymerase chain reaction
PDL	Poly-D-Lysin
PFA	Paraformaldehyde
PNS	Peripheral nervous system
PMSF	Phenylmethylsulfonylfluoride
P/S	Penicillin/Streptomycin
Q	Glutamine
RGCs	Retinal ganglion cells
RING	Really interesting new gene
RNF	RING finger protein
RF	RING finger

RFP	Red fluorescence protein
RT	Room temperature
RT-PCR	Reverse transcription PCR
sec	second
Ser	Serine
SDS	Sodium dodecyl sulphate
SOCS3	Suppressor of cytokine signaling 3
Sprr1	Small proline rich protein 1
SSC	Trisodium citrate and sodium chloride solution
STAT3	Signal transducers and activators of transcription 3
Taq	Thermus aquaticus
TBE	Tris, boric acid and EDTA
TGN	Trans-Golgi Network
TEMED	N,N,N',N'-Tetramethylethylenediamine
Thr	Threonine
T_m	melting temperature
TM	Transmembrane domain
TNF	Tumor necrose factor
TRPC	Transient receptor potential cation channel
U	Unit
V	Volt
v/v	Volume pro volume
w/o	without
WT	Wild type

1 Introduction

The nervous system is a wired complicated communication system of the body. The important functions of the nervous system are perception and integration of sense as well as cerebration. It can be divided into the central nervous system (CNS) and the peripheral nervous system (PNS). The CNS is composed of the brain, spinal cord and the optic nerve. The brain controls effector cells, which carry out the physiological responses ordered by the brain. Nerves connect the brain to effector cells. Thus, if nerves are damaged, the signal to effector cells is interrupted, and neurons are unable to induce effective functions such as muscle movements, or signal transmissions to the brain such as the optic signal. If neurons are damaged, the CNS has a very limited regenerative capacity. This results from the environment of the injury site, which includes myelin proteins, astrocytic gliosis and cell surface molecules.

In the visual system, the optic nerve, which contains the axons of retinal ganglion cells (RGCs), has been used as an excellent experimental model to study neuroprotection and axonal regeneration of adult CNS neurons (Berkelaar et al., 1994; Fischer et al., 2000; Fischer et al., 2004a, 2004b; Harvey et al., 2006). Adult RGCs exhibit little or no spontaneous regenerative responses after injury to regenerate axons (Caroni and Schwab, 1993; Schwab et al., 1993; Chen et al., 1995). Berkelaar et al. (1994) showed that all RGCs in adult rats survived for 5 days after intraorbital optic nerve transection, reducing the survival rate to approximately 50% by day 7 and to less than 10 % on day 14. Although most RGCs undergo apoptosis after axotomy and do not regenerate axons in the mature optic nerve, there are several evidences that either a lens injury (LI) or injections of the glucose polymer zymosan into the vitreous body of the eye induce intraocular inflammation which enables RGCs to survive an injury and reactivate their intrinsic growth program (Fischer et al., 2000; Fischer et al., 2001; Fischer et al., 2004a; Leon et al., 2000; Hauk et al., 2008; Müller et al., 2007; Yin et al., 2003).

1.1 The visual system

The eye enables human beings to perceive the light between 400 and 750 nm wavelength as well as the contrast and it is connected to the brain via the optic nerve (Lüllmann-Rauch, 2002; Hick, 2002). The anatomy of human eye is shown in Figure 1-1. The sclera covers the outside of the eye and is composed of tough

network-formic connective tissue. It bears up the intraocular pressure. Light, which enters through the pupil, is focused by the cornea and the lens onto the retina. Cornea is the transparent window of eye and has no blood vessel (Lüllmann-Rauch, 2002). Lens is an epithelial organ and composed of lens fibers, lens epithelial layer and lens capsule. Certain lens proteins, crystallins have been reported that they strongly enhanced axon regeneration from retinal explants in culture (Fischer et al., 2008). Lens is connected to zonule fibers, which keep the position of lens. The iris, which is the foremost part of uvea, controls the amount of the light and the ciliary muscles which are connected to the lens via zonule fibers can change the shape of the lens to achieve a sharp focus at the retina. The image which is formed on the retina is transmitted to the brain by the optic nerve. The fovea is the highest sharp point of vision in retina, which contains the largest concentration of cone cells in the eye (Lüllmann-Rauch, 2002; Kolb et al., 2007). In contrast, however, in some nocturnal animals such as the rat, there is no fovea.

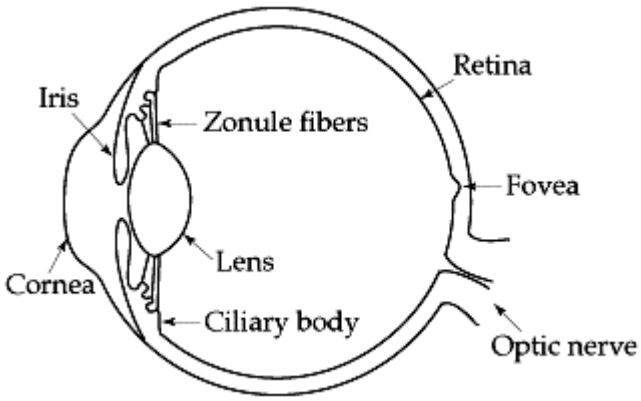

Figure 1-1: Anatomy of the human eye (from http://thalamus.wustl.edu/course/eyeret.html)

The retina is the part of brain and has a layered structure. The structure of the retina is illustrated in Figure 1-2. The light signal enters first from RGCs layer and penetrates the entire retina to reach the photoreceptors which are divided into rods and cones. The photoreceptors convert light impulse to electrochemical signals. The axons of photoreceptors make contact with the dendrites of bipolar cells and horizontal cells which process then the signals to RGCs and amacrine cells. The cells of the RGCs layer send their axons through the optic fiber layer to form the optic nerve and finally connected to brain. About 100,000 RGCs exist in

retina of rodents and there are at least twice as many ganglion cells in the retina of the newborn rat as in the adult rat (Perry et al., 1983). RGCs are the only cells in the retina that connect to the brain and they vary significantly in terms of their size, connections, and responses to visual stimulation (Lüllmann-Rauch, 2002; Inatani M, 2005). Müller cells, a special form of glial cells, are typical glial cells in the retina (Lüllmann-Rauch, 2002). These cells span the entire thickness of the retina and fill in the gaps between the neurons with their branches. The function of Müller cells has not been well understood so far, but in recent year it has been reported that these cells function for regeneration of RGCs (Müller et al., 2007; Hauk et al., 2008).

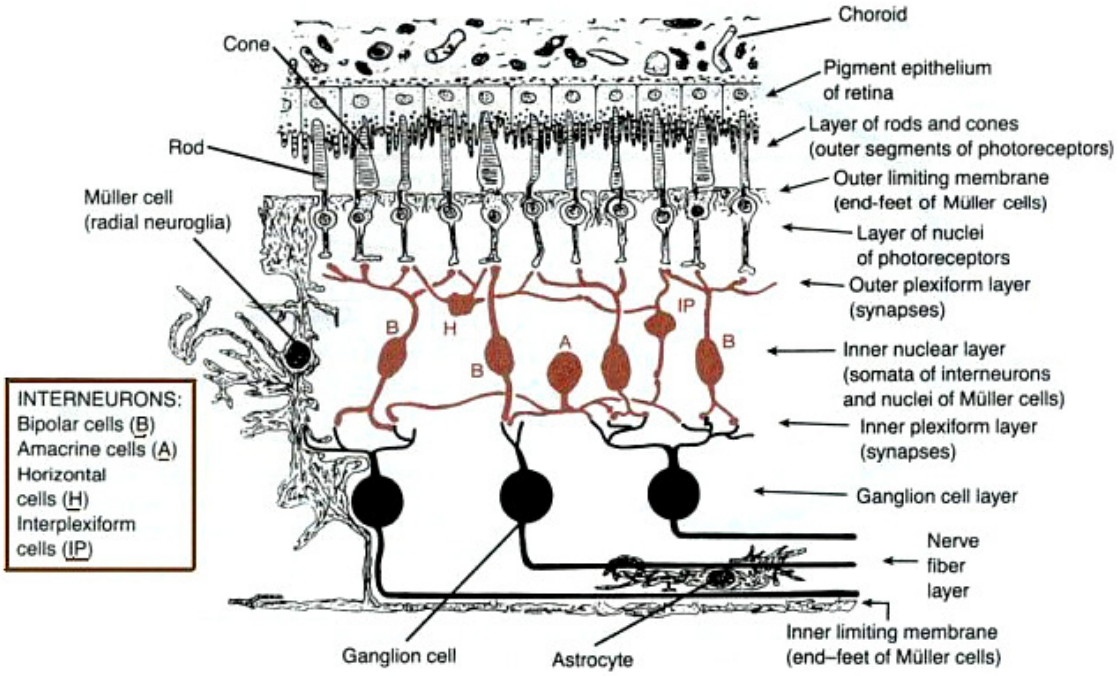

Figure 1-2: Structure of the retina (from http://instruct.uwo.ca/anatomy/530/retina.jpg)

This schematic drawing shows the layered-structure of the retina. Bipolar cells (B), Amacrine cells (A), Horizontal cells (H) and interplexiform cells (IP) belong to interneurons and Müller cells and astrocytes belong to the glial environment of the retina. RGCs, the biggest cells in retina, are the only cells in the retina that connect to the brain.

1.2 Difference of glial environment between CNS and PNS

Axons in the adult CNS fail to regenerate after injury, while those in the PNS are capable of a long distance growth and a successful target reinnervation. This

difference, at first, results from the different responses of the glial environment. The CNS glia is composed of astrocytes and oligodendrocytes and the PNS glia is composed of Schwann cells. These glial cells express different myelin inhibitory proteins which can contact and interact with nerve cells via specific receptors and so respond differently during regeneration after injury.

1.2.1 Myelin inhibitory proteins

Growth inhibitory proteins present in CNS myelin are myelin-associated glycoprotein (MAG), Nogo-A and oligodendrocyte myelin glycoprotein (OMgp) (Schwab et al., 1993; McKerracher et al., 1994; Chen et al., 2000; Qiu et al., 2000; Grandpre and Strittmatter, 2001; Wang et al., 2002a; Wang et al., 2002b; Chaudhry and Filbin, 2007). All three proteins are localized on the inner lamella of the myelin sheath and make direct contact with axons (GrandPre et al., 2000; McKerracher et al., 1994; Wang et al., 2002b). Nogo is expressed by oligodendrocytes but not by Schwann cells and has three forms, Nogo-A, -B, and –C, which are generated from Nogo gene by alternate splicing, sharing a highly conserved 180 amino acid C-terminal domain (GrandPre et al., 2000; Dodd et al., 2005). The inhibitory activity of Nogo-A is located in the N-terminal part of the molecule, called NiG (Chen et al., 2000; Fournier et al., 2001) and the Nogo-66 domain (GrandPre et al., 2000; Fournier et al., 2001). MAG is a type I membrane protein composed of 5 extracellular immunoglobulin-like domains, whereas OMgp is a glycosylphosphatidyl-inositol (GPI) anchored protein (Domeniconi et al., 2002; Liu et al., 2002; Wang et al., 2002b). Unlike Nogo-A, MAG is expressed by both CNS oligodendrocytes and PNS Schwann cells (Schachner and Bartsch, 2000). MAG promotes embryonic and neonatal neurite outgrowth (Schachner and Bartsch, 2000; DeBellard et al., 1996). Depending on the developmental stage of the neuron, MAG can inhibit neurite outgrowth in vitro (Mukhopadhyay et al., 1994; DeBellard et al., 1996). This suggests that MAG can function as both promotion and inhibition of neurite outgrowth (Schachner and Bartsch, 2000; DeBellard et al., 1996). OMgp is often found in membranes of oligodendroglia-like cells that encircle nodes of Ranvier and might function to prevent collateral sprouting (Huang et al., 2005). In addition to these myelin inhibitors, some other myelin-associated components were identified during development, such as Ephrin B3 and Semaphorin 4D (Liebl et al., 2003; Benson et al., 2005; Moreau-Fauvarque et al., 2003). They play critical roles in axon path finding during embryonic development, but it is also proposed that they may function as inhibitors of regeneration in the mature CNS (Liebl et al., 2003). Benson et al. (2005) showed that Ephrin B3 is ex-

pressed in postnatal myelinating oligodendrocytes and functions as a myelin-based inhibitor combined through the co-receptor p75.

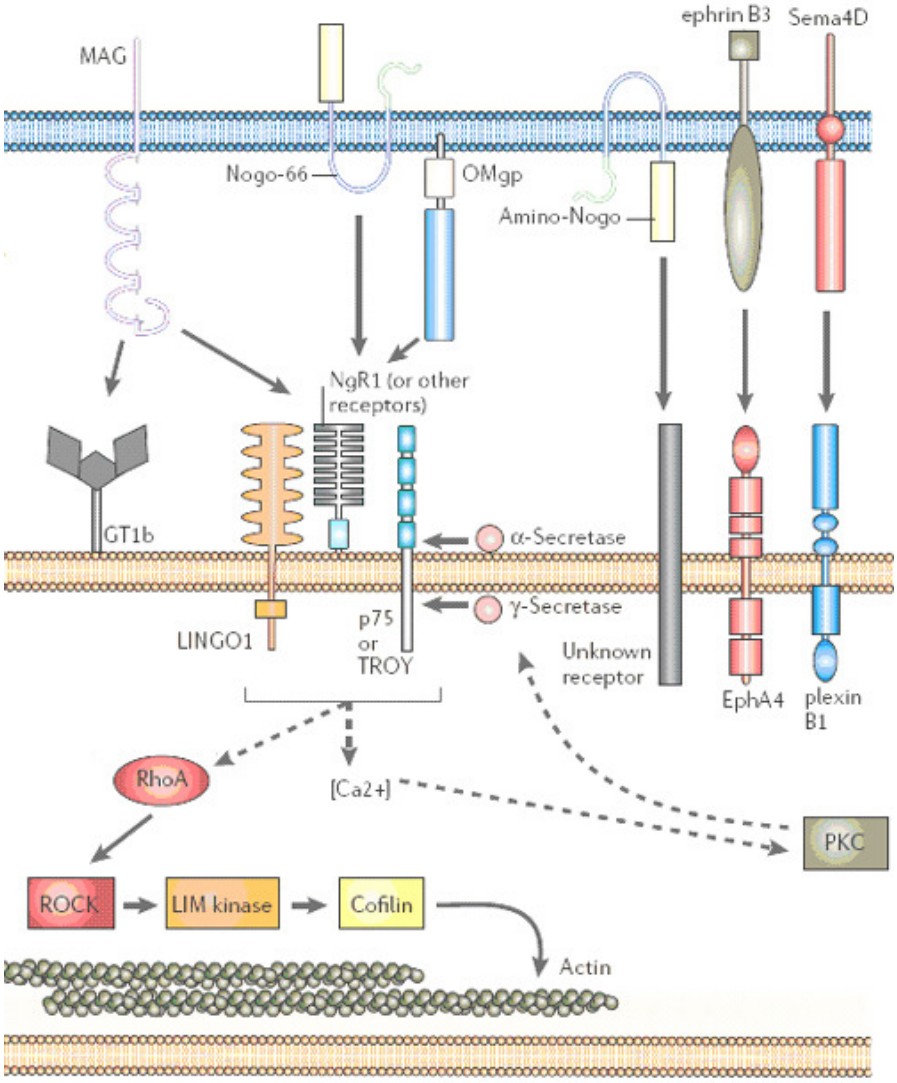

Figure 1-3: Myelin inhibitory proteins and intracellular signaling mechanisms.

The myelin inhibitory proteins of the adult CNS glial environment are myelin-associated glycoprotein (MAG), Nogo-A, oligodendrocyte myelin glycoprotein (OMgp), ephrin and semaphorin 4D (Sema4D). The neuronal receptors and intracellular signaling pathways are shown. These inhibitory signals activate finally RhoA and cause the rise in intracellular calcium. The signals downstream of RhoA are well characterized (solid arrows), but the relation between RhoA and the function of calcium influx is still not well known (dashed arrows) (modified from Yiu and He, 2006).

The Nogo-receptor (NgR) is a GPI-linked protein and can bind Nogo, MAG, and OMgp. The p75 interacts with the NgR as a co-receptor and this complex medi-

ates repulsive signaling by myelin-associated glycoprotein (Wang et al., 2002a; Wong et al., 2002). But many CNS neuron types that are inhibited by myelin, such as RGCs, do not express p75 in the adult CNS (Park et al., 2005). Park et al. (2005) showed that a TNF receptor family member, TROY could interact with NgR and its interaction was nearly eight fold stronger than the interaction between p75 and NgR. They showed that TROY can substitute for p75. Other evidences have revealed the requirement for another co-receptor known as LINGO1, a transmembrane protein that can bind to both NgR and p75 (Mi et al., 2004).

The signaling mechanisms for the transduction of the inhibitory properties of myelin inhibitory proteins are not well known. So far, the best characterized pathway involves RhoA and its effector, RhoA-associated serine-threonine kinase (ROCK). RhoA is a small GTPase protein which is known to regulate the actin cytoskeleton in the formation of the stress fibers. Small GTPases of the Rho family such as RhoA, Rac1 and Cdc42 (cell division cycle 42) are known regulators of the actin cytoskeleton (Luo, 2000; Dickson, 2001; Maekawa et al., 1999). Rho proteins switch their states by cycling between an inactive GDP-bound and an active GTP-bound state (Bishop and Hall, 2000). In the active GTP-bound state, RhoA can bind with ROCK, which regulates growth cone motility negatively (Bito et al., 2000) and induce the growth cone collapse via activation of LIM kinase 1 (LIMK1). LIMK1 is a critical regulator of the cellular actin cytoskeleton (Arber et al., 1998). It is activated through phosphorylation and phosphorylates further the actin depolymerising factors (ADF)/cofilin, which depolymerize actin filaments (Bamburg, 1999).

The exact RhoA/ROCK inhibitory signal transduction mechanism is not well known. However, inhibiting RhoA using *Clostridium botulinum* C3 transferase and inhibiting ROCK using Y27632 (Ishizaki et al., 2000; Lingor et al., 2008) promotes axon outgrowth on inhibitory substrates (Niederöst et al., 2002).

In addition to the myelin inhibitory proteins involved in the failure of regeneration in CNS neurons, the astrocytic gliosis and the formation of the glial scar are the next barrier for axonal regeneration.

1.2.2 The glial scar

The glial scar is formed by activated astrocytes. The CNS injury activates and changes astrocytes and microglia with morphological and functional effects (Fitch et al., 1999). The activated glial cells enter the site of primary injury. They clear up first the cell debris and block it to prevent secondary injurious mechanisms.

Following this, microglia, which is accompanied by invasion of blood born macrophages, can be activated and produces tumor nekrose factor-α (TNF-α) and nitrogen monoxide (NO) (Bunge et al., 1997; Fawcett and Asher, 1999; Fitch et al., 1999). After the invasion of phagocytes, an inhibitory chondroitin sulphate proteoglycan (CSPGs) which is released by reactive astrocytes and platelet-derived growth factor receptor a (PDGFRa) enter into the glial scar (Fawcett and Asher, 1999). The formation of the glial scar can be finished by a migration and proliferation of astrocytes. Astrocytes respond to the CNS injury with their morphological change and they synthesize more glial fibrillary acidic protein (GFAP). These changes can be observed as early as 24 h after CNS injury (Schnell et al., 1999). With sealing the site of injury from the environment and reconstructing the damaged areas, this glial scar formation in the CNS can prevent further infections and damages (Bush et al., 1999; Stichel and Muller, 1998). In comparison to these responses of the CNS glia after injury, the PNS glia, Schwann cells, responds differently to injury.

1.2.3 Schwann cells

Schwann cells were first described by Theodore Schwann and they are derived from neural crest cells, and are divided into two types either myelinating or non-myelinating Schwann cells after birth (Jessen et al., 1994; Jessen and Mirsky, 2005). Both play an important role in the maintenance and regeneration of axons of the neurons in the PNS (Jessen et al., 1994). Both myelinating and non-myelinating Schwann cells can differentiate to immature Schwann cells after axonal interaction stops. Once axonal contact is re-established, these cells become myelinating or non-myelinating depending on the axonal signal (Jessen and Mirsky, 2005). Mature Schwann cells are able to block apoptosis by releasing growth factors including insulin-like growth factors (IGFs), platelet derived growth factor-BB (PDGF-BB), and neurotrophin-3 (NT-3) (Jessen and Mirsky, 2005). One of the most important functions of the Schwann cell is to myelinate the axons of the PNS. They also assist in neuronal survival and signal the formation of various structures within the PNS (Jessen and Mirsky, 2005; Burstyn-Cohen et al., 1998). After an injury occurs in the PNS, the Schwann cell helps to phagocytize the damaged end of the axon and then forms the regeneration tube of the axon that is connected to the cell body (Burstyn-Cohen et al., 1998). Schwann cells are also able to attract injured neurons by secreting neurotrophic factors such as nerve growth factor (NGF) to help axon elongation. They also promote elongation after injury by secreting F-Spondin, a developmental protein (Burstyn-Cohen et

al., 1998). Due to their regenerating effect in the PNS, the Schwann cell transplantation into the damaged CNS target area was often tested in the last years. Those experiments showed improved healing and regeneration effects suggesting the better possibility for treating demyelinating disorders and spinal cord injuries (Kamada et al., 2005; Kohama et al., 2001; Bachelin et al., 2005). For a complete recovery, however, the reduced intrinsic capacity to regenerate axons is a next known obstacle in the adult CNS.

1.3 Changes of intrinsic capabilities for axonal regeneration

The injured adult CNS may react less efficiently to neurotrophic factors than the embryonic neurons, which may also react differently to myelin-associated inhibitors. This is one of the reasons for the reduced intrinsic capability of the injured adult CNS for regeneration. In the last years, changes of intrinsic factors were often observed during successful neuronal regeneration. The cellular levels of the second messenger cyclic AMP (cAMP) are related to the CNS axonal regeneration. Some neurotrophins, brain-derived neurotrophic factor (BDNF) and glia-derived neurotrophic factor (GDNF) could block the inhibitory effects of myelin-associated glycoproteins (Cai et al., 1999) and finally elevated neuronal cAMP levels to enhace the axonal regeneration. A cAMP elevation upregulates further the expression of arginase I, a key enzyme in polyamine synthesis which can overcome axonal growth inhibition by myelin-associated inhibitors. One transcription factor which seems to be engaged in the upregulation of arginase I expression is the cAMP response element binding protein (CREB). CREB is a well known transcription factor of neuronal responses to neurotrophins and its activity results in enhanced neuronal survival and regeneration (Watson et al., 2001; Finkbeiner et al., 1997). The protein Bcl-2, an apoptotic regulator, seems to play a role in enhancing the intrinsic axonal regeneration capacity of RGCs (Chen et al., 1997; Holm and Isacson, 1999; Yang et al., 1995; Adams and Cory, 1998; Adams and Cory, 2001). Chen et al. (1995) showed that the adult CNS neurons have a diminished intrinsic regenerative capacity compared to young neurons in RGCs. They showed that embryonic retinal axons could regrow and overcome the myelin inhibitory effect but adult retinal axons lose their ability for reinnervation from postnatal day two. They showed further that this regenerative ability in embryonic retinal axons could be changed between E16 and E18 retinal axons and this is correlated with a drastic decrease in the level of the anti-apoptotic protooncogene Bcl-2 (Chen et al., 1997). In contrast, adult PNS neurons keep the Bcl-2 expression function for regeneration throughout adulthood (Merry et al.,

1994). These observations suggested that Bcl-2 has a role in enhancing the intrinsic axonal regeneration capacity of RGCs.

Fischer et al. (2000) showed that RGCs failed to regenerate and undergo apoptosis after optic nerve crush (ONC), but they could switch into the regeneration state after lens injury (LI) and intravitreal injection of yeast wall extract, zymosan. The activated macrophages stimulated by inflammation have been suggested to be a source of factors for these beneficial effects of LI or zymosan injection (Yin et al., 2003; Leon et al., 2000). And Yin et al. (2006) showed that oncomodulin driven by macrophages could be a major factor of these LI or zymosan injection effects for the regeneration of RGCs. However, Hauk et al. (2008) have shown recently that the effect of regeneration in RGCs by LI and zymosan injection is correlated with activated astrocytic glial cells and Müller cells, not macrophages. Müller et al. (2007) confirmed that LI or zymosan effect and elevated intracellular cAMP levels result in a strong regeneration of RGCs. They showed that this LI induced upregulation of ciliary neurotrophic factor (CNTF) which was produced in retinal astrocytes and this CNTF finally activated the transcription factor signal transducers and activators of transcription 3 (STAT3) in RGCs. These observations suggest that CNTF can be one of the major contributors to enhance the intrinsic capacity for axonal regeneration in RGCs. However, it is still not well known which genes are activated by STAT3 in RGCs. The known upregulation of SOCS3 (suppressor of cytokine signaling 3) by STAT3 inhibits the STAT3 activation as a negative feedback pathway (Yasukawa et al., 2001). Fischer et al. (2004b) showed the upregulation of genes after ONC only, and ONC with additional LI treatment through microarray analysis, such as sprr1 (small proline rich protein 1), gap43 (growth associated protein 43), Calcineurin, Cebp-δ, and some unknown genes.

1.4 LINA, a new RING finger protein promoting neurite outgrowth

Fischer et al. (2004b) showed that RGCs could change their intrinsic capacity for regeneration 4 days after lens injury (LI) and ONC in rats. They showed that RGCs could regenerate their axons through reactivation of the intrinsic growth program *in vivo*. Additionally, they analyzed the change of the gene expression pattern in RGCs using microarrays when RGCs enter into the state of regeneration. Among those genes which were specifically upregulated in the regenerative state, in our lab we chose to examine one gene from expression sequence tags (ESTs) and cloned it. This gene, which encodes a RING (Really Interesting New Gene)-finger protein, has been so far uncharacterized and its sequence is un-

known in rats. It has been known as [redacted] in the mouse though. Cloning of this sequence showed a 100% identity with the mouse protein sequence. In our lab we named this rat protein Lens Injury induced Neurite outgrowth promoting Activity (LINA).

Many recent reports suggest that proteins possessing a RING finger motif have diverse functions in cells. They appear to be involved in development, oncogenesis, cell cycle control and apoptosis. Structurally, the RING-finger is a specialized type of zinc-finger which consists of 40 to 60 amino acids that binds two zinc atoms (Borden and Freemont, 1996). There are two different variants, the C_3HC_4-type and a $C_3H_2C_3$ type, which are related with the different cysteine (C)/histidine (H) pattern (Freemont, 1993; Borden and Freemont, 1996; Schwabe and Klug, 1994). The latter type is referred to as RING-H2 finger. LINA belongs to this type. It has been shown that many RING-finger proteins as well as the zinc finger protein have a DNA binding activity, whereas it is thought that most of the RING-H2 finger proteins and a few of the RING finger proteins do not bind DNA (Freemont, 1993) but are associated with other functions. Robinson et al. (1991) characterized one yeast protein containing a RING finger motif, Vps18p. They showed that through a mutation of the first zinc finger of this protein, yeasts were defected in the sorting and transport of vacuolar enzymes, suggesting that the RING finger motif may be required for vacuolar protein sorting (Robinson et al., 1991).

Many RING finger proteins have also been reported to be involved in ubiquitin mediated protein modification. Ubiquitin is a protein, which is found in all eukaryotic cells. It consists of 76 amino acids and its sequence is conserved in all species (Joazeiro and Weissman, 2000). Ubiquitin participates in the post-translational protein modification, namely ubiquitination, in which it can be attached to other proteins. Ubiquitination is an ATP-dependent process and three enzymes are involved, an ubiquitin-activating enzyme (E1), an ubiquitin-conjugating enzyme (E2) and an ubiquitin ligase (E3) (Herschko and Ciechanover, 1998). The E1 enzyme transfers the ubiquitin molecule to a cysteine residue on the E2 enzyme in an ATP-dependent manner. The E2 enzyme then either transfers the ubiquitin directly to a substrate, or to an E3 ligase, which can also ubiquitinate a substrate (Herschko and Ciechanover, 1998; Scheffner et al., 1995; Schwarz et al., 1998). Ubiquitination is an important process in the cell. It controls many signaling proteins, such as cell cycle control proteins (Gmachl et al., 2000) and removes misfolded or damaged proteins that could be harmful to the cell. Many proteins containing RING fingers function as E3 ubiquitin ligases (Freemont, 2000; Fang et al., 2000; Baer et al., 2002; Ogawa et al., 2008). On-

coprotein Mdm2, containing a RING finger domain has been reported as an E3 ubiquitin ligase for tumor suppressor p53 (Fang et al., 2000). Fang et al. (2000) showed further that Mdm2 functions in its own ubiquitination requiring no other substrate protein. Another RING finger protein, BRCA1 binds together with BARD1 as a heterodimer and functions as an E3 ubiquitin ligase participating in suppressing tumor formation in normal cells (Baer et al., 2002). Recently, a novel RING finger gene, Rines/RNF180 was identified and characterized as a new E3 ubiquitin ligase associated with the ubiquitin-proteosome pathway (Ogawa et al., 2008)

The function of the RING finger domain in axonal regeneration is at present poorly known. However, Araki et al. (2001) identified and characterized a new gene, Nin283 containing both zinc finger and RING finger domains, which was upregulated after nerve injury in Schwann cells. They showed that this protein was highly expressed in the CNS as well as PNS and located in the endosome/lysosome compartment, speculating that this protein may participate in the ubiquitination. Nakayama et al. (1995) showed a novel RING-H2 motif protein, Neurodap1, which is downregulated by facial nerve axotomy. Through the analysis of subcellular localization of this protein, they speculated that Neurodap1 might be linked to the secretory or protein sorting machinery and might play an important role in protein sorting from the Golgi-network to the postsynapse in neurons (Nakayama et al., 1995). Tursun et al. (2005) investigated the role of RNF6 containing a RING finger during the mouse embryogenesis and also in cultured hippocampal neurons. This group showed the upregulation of RNF6 in developing axonal projections of motor neurons and DRG neurons in mouse embryos. They also demonstrated that RNF6, as an E3 ubiquitin ligase, binds to LIMK1 and mediates polyubiquitination of LIMK1 for proteosomal degradation and finally regulates the growth cone actin dynamics (Tursun et al., 2005). A novel RING finger protein, MIR (myosin regulatory light chain interacting protein) was also found to play a role in neurite outgrowth (Olsson et al., 1999). They showed that overexpression of MIR in PC12 cells abrogated neurite outgrowth induced by NGF, suggesting that MIR interacts with the cytoskeleton and regulates cell motility (Olsson et al., 1999).

As a new RING-finger protein whose gene expression was upregulated by LI in RGCs, it is interesting to investigate the functional effect of LINA in neurite outgrowth and to understand the characteristic of this protein.

Here I reported the characterization of a so far uncharacterized RING finger protein, LINA, the gene expression of which was upregulated in the regenerating RGCs of the rat. The aims of this work are:

1. Functional characterization of LINA for neurite outgrowth in PC12 cells.
2. Biochemical characterization of the structural domains of the LINA protein by generating different LINA depleted variants.
3. Characterization of the subcellular localization of exogenous LINA.
4. Investigation of endogenous LINA expression in retina and rat brain using anti-LINA antibodies.
5. Investigation of the LINA expression on mRNA level using *in-situ* Hybridization method.

2 Material

2.1 Technical equipments

4-well-Plate	Sarstedt Inc., Newton, NC, USA
Autoclav	Systec GmbH Labor-Systemtechnik, Wettenberg, Germany
Weight scale, BP110S	Sartorius, Göttingen, Germany
Fluorescence microscopy	Zeiss, Oberkochen, Germany
	Integrated Camera; Fluorescence filter 450-490 nm / 510-560 nm / 395-440 nm
Gel documentation system 1000	BIO RAD, Hercules, CA, USA
Gel combs	BIO RAD, Hercules, CA, USA
Hand gloves	Kimberly-Clark, Roswell, GA, USA
Incubator (Bacterium)	Biometra, Göttingen, Germany
Incubator (cell culture), HERA cell	Heraeus, Hanau, Germany
Cool centrifugation, 5417R	Eppendorf, Hamburg, Germany
Suprafuge 22 + Megafuge 1.OR	Heraeus, Hanau, D
Laborweight scale, PT 610	Sartorius, Göttingen, Germany
Light microscopy	Leica, Wetzlar, Germany
Parafilm	„M“American National Can TM, Chicago, USA
PCR Tubes	Biozym Biotech Trading GmbH, Wien, A
Pipettes	Abimed HAT, Langenfeld, Germany
Reaction tubes	Sarstedt Inc., Newton, NC, USA
RNase Zap-tissue	Ambion, Austin, TX, USA
Falcon	Becton Dickinson Labware, Franklin Lakes, NJ, USA
Shaker	Gesellschaft für Labortechnik, Burgwedel, D

Clean bench, HERA safe	Heraeus, Hanau, Germany
T3 Thermocycler	Biometra, Göttingen, Germany
Table centrifugation, Biofuge pico	Heraeus, Hanau, Germany
Vortexes	Bender & Hobein, Zürich, CH
Water bath K15 + C1	HAAKE, Vreden, Germany

2.2 Consumable Materials

Cellstrainer (100 µm, Falcon Nr.352360)	Firma Becton Dickinson, Heidelberg
Injection needle (steril, 10 ml)	Aesculap, Tuttlingen
Scalpel	Aesculap, Tuttlingen
Electroporation cuvets (1 mm)	Bio-Rad, München
Tissue culture flask T 25 (50 ml)	Greiner, Frickenhausen
Tissue culture petri dish	Greiner, Frickenhausen
Cryotubes	Roth, Karlsruhe
Nylon Membranes	Amersham
Pasteur pipettes	Brand, Wertheim
PCR-tubes	Fischer, Ulm
Petri dish	Greiner, Frickenhausen
Pipette tips, filtered (10 µl, 100 µl, 1000 µl)	Sarstedt
Pipettes steril (10 ml, 25 ml)	Invitrogen, Groningen, NL
Reaction tubes (1.5 ml, 2 ml)	Eppendorf, Hamburg
Sterilfilter (0.2 µm)	Sartorius, Göttingen
Poly-prep Chromoatography columns	BioRad
Whatmann paper	BioRad

2.3 Plasmids

pAAV-IRES-hrGFP	Stratagene, Amsterdam, NL
pCR2.1-HIS-TOPO	Invitrogen, Calsbad, CA, USA

pEGFP-N2	Clontech, mountainview, CA, USA
pcDNA3-RBP2N-mcherry	Internal medicine I, university Ulm
pCS2+	Biochemistry, university Ulm
pGEX-4T-1	Anatomy and cell biology, university Ulm

2.4 Enzymes

Eco*R* I	Invitrogen, Calsbad, CA, USA
Xho I	Invitrogen, Calsbad, CA, USA
Sac II	New England Biolabs, Ipswich, MA, USA
Sma I	New England Biolabs, Ipswich, MA, USA
Not I	New England Biolabs, Ipswich, MA, USA
Kpn I	New England Biolabs, Ipswich, MA, USA
BamH I	New England Biolabs, Ipswich, MA, USA

2.5 Antibodies

Rabbit Anti-HA	Sigma, St.Louis, MO, USA
Mouse Anti-Flag	Sigma, St.Louis, MO, USA
Rabbit Anti-GST	Sigma, St.Louis, MO, USA
Mouse Anti-ß-actin	Sigma, St.Louis, MO, USA
Rabbit Anti-LINA	Invitrogen, Calsbad, CA, USA
Guinea pig Anti-LINA	PINEDA, Berlin, Germany
Mouse Anti-ß III tubulin (TUJ1)	Covance, Berkeley, CA, USA
Anti-Rabbit peroxidase coupled	Sigma, St.Louis, MO, USA
Anti-Mouse peroxidase coupled	Sigma, St.Louis, MO, USA
Anti-Guinea pig peroxidase coupled	Sigma, St.Louis, MO, USA
Alexa Fluor® goat Anti-Mouse 594	Molecular Probes, Eugene, USA
Alexa Fluor® goat Anti-Rabbit 488	Molecular Probes, Eugene, USA
Alexa Fluor® goat Anti-Rabbit 594	Molecular Probes, Eugene, USA
Alexa Fluor® goat Anti-Mouse 488	Molecular Probes, Eugene, USA

2.6 Reagent kits

ProFound HA Tag IP/Co-IP kit	PIERCE
TOPO TA cloning kit	Invitrogen
MaxiPreps	Invitrogen
QuickChange Site-Directed Mutagenesis kit	Stratagene
AAV Helper-Free System	Stratagene
QIAquick DNA purification kit	Qiagen
QIAquick Gel extraction kit	Qiagen
Mmessage Mmachine SP6 kit	Ambion
RNeasy Mini Kit	Qiagen
WizardPlus SV Minipreps	Promega

2.7 Chemicals and reagents

Agarose	GIBCO BRL, Paisley, Scotland, UK
Ampicillin	Sigma, St. Louis, MO, USA
Acetic acid	Sigma, St. Louis, MO, USA
Kanamycin	Sigma, St.Louis, MO, USA
Ampuwa (sterile)	Fresenius, Bad Homburg, D
ß-ME (14.3 mol/l)	Sigma, St. Louis, MO, USA
Bromphenolblue	Pharmacia Biotech, Uppsala, S
BSA	PAA Laboratories GmbH, Pasching, Austria
EDTA	Sigma, St. Louis, MO, USA
Ethanol	Apotheke Uniklinik Ulm, D
Ethidiumbromid	Sigma, St. Louis, MO, USA
FCS	Invitrogen, Calsbad, CA, USA
D(+)-Glucose-Monohydrate	AppliChem, Darmstadt, D
Glycerine (p.a.)	J.T. Baker, Deventer, NL
HCl (>=37%)	Riedel-de Häen, Seele, D

HEPES	Sigma, St. Louis, MO, USA
HBSS	GIBCO BRL, Paisley, Scotland, UK
Isopropanol	Furka Chemie GmbH, Buchs, CH
KCl	AppliChem, Darmstadt, D
Lipofectamine™ (2 mg/ml)	Invitrogen, Calsbad, CA, USA
Methanol	MERCK, Darmstadt, D
$MgCl_2$ (50 mM)	Invitrogen, Calsbad, CA, USA
Natriumphosphate	Riedel-de Haen, Seele, D
Natriumacetate	Merck, Darmstadt, D
Nerve Growth Factor	SIGMA, St. Louis, MO, USA
PBS (10 x, pH 7.4, -$CaCl_2$, -$MgCl_2$)	GIBCO BRL, Paisley, Scotland, UK
Penicillin/Streptomycin (10 mg/ml)	Biochrom AG, Berlin, D
PFA (10% Formalin)	SIGMA, St. Louis, MO, USA
Phenol/Chloroform/Isoamylalcohol	Invitrogen, Calsbad, CA, USA
Poly-L-Lysin	SIGMA, St. Louis, MO, USA
Tris	BIO RAD, Hercules, CA, USA
dNTP (10 mM)	Invitrogen Calsbad, CA, USA,
RNA*later*™	QIAGEN, Hilden, Deutschland
1 kb plus DNA Ladder (1 µg/µl)	Invitrogen, Calsbad, CA, USA
Triton-X-100	Sigma, St. Louis, MO, USA
$CaCl_2$	Sigma, St.Louis, MO, USA
Protein weight marker	Fermentas
Protease Inhibitor cocktail	AppliChem, Darmstadt, D
4',6-diamidino-2-phenylindol (DAPI)	Sigma, St. Louis, MO, USA
Coomasie Blue R250/G250	Sigma, St. Louis, MO, USA
DMSO	Sigma, St. Louis, MO, USA
NaCl	Sigma, St. Louis, MO, USA
APS	Sigma, St. Louis, MO, USA
TEMED	Sigma, St. Louis, MO, USA

Acrylamid solution	BIO RAD, Hercules, CA, USA
ECL Detection reagent	Amersham
Glycin	Applichem, Darmstadt
Tris	USB, Ohio, USA
Tween 20	Sigma, St. Louis, MO, USA
SDS	USB, Ohio, USA
Milk powder	Roth
Glutathione-Sepharose	GE-Health care
Glutahtione, reduced	SERVA
Lysozyme	SERVA
Dnase I	Roche
Rnase I	Qiagen

2.8 Buffers

DNA-sample buffer (6 x)	40% Saccharose (w/v), 0.2% SDS (w/v), 0.05% Bromphenolblue (w/v), 0.05% Xylencyanol (w/v), 0.125 M Tris pH 8, 10 mM EDTA
TBE (10 x)	900 mM Tris, 900 mM Boric acid, 25 mM EDTA
10 x PCR Buffer (-$MgCl_2$)	Invitrogen, Calsbad, CA, USA
TBS-T (1 x)	20 mM Tris, 137 mM NaCl, 0.1% Tween 20, pH 7.6
Running Buffer (10 x)	250 mM Tris, 1920 mM Glycin, 1% SDS
Transfer Buffer (1 x)	25 mM Tris, 192 mM Glycin, 20% Methanol

Protein sample buffer (2 x)	200 mM Tris/HCl, 6% SDS, 20% Glycerine, 0.1% Bromphenolblue, 4% 2-ß-ME
Protein lyses buffer	1 x PBS, 10 mM EDTA, 1% Triton X-100, 0.1% SDS, Protease Inhibitor cocktail
TE buffer (10X)	100 mM Tris-HCl, 10 mM EDTA
Milk blocking buffer	5% skimmed milk powder, 1% BSA in TBS-T
Stripping Buffer	100 mM ß-mercaptoethanol, 2% SDS, 62.5 mM Tris/HCl, pH 6.7
Stacking gel buffer	1.0 M Tris/HCl, pH 6.8
Running gel buffer	1.5 M Tris/HCl, pH 8.8
Permeabilation solution (for Hippocampus cell)	500 µl 20% Triton-X-100 1 ml 10% Na-Citrate with 1 x PBS till 50 ml
Blocking solution (for Hippocampus cell)	0.5% Fish gelatine 0.1% Ovalbumin in PBS

2.9 Cell and Bacterial culture and medium

2.9.1 PC12 cells and medium

The PC12 cell line which responds to nerve growth factor (NGF) has been established from a transplantable rat adrenal pheochromocytoma (Greene and Tischler, 1976).

PC12 cell medium: 10% horse serum, 5% fetal calb serum, inactivated at 56°C for 30 min (FCSi), 100 U penicillin and streptomycin in Dulbecco's Modified Eagle Medium (DMEM).

2.9.2 HEK293 cells and medium

The HEK 293 cell line is derived originally from an embryonic human kidney.

HEK 293 cell medium: 10% FCSi, 100 U penicillin and streptomycin in DMEM.

2.9.3 RGCs and medium

Primary retinal ganglion cells were isolated and cultured from an adult rat retina.

RGCs medium: 2% B27, 2% penicillin and streptomycin in DMEM

2.9.4 Hippocampus cells and medium

Primary hippocampus cells were isolated and cultured from an embryonic rat brain (E18 - E20).

Hippocampus cell medium: 10% FCSi, 1% Glutamine, 1% penicillin and streptomycin in DMEM

2.9.5 Escherichia coli (*E. coli*) DH 5α ™ and medium

DH 5α™ competent cells are recommended for routine subcloning into plasmid vectors (Invitrogen).

Luria-Bertani-Medium (LB-Medium, from Invitrogen):

10 g/l trypton, 5 g/l yeast extract, 10 g/l NaCl and 100 mg/l ampicillin

Luria-Bertani-Agar (LB-Agar, from Invitrogen):

10 g/l trypton, 5 g/l yeast extract, 10 g/l NaCl, 15 g/l agar and 100 mg/l ampicillin

2.10 Rat animal material

For experimental procedures adult Sprague-Dawley albino rats (*Rattus norwegicus*) weighing 180 - 220 g were used and obtained from Charles River Laboratories or from the own breed. Animals were maintained in a temperature-controlled room (about 20°C), 50 - 55% humidity on a 12 h light and 12 h dark cycle in Makrolon® Type IV cages. Rats were given a normal laboratory animal diet (sniff M-Z, sniff Versuchstierdiäten GmbH, Germany) and supplied with drinking water *ad libitum*. Any experiment with animals was approved by the local authorities (Regierungspräsidium Tübingen) and regarding matters which under the Federal Constitution Act are implemented.

2.11 Oligonucleotide

Oligonucleotides were ordered from the company ThermoFischer (Ulm, Germany), delivered as lyophilized pellets and dissolved in distilled water to a final concentration of 100 pmol/µl.

2.11.1 Cloning primer for LINA and LINA variants

All LINA variants were tagged with either HA peptide (human influenza hemagglutinin) or FLAG at the carboxyl terminus. All primers used for cloning were listed below;

LINA:
Forward: 5´-CATTGATGCACCCATTCCAGTGGTGTAA-3´
Reverse: 5´- GCAAGGAGCGCTTACACCAATTCAT-3´

LINA with Eco*R* I & Xho I site:
Forward with Eco*R*I site: 5´- GTCAAATTGAATTCCCTTGACTCCACTCCT CC-3´
Reverse with Xho I site: 5´-GTTATATTCTCGAGGCAAGGAGCGCTTACA CC-3´

LINA-HA-tag:
Forward with Eco*R*I site: 5´- GTCAAATTGAATTCCCTTGACTCCACTCCT CC-3´
Reverse with Xho I site: 5´-ATATTCTCGAGTTAAGCATAATCTGGAACA TCATATGGATACATCACCAATTCATCCAGCAGGAT-3´

$LINA^{C93A}$:
Forward: 5´- GCTCTATGGGCAGACCGCTGCAGTTTGTCTGG-3´
Reverse: 5´-CCAGACAAACTGCAGCGGTCTGCCCATAGAGC-3´

N-terminal HA-tag-LINA with Eco*R* I site:
Forward with HA-tag and EcoRI site: 5´-GCATTGAATTCATGTATCCATATGATG TTCCAGATTATGCTTTGATGCACCCATTCCAGTGGTGTAACGGGT-3´
Reverse with Xho I site: 5´-GTTATATTCTCGAGGCAAGGAGCGCTTACA CC-3´

$LINA^{36-155}$-HA-tag:
Forward: 5´-GCCTTTGAATTCATGAACATCTACATGGTCATC-3´
Reverse: same reverse primer like LINA-HA

LINA$^{60-155}$-HA-tag:
Forward: 5´-GCCAATGAATTCATGATCAGCAAACTCCGGAAC-3´
Reverse: same reverse primer like LINA-HA

LINA^{IgK}-HA-tag:
Forward: 5´-GCCTTTGAATTCATGAACATCTACATGGTCATC-3´
Igk forward: 5´-ATGGAGACAGACACACTCCTGCTATGGGTACTGCTGCTCTG GGTTCCAGGTTCCACTGGTGACGCAGAATTCCGACATGACTCAGGA-3´
Reverse: same reverse primer as LINA-HA

LINA-FLAG-tag:
Forward: same forward primer as LINA-HA
LINA w/o stop codon with Xho I restriction site reverse: 5´-TTTGTCCTCGAGCAC CAATTCATCCAGCAG-3´

LINA$^{1-133}$ HA-tag with Xho I site:
Forward: same forward primer like LINA-HA
Reverse: 5´-ATATTCTCGAGTTAAGCATAATCTGGAACATCATATGGATCATG CACATGGGGCAGACGCAACGCAC-3´

LINA^{N20Q}:
Forward: 5´- GGGGCTGGTGAGTACCCAAAAGTCCTGCTCAATGCC-3´
Reverse: 5´-GGCATTGAGGACTTTTGGGTACTCACCAGCCCC-3´

LINA$^{70-155}$-FLAG-tag:
Forward with Eco*R* I site: 5´- GCCAATGAATTCATGGAGCGATACGGC TA-3´
LINA w/o stop codon with Xho I cutting site reverse

LINA$^{80-155}$-FLAG-tag:
Forward with Eco*R* I site: 5´- GCCAATGAATTCATGAAAGGTGATGCT AA-3´
LINA w/o stop codon with Xho I restriction site reverse

LINA$^{w/o\ 80-92aa}$-FLAG-tag:
A: Eco*R* I LINA forward
B: Reverse: 5´- CAGACAAACTGCACAAAGCACCACCTCCTT-3´

C: Forward: 5´-AAGGAGGTGGTGCTTTGTGCAGTTTGTCTG-3´

D: LINA w/o Stop codon with Xho I restriction site reverse

LINA$^{w/o\ RF}$-FLAG-tag:

A: Eco*R* I LINA forward

B: Reverse: 5´- GCAATGGGCTTGTTGGTCTGCCCATAGA-3´

C: Forward: 5´-TCTATGGGCAGACCAACAAGCCCATTGC-3´

D: LINA w/o stop codon with Xho I restriction site as reverse.

LINA-GFP fusion construct:

Forward with Sac II restriction site: 5´- GTTAAACCGCGGCCGGGCGGA TCCGAATT-3´

Reverse with Sma I restriction site: 5´- GCATACCCGGGCACCAATTCATCCAG-3´

LINA-RFP fusion construct:

Forward with *Kpn* 1 restriction site: 5´-GCCAATGGTACCATGCACCCA TTCCAGT-3´

Reverse with Xho I restriction site without stop codon.

3 Experimental Methods

3.1 Cell culture

3.1.1 Cell freezing and defreezing

The cells were frozen and kept in liquid nitrogen for a long time storage. Cells were first harvested with trypsin and then trypsin was inactivated by adding the medium. The cell pellet was obtained by the centrifugation at 900 x g, 5 min, at room temperature (RT). The cell pellet was finally resuspended with 40% FCS, 10% DMSO in DMEM and stored at -80°C in an ethanol containing cryobox for slow cooling for 1 day and then finally stored in liquid nitrogen.

For defreezing, the frozen cells were taken from liquid nitrogen and quickly melted in a water bath at 37°C and cultured in fresh cell medium. The medium was changed the next day to remove DMSO.

3.1.2 PDL and laminin coating

For PC12 cells, RGCs, Hippocampus cell cultures, the culture plates were first coated with PDL (poly-D-Lysine). The plates were coated with 250 µl PDL (1 µg/µl) and incubated at RT for 1 hour (h) and finally washed with dH_2O three times each 10 min and air dried. For RGCs cultures, the PDL coated plates were further coated with laminin. 20 µl laminin (1 mg/ml) was diluted with 1 ml HBSS. 250 µl from this laminin-HBSS mix was added to each well (4-well plate) and incubated at least 1 h at 37°C.

3.1.3 Transfection of PC12 cells

For DNA transfection in PC12 cells, Lipofectamine™ 2000 (Invitrogen) was used according the manufacturer´s protocol. Briefly, 2 µl lipofectamine were diluted in 50 µl DMEM (per 1 well in 4-well plate) and incubated at RT for 5 min. During this time, 800 ng DNA were diluted in 50 µl DMEM (per 1 well in 4-well plate). These two dilutions were next combined and incubated at RT for further 20 min. The medium of cells was changed into 500 µl DMEM and finally the incubated mixture of DNA and lipofectamine was added to each well and the cells were incubated with this mixture for 4 - 6 h. Medium was then changed by addition of NGF (end concentration 100 ng/ml).

3.1.4 Transfection of HEK293 cells by calcium phosphate method

The principle of calcium phosphate transfection is based on slow mixing of HEPES-buffered saline containing sodium phosphate and a $CaCl_2$ solution containing the DNA. A DNA–calcium phosphate co-precipitate forms which adheres to the cell surface and can be taken up by the cell, presumably by endocytosis (Jordan M and Wurm F, 2004)

3.1.4.1 Material required for 10 cm petri-dish

560 µl 2 x HBS: 280 mM NaCl, 50 mM HEPES, 1.5 mM Na_2HPO_4, 10 mM KCl, 12mM dextrose, pH 6.99 - 7.05, sterile filtered

DNA/Calcium mix: 50 µl 10 x TE buffer, pH 7.5 sterile filtered, 15 µg DNA, 60 µl 2.5 M $CaCl_2$, sterile filtered, rest volume with dH_2O to total 560 µl volume

3.1.4.2 Procedure

First, the DNA/Calcium mix was prepared as above and mixed gently. The DNA/Calcium mix was then combined in the 2 x HBS drop by drop and finally incubated in water bath at 37℃ for 10 min. This transfection mixture was finally added to each cell plate and incubated and the medium was changed after 12 - 16 h.

3.1.5 Dissociated RGCs cell culture

Rats were killed with 14% chloral hydrate (i.p.) and their eyes were removed. Retinas were ophthalmologically screened to exclude ischemia. Then retinas were rapidly dissected free from connective tissue and dissociated enzymatically to obtain a suspension of cells. Each retina was incubated at 37℃ for 30 min in DMEM, L-cysteine (1:1000, 0.3 mg/ml, Sigma), papain (10 U/ml). The tissue was washed twice with 5 ml DMEM and mechanically dissociated in 5 ml of DMEM containing 1:50 B27 supplement and 1:50 Penicillin/Streptomycin by triturating with pipettes. The cell suspension was sorted using a cell strainer. 500 µl of cell suspension was plated on each multiwell (4-well plates, Nunc). Plates were precoated with PDL followed by 20 µg/ml laminin.

3.1.6 Hippocampal cell culture

Embryonic rat hippocampuses were provided from the Institute of Anatomy and Cell Biology at Ulm University. The procedure of rat hippocampal cell culture is as follows; rat hippocampal cells were obtained from 18 - 20 day-old embryos (E18 - E20). The hippocampus was dissected away from the rat embryos and the col-

lected tissues were washed with 10 ml Ca^{2+}- and Mg^{2+}-free Hank's balanced salt solution (HBSS, Gibco) three times on ice and incubated in 0.25% trypsin in HBSS for 20 min at 37°C (1800 µl HBSS + 200 µl 2.5% trypsin solution). After trypsination the tissues were rinsed in a 5 ml HBSS five times for 5 min and moved to a new tube containing DNase I (end concentration 0.01%). Then, the tissue was mechanically dissociated ten times with pipettes to obtain single cells. The cell suspension was sorted using a cell strainer and 18 ml DMEM was added. The cells were counted with a Neubauer-Kammer and 50,000 cells were prepared per well. The DMEM was changed with hippocampus culture medium after 24 h.

3.1.7 Myelin isolation and preparation

3.1.7.1 Isolation of crude myelin

Rats were decapitated and the entire brain was removed and weighed. The brain was homogenized on ice with a Dounce homogenizer in 20 volume (w/v) of 0.32 M sucrose, using 5 strokes of the loose pestle and 5 strokes of the tight pestle. The homogenate was layered over 8 ml of 0.85 M sucrose and centrifuged at 75,000 x g for 30 min. The layer of crude myelin which formed at the interface of the two sucrose solutions was collected with a Pasteur pipette. This crude myelin layer was resuspened in water and brought to a final volume of 60 ml. This suspension was centrifuged at 75,000 x g for 15 min. The supernatant fluid was discarded. The crude myelin pellets were again dispersed in a total volume of 60 ml of water and centrifuged at 12,000 x g for 10 min. The loosely packed pellets were again dispersed in water and centrifuged at 12,000 x g for 10 min. The myelin pellets were next suspended in 30 ml of 0.32 M sucrose. This suspension was layered over 0.85 M sucrose and centrifuged at 75,000 x g for 30 min. The purified myelin was removed from the interface with a Pasteur pipette and aliquoted and stored at -80°C.

3.1.7.2 Preparation of myelin and coating the plates

1/10 volume of 10 x PBS and 60 mM ß-octyl glucoside (Sigma) was added to the myelin and incubated with rotation for 2 h at RT. The myelin was centrifuged at 14,000 x g for 10 min and diluted with water 1:50. The 4 well plate chamber cell plates were at first incubated shortly with nitrocellulose-methanol solution and sucked out instantly and air dried. After that, the plates were incubated with PDL or PLL (poly-L-Lysine) for 1 h and washed three times with water and air dried.

Finally the prepared myelin was added on the plates and incubated at 37℃ for 30 min.

3.2 Surgical methods

These surgical procedures were performed by Prof. Dr. Dietmar Fischer.

3.2.1 Optic nerve crush (ONC)

Rats were anaesthetized by intraperitoneal injections of ketamine (60–80 mg/kg body weight) and xylazine (10–15 mg/kg body weight). The head of rats was shaved first and positioned in a stereotaxic apparatus (Kopf Instruments, Tujunga, CA). A 1.0–1.5 cm skin was incised close to the superior orbital rim and the right orbita was opened leaving the supraorbital vein intact. After subtotal resection of the lachrymal gland, the superior extraocular muscles were spread. The optic nerve was surgically exposed under a microscope and the epineurium was longitudinally opened. Then, the optic nerve was crushed 1 mm behind the eye for 10 sec using a jeweller's forceps. Optic nerve crush (ONC) was verified by the appearance of a translucent region at the lesion site.

3.2.2 Lens Injury (LI)

A lens injury (LI) was induced by a retrolenticular approach. The lens capsule was punctured with the tip of a microcapillary tube. A successful LI was verified by an apparent puncture of the lens and a cataract which forms during the following days.

3.3 Molecular biological methods

3.3.1 Cloning of LINA

The cDNA encoding LINA was first amplified by polymerase chain reaction (PCR) using the forward primer: 5´-CATTGATGCACCCATTCCAGTGGTGTAA-3´ and reverse primer: 5´- GCAAGGAGCGCTTACACCAATTCAT-3´. The RNA was isolated from the retinal ganglion cell line using the RNA isolation kit from Qiagen according the manufacturer´s protocol and was used as a template for PCR. For the PCR reaction, 100 ng of template, 10 pmol each primer, 10 mM dNTPs, 50 mM $MgCl_2$, and 2.5 unit *Taq* polymerase were used. The denaturation temperature of PCR was 95℃ for 30 seconds and the annealing temperature of PCR was 55℃ for 30 seconds and the extension was 1 min at 72℃ for 35 PCR cy-

cles. As a negative control, PCR with no template was always included to avoid the contamination.

DNA fragments amplified by PCR were next separated by an agarose gel electrophoresis. 1% agarose gel (w/v) was used to separate the DNA fragments between 0.5 and 10 kb. Gel electrophoresis was done by 80 V for 20 min using TAE (Tris-acetate-EDTA) buffer. After agarose gel electroporation, the amplified DNA fragments were excised from the gel. Using the Gel extraction kit (Qiagen), the amplified DNA was isolated and purified according the manufacturer´s protocol. This purified cDNA of LINA was next cloned to the pCR2.1 vector (Invitrogen) according the manufacturer´s protocol. The cDNA sequence of LINA was then verified by sequencing. The verified cDNA of LINA was next amplified using the primers containing the Eco*R* I and Xho I restriction sites to clone into the expression vector pAAV-IRES-hrGFP (Stratagene) generating pAAV-IRES-hrGFP-LINA^{WT}. Following primers were used; forward primer with Eco*R* I site: 5´-GTCAAATTGAATTCCCTTGACTCCACTCCTCC-3´, and reverse primer with Xho I site: 5´-GTTATATTCTCGAGGCAAGGAGCGCTTACACC-3´. This PCR product and vector were digested with Eco*R* I and Xho I enzymes for 2 h at 37°C. After inactivation of the enzymes at 65°C for 20 min, the digested vector and the cDNA of LINA were ligated for 1 h at RT and finally transformed into *E.coli* DH 5 α. The positive colonies were selected by the ampicilin selection, since the plasmid contained the ampicilin resistant gene. The cloned plasmids from positive colonies were next isolated using MiniPrep Kit (Promega) and finally verified by sequencing.

In order to detect the expression of LINA in cells, either hemagglutinin (HA)-tag or FLAG-tag was added to the C-terminus of LINA. HA-tagged LINA was generated by PCR using the pAAV-IRES-hrGFP-LINA^{WT} as a template with following primers; forward: 5´-GTCAAATTGAATTCCCTTGACTCCACTCCTCC-3´, reverse: 5´-ATATTCTCGAGTTAAGCATAATCTGGAACATCATATGGATACATCACCAATTC ATCCAGCAGGAT-3´. The reverse primer encodes an Xho I site, followed by a HA-tag and an overlap with the C-terminus of LINA to generate the HA-tag at the C-terminus of LINA. This PCR product was digested with Eco*R* I and Xho I and cloned into the pAAV-IRES-hrGFP vector to generate the pAAV-IRES-hrGFP-LINA-HA. The identity of the construct was verified by sequencing.
The FLAG-tagged LINA was generated by PCR using the pAAV-IRES-hrGFP-LINA^{WT} as a template with a forward primer that encoded an Eco*R* I site, followed by an overlap with the N-terminus of LINA and a reverse primer that encoded a Xho I site, followed by an overlap with the C-terminus of LINA without stop codon,

since the pAAV-IRES-hrGFP plasmid contains a FLAG-tag sequence in its own open reading frame. The amplified PCR product was then cloned into the pAAV-IRES-hrGFP plasmid using the Eco*R* I and Xho I restriction sites to generate a pAAV-IRES-hrGFP-LINA-FLAG construct. This new construct was verified by sequencing.

3.3.2 Cloning of LINA-GFP (Green fluorescence protein) and LINA-RFP (Red fluorescence protein) fusion protein

To determine the subcellular localization of the LINA protein, a LINA-GFP and a LINA-RFP fusion constructs were generated. Using a forward primer containing a Sac II site 5´- GTTAAACCGCGGCCGGGCGGATCCGAATT-3´ and a reverse primer containing a Sma I site 5´- GCATAC CCGGGCACCAATTCATCCAG-3´, cDNA encoding LINA was amplified by PCR and finally cloned into the vector pEGFP-N2 (Clontech, CA, USA) using the Sac II and Sma I restriction sites. The identity of the cloned LINA-GFP fusion construct was confirmed by sequencing.

In order to construct a LINA-RFP fusion protein, cDNA encoding LINA was amplified using a forward primer which contains a *Kpn* I restriction site as follows: 5´-GCCAATGGTACCATGCACCCATTCCAGT-3´. As a reverse primer, the primer containing an Xho I restriction site without stop codon was used. The amplified cDNA was then digested with the restriction enzymes *Kpn* I and Xho I and cloned into the vector pcDNA3-RBP2N-mcherry (provided by Dr. Franz Oswald, Institute of Internal Medicine 1 at Ulm University). This new construct was verified by sequencing.

3.3.3 Phenol/Chloroform DNA purification

The isolated plasmid DNA was further purified by the phenol/chloroform method. The same volume of Phenol/Chloroform was added to the DNA solution and well mixed. The mixture was separated with centrifugation at 13,000 x g for 10 min into two phases, the DNA containing water phase and the protein containing phenol phase. The DNA containing water phase supernatant was carefully collected in a new tube. 10% 3 M NaAc (v/v) and 2.5 fold pure ethanol (v/v) were then added. The DNA solution was stored at -20°C for 1 h to precipitate and finally centrifuged at 13,000 x g for 20 min, 4°C. The DNA pellet was finally washed with 70% ethanol and dried. The dried DNA pellet was resolved with dH_2O and the concentration and purity were measured with a photometer.

3.3.4 Site-directed Mutagenesis

In order to generate a point mutation, the QuickChange II site-directed mutagenesis kit (Stratagene) was used according the manufacturer´s protocol. Briefly, the QuickChange II site-directed mutagenesis method was performed using *PfuUltra*TM high-fidelity (HF) DNA polymerase for the highest fidelity (Stratagene). Primers, each complementary to opposite strands of the vector, contained the desired mutation and bound to the double-stranded DNA vector which contained the insert of interest (Stratagene). During the PCR, the *Pfu Ultra* HF DNA polymerase amplified a mutated plasmid by extension of the primers and generated a mutated plasmid containing staggered nicks. After PCR, the product was treated with *Dpn* I to digest the parental DNA template and to select for mutation containing synthesized DNA. The nicked vector DNA containing the desired mutations was then transformed into XL1-Blue supercompetent cells for the selection. Two LINA variants, $LINA^{C93A}$ and $LINA^{N20Q}$ were generated using the site-directed mutagenesis. For the $LINA^{C93A}$, the following primers were used: forward: 5´-GCTCTATGGGCAGACCGCTGCAGTTTGTCTGG-3´, reverse: 5´-CCAGACAAACTGCAGCGGTCTGCCCATAGAGC-3´. These primers contained the point mutation at the 93th amino acid cysteine (C) to alanine (A) by substituting the two original bases TG with GC of the LINA cDNA. For the $LINA^{N20Q}$, forward primer: 5´-GGGGCTGGTGAGTACCCAAAAGTCCTGCTCAATGCC-3´, and reverse primer: 5´-GGCATTGAGGACTTTTGGGTACTCACCAGCCCC-3´ were used. These primers contained a point mutation at the 20th amino acid asparagine (N) to glutamine (Q) by substituting three original bases AAC with CAA of the LINA cDNA. The pAAV-IRES-hrGFP-$LINA^{WT}$ was used as a template. After the amplification with PCR, the parental DNA template vectors were digested with *Dpn* I endonuclease and the nicked vectors containing the mutations were then transformed into XL-1 Blue supercompetent cells. The point mutation in the new constructs was then verified by sequencing.

3.3.5 *In vitro* Mutagenesis by Overlap Extension and Splicing PCR

Two LINA depleted mutants, $LINA^{w/o\ 80\text{-}92aa\text{-}Flag}$ (LINA without 80-92 amino acids) and $LINA^{w/o\ RF\text{-}Flag}$ (LINA without RING-finger domain) were generated by using the *in vitro* Mutagenesis by an overlap extension and splicing PCR strategy. The principle of this method is shown in the following Figure 3-1.

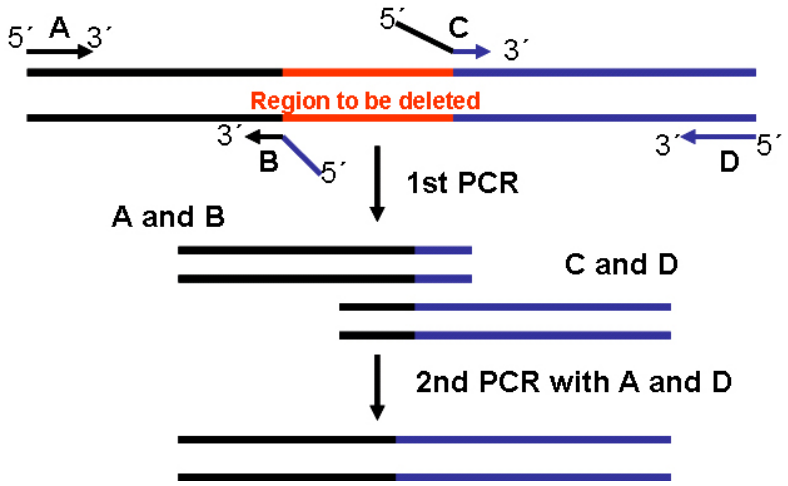

Figure 3-1: Principle of *in vitro* mutagenesis by overlap extension and splicing PCR (modified from Lottspeich et al. (1998))

Two primers (B and C in Figure 3-1) were designed so that their 3´-regions correspond to the sequence adjacent to the deletion end point and their 5´-regions contained the sequence complementary to the other primer sequence. Two DNA fragments were amplified by 1st PCR using the combination of either primer A and B, or C and D. These amplified fragments were then purified using the gel extraction kit (Qiagen) to remove the original primers. The ends of the two DNA fragments were complementary and could work for a 2nd PCR amplification with the two flanking primers A and D. Finally, the 2nd PCR reaction yielded a product lacking the region targeted for deletion.

The construct, pAAV-IRES-hrGFP-LINA^{WT} was used as a template. The primers are shown in the primer lists (2.11.1). The amplified PCR products were then digested by the restriction enzymes Eco*R* I and Xho I and cloned into the expression vector pAAV-IRES-hrGFP to generate pAAV-IRES-hrGFP-LINA$^{w/o\ 80\text{-}92aa}$ and pAAV-IRES-hrGFP-LINA$^{w/o\ RF}$. These new constructs were verified by sequencing analysis.

3.4 Protein biochemical methods

3.4.1 Protein Isolation

The transfected cells overexpressing the protein were collected and centrifuged by 900 x g for 5 min at RT. The supernatant was discarded and the cell pellet was resuspended with lysis buffer (20 mM Tris-HCl, pH 7.5, 10 mM KCl, 250 mM

sucrose, 10 mM NaF, 1 mM DTT, 0.1 mM Na_3VO_4 and 1 mM PMSF and protease inhibitor cocktail, 1% SDS, 0,1% Triton-X100) and incubated on ice for 1 h. The cells were homogenized by ultrasonification for 4 x 3 sec and finally centrifuged at 5000 rpm, 10 min, at 4°C. The supernatant was collected and the cell debris was discarded.

3.4.2 Bradford test

The Bradford test is often used as a quantitative protein asssay. It is based on the binding of coomasie brilliant blue G to a protein sample and this binding results in a stable blue form. This test required a series of standard solutions with a different, known concentration of protein. BSA (Bovine serum albumin) was often used as a standard protein. A standard curve was first achieved using BSA with concentrations of 0, 10, 20, 30, 40, 50, and 100 µg/ml. Protein samples were diluted 1/10 in the same buffer in which they were dissolved. The absorbance of samples was measured at 595 nm twice and the concentration of protein samples was calculated according to the standard curve.

3.4.3 Western Blot Analysis

After determining their concentrations by a Bradford test (3.4.2), protein samples were diluted with same volume of 2 x sample buffer (Laemmli buffer). This sample buffer contained sodium dodecyl sulphate (SDS) as a detergent, bromophenol blue for visualizing the sample in the gel, glycerol for the densitiy of the sample, ß-mercaptoethanol for breaking up disulfide bonds and tris-glycine buffer at pH 6.8. The protein samples were denaturated by boiling at 95°C for 5 min and finally cooled on the ice for SDS polyacrylamide gel electrophoresis (SDS-PAGE). The SDS gels were composed of two different gels, stacking gel and running gel which had different pH values and different composition of acrylamid (shown in Table 1). A 1.2 mm thick SDS-PAGE mini gel (Bio-Rad) was run at 100 V constant for the stacking gel and 200 V for the running gel until the bromophenol tracking dye reached the bottom of the running gel. The 10% running gel was used for separating proteins around 20 - 200 kDa and 12% running gel was used for 14 - 70 kDa proteins.

Table 1 : Gel solution mixture per 1 gel

	Stacking gel	Running gel (10%)	Running gel (12%)
H_2O	1500 µl	3125 µl	2342 µl
Acrylamid (30%)	375 µl	2500 µl	2800 µl
Stacking (pH 6.8) /Running (pH 8.8) gel buffer	625 µl	1875 µl	1875 µl
SDS (10%)	25 µl	75 µl	75 µl
TEMED	3.75 µl	12.5 µl	12.5 µl
APS (40%)	7.5 µl	6.25 µl	6.25 µl
Total	2536 µl	7593 µl	7593 µl

Following electrophoresis, the gel was electro-blotted at 50 V for 2 h to transfer the proteins to a nitrocellulose membrane (Amersham). The gel and membrane were sandwiched between two stacks of filter papers that had been pre-wet with transfer buffer. The membrane was placed to the anode, and the gel was placed to the cathode. After blotting, the protein standards (Fermentas) were marked and the membrane was incubated in 5% skimmed milk blocking buffer in TBS-T at RT for 1 h on a shaker to block the unspecific binding of the primary antibody on the membrane. The membrane was then incubated with the diluted primary antibody at 4°C overnight. After washing three times for each 10 min, the secondary antibody diluted in TBS-T was applied and incubated at RT for 2 h. After another step of washing, the location of the secondary antibody was determined by adding enhanced chemiluminescent detection solution (ECL). This system used a horseradish peroxidase (HRP) conjugated secondary antibody that was in conjunction with a chemiluminescent substrate, luminol, and finally generated a signal on film. After detection of protein, the membrane was usually stripped for further analysis, such as detecting the ß-actin to assess the amount of protein used. The membrane was incubated with stripping buffer for 30 min at 50°C twice and then washed with TBS-T for 10 min. The washed membrane was again blocked in 5% skimmed milk buffer for 1 h and incubated further with another antibody for immunodetection. The dilutions of the different primary antibodies and second antibodies were as follows;

Primary antibodies:

Rabbit anti-HA-antibody (Sigma): 1/3000, mouse anti-FLAG-antibody (Sigma): 1/2000, rabbit anti-LINA antibody (Invitrogen): 1/1000, guinea pig-anti-LINA antibody (PINEDA, Berlin): 1/1000, mouse anti-ß-actin-antibody (Sigma): 1/5000

Secondary antibodies:

HRP-goat-anti-rabbit (Amersham): 1/20,000, HRP-goat-anti-mouse (Sigma): 1/80,000, HRP-goat-anti-Guinea pig (Sigma): 1/20,000

3.4.4 Coomasie brilliant blue staining

Visualization of protein bands was carried out by incubating the gel with a staining solution. With Coomasie Blue staining, a protein amount of 50 ng – 500 ng can be detected. First 0.5% coomasie blue G250 in methanol solution was mixed with 0.5% coomasie blue R250 in water solution. Then 10% of acetic acid (v/v) was added to this mixture and filtered. Gels were incubated with this mixed staining solution for 30 min and washed with decolouring solution (13% acetic acid, 25% methanol in water).

3.4.5 Cross Linking

When two or more proteins have a specific interaction or affinity, those interactions can be investigated using cross linking reagent, ethylene glycolbis: succinimidylsuccinate (EGS), which can capture protein-protein complexes by a covalent binding. Cross linking experiment was carried out according the manufacturer´s procotol (PIERCE). Briefly, the protein samples were prepared in reaction buffer (PBS, 0.5% Triton-X100, pH 7.2, protease inhibitor) and then the cross-linker solution, 25 mM EGS solution dissolved in DMSO, was added to the protein sample at a final concentration of 2.5 mM. This reaction mixture was then incubated on ice for 2 h and quenched for 15 min with a quenching solution (1 M Tris, pH 7.5) at a final concentration of 25 mM. The reaction mixture was then further incubated for an additional 15 min and analyzed by western blotting.

3.4.6 Co-immunoprecipitation

Co-IP is often used for the analysis of protein interaction. In principle, it works as follows. An antibody specific for the protein of interest is used and incubated with a protein lysate. The antibody-protein complex is then precipitated using beads which are usually coupled with antibody. If there are any proteins that bind to the

first protein, they can also be precipitated and this co-precipitated protein can be identified by western blot analysis.

The different LINA depleted mutants were transfected in ca. 80% confluent HEK293 cells with $CaCl_2$ transfection and the medium was changed after 12 - 16 h. 24 h after transfection, the cells were harvested with centrifugation in 900 x g for 5 min. Total cell protein was extracted from the cell pellets using the lysis buffer (1 x PBS, 10 mM EDTA, 1% Triton-X-100) with 1/100 protease inhibitor (Calbiochem).
200 µl lysate was incubated with 6 µl anti-HA agarose slurry (10 µg anti-HA antibody) in a spin column (ProFound™ Mammalian HA Tag IP/Co-IP kit, PIERCE) with gentle end-over-end mixing overnight at 4°C. The overnight incubated lysate was washed three times with TBS-T and eluated three times with each 10 µl elution buffer and immediately neutralized by adding 1.5 µl of 1 M Tris, pH 9.5 per 30 µl elution buffer. The eluent was treated with reducing sample buffer and heated at 95°C for 5 min and analyzed further by western blotting.

3.4.7 Membrane fragmentation

HEK 293 cells expressing LINA-HA and different LINA depleted mutants were collected in lysis buffer (20 mM Tris-HCl, pH 7.5, 10 mM KCl, 250 mM sucrose, 10 mM NaF, 1 mM DTT, 0.1 mM Na_3VO_4, 1 mM PMSF and protease inhibitor cocktail). The cells were broken by repeated passage through a 21-G needle. The intact cells and nuclei were removed by the centrifugation at 500 x g for 10 min and sucrose was added to final concentration of 2 M sucrose. This was overlaid with 1.7 M and 0.8 M sucrose in 20 mM Tris-HCl (pH 7.5) and centrifuged for 20 h at 130,000 x g, 10°C. The 1.7/0.8 M interface membrane peak was collected and diluted two fold with 20 mM Tris-HCl. Finally membranous fractions were pelleted at 150,000 x g for 30 min. Proteins from the soluble 2 M fraction were diluted two-fold with 20 mM Tris-HCl and precipitated with 10% trichloroacetic acid on the ice for 60 min. These membranous fraction and cytosolic fraction were further analyzed by western blotting.

3.4.8 GST-fusion protein

First, the cDNA encoding amino acids 60-155 of LINA was cloned into the glutathione S-transferase (GST) encoding bacteria expression vector pGEX-4T-1 using the restriction sites Eco*R* I and Xho I to generate GST-LINA$^{60\text{-}155}$. The construct was verified by sequencing. This GST-LINA$^{60\text{-}155}$ construct was next transformed into the *E.coli* BL-21(DE3) to express the GST fusion protein.

3.4.8.1 Induction of GST- fusion protein

200 µl bacterial preculture was grown in 6 ml LB medium with ampicillin for about 2 h at 37°C. The density was measured in OD_{600}. When the OD reached a value between 0.4 and 0.5, the bacterial preculture was divided into two 3 ml cultures. One culture was further grown without addition of isopropyl ß-D-thiogalactoside (IPTG), and the other was grown with addition of 1 M IPTG to the final concentration of 1 mM and the protein production was stimulated at 37°C. After 30 min, 1 h, 2 h, 3 h, 4 h and 5 h, 100 µl probes from each culture were collected and centrifuged. The bacterial pellet was lysed in probe buffer with DNase and the protein was denaturated at 95°C for 5 min. The proteins from each culture were loaded in 12% SDS gel and finally stained with coomasie blue. The coomasie blue stained gel showed the different pattern of induced GST-fusion protein depending on the different time. I observed the increase of GST-fusion protein from 30 min to 2 h-induction and no difference between 2 and 3, 4 and 5 h-induction. The 2 h-induction after the addition of IPTG was decided to be the optimal induction time. Finally, the 5 ml preculture was added and grown to 300 ml LB medium with ampicillin for a big scale protein expression culture. 1 M IPTG was added in culture to the final concentration of 1 mM and the protein was induced for 2 h. The bacteria were then harvested with centrifugation for 15 min at 4°C, 4500 rpm and the pellet was preserved at -20°C for next purification.

3.4.8.2 GST-fusion protein purification with affinity chromatography

Material: PBS, 10 mg/ml lysozyme (stock) in 10 mM Tris-HCl pH 8.0, DNase I 100 mg/ml in DNase dilution buffer (10 mM Tris-HCl pH 7.5, 150 mM NaCl, 1 mM $MgCl_2$), RNase I 100 mg/ml.

All bacterial pellets were resuspended with 12 ml PBS and the lysozyme was added to a final concentration of 1 mM. The resuspension was incubated on ice for 30 min. After that 10 ml of 0.2% Triton X-100 was added and well mixed. Stock DNase I and RNase I were added with dilution of 1:20,000. 1 M $MgCl_2$ was then added to an end concentration of 1 mM $MgCl_2$. The resuspension solution was incubated at 4°C on a rotator for 20 min. The insoluble debris was removed by centrifugation at 3,000 x g for 30 min at 4°C with SS34 Sorvall Rotor (Beckman). The supernatant was collected in a fresh tube and dithiothreitol (DTT) was added to a final concentration of 1 mM and finally the supernatant was filtered with a 0.45 µm filter. For preparing the glutathione sepharose column, 1 ml of end volume of glutathione-sepharose was washed four times with 10 ml PBS. All steps were done at 4°C. The PBS in glutathione-sepharose resin was carefully

removed and the cell lysate was combined with glutathione-sepharose and incubated at 4°C overnight with rotation. The mixture was loaded on the column and washed with 10 x 2 ml PBS at 4°C. The unbound protein was collected and the absorption was measured at 280 nm to check the quality of the washing step. The decrease of the amount of unbound protein was observed and finally the bound GST fusion protein was eluted from the resin using glutathione elution buffer (30 mM glutathione in 50 mM Tris-HCl pH 8.00). Each fraction was collected with 300 µl elution buffer and the absorbance was measured at 280 nm with a photometer.

3.4.9 Affinity Chromatography for purification of anti-LINA Antibody

The column matrix bound with the synthetic peptide sequences (NKPIAGPTETSQS) was equilibrated with PBS first and the rabbit serum was diluted with an equal volume of PBS into 7 ml. The diluted serum was slowly rotated with the peptide-bound matrix overnight at 4°C. The Flow through was collected from the column for further use and the column was washed three times with 10 ml PBS and twice with 10 ml 10 mM Na-phosphate, pH 6.8. The antibody was eluted from the column with 10 fractions each 500 µl of 0.1 M glycin-buffer, pH 2.4. The collected fraction was loaded with 35 µl of 2 M K_2HPO_4. Each fraction was mixed gently and cooled on ice immediately. The purified serum was aliquoted in 100 µl portions and an equal volume of glycerol (ultra pure) and 10% Na-azide solution were added to obtain a final concentration of 0.05% azide and stored at -80°C. For the regeneration and storage of the column for further use, the column was washed once with 10 ml 10 mM Na-phosphate buffer, pH 6.8, then washed twice with 10 ml PBS containing 1 M NaCl and finally twice with 10 ml PBS containing 0.05% sodium azide and kept at 4°C.

3.5 Immunocytochemistry and Immunohistochemistry

3.5.1 Immunocytochemistry

The cells were fixed with 4% paraformaldehyde for 20 min, followed by 100% methanol for 10 min for permeabilization. Cells were then incubated with 2% BSA in TBS-T solution for 30 min for blocking the unspecific binding of antibody. After blocking, the cells were incubated with different first antibodies (rabbit anti-HA antibody; dilution 1/700, mouse anti-TGN38 antibody; dilution 1/50, purified rabbit anti-LINA antibody; dilution 1/100) in 2% BSA in TBS-T solution at 4°C overnight. Next day, the cells were washed with PBS three times for 10 min and incubated

with different secondary antibodies including anti-rabbit IgG conjugated to Alexa Fluor® 594 (1:1000, molecular probes), anti-mouse IgG conjugated to Alexa Fluor® 488 (1:1000, molecular probes). The nuclei were stained with 4',6-diamidino-2-phenylindol (DAPI). DAPI was diluted in water 1/100,000 and incubated for 1 min for staining. The staining was analyzed under a fluorescent microscope (Zeiss, Göttingen).

3.5.2 Immunohistochemistry

Animals were anesthetized and perfused through the heart with PBS, followed by 4% paraformaldehyde. Eyes and brain were dissected and then postfixed overnight, transferred to 30% sucrose overnight (4℃), and embedded with tissue-tek. Frozen sections were cut on a cryostat, thaw-mounted onto coated glass slides (Superfrost Plus) and stored at -80℃ until additional use. The staining procedure is same as immunocytochemistry. As primary antibody, I used affinity chromatography- purified rabbit anti-LINA antibody at a dilution of 1:50. To visualize RGCs in retina and neuronal cells in brain, I used the monoclonal mouse ßIII-tubulin antibody at a dilution of 1:1000. Secondary antibodies included an anti-rabbit IgG conjugated to Alexa Fluor® 594 (1:1000, molecular probes) and anti-mouse IgG conjugated to Alexa Fluor® 488 (1:1000, molecular probes). The nuclei were stained with DAPI and the sections covered using mowiol and analyzed under a fluorescent microscope.

3.5.3 Haematoxylin and eosin staining (HE staining)

The tissue sections were put into water first and then placed in haematoxylin solution for 5 min. After incubation, the tissue sections were washed in tap water and placed then in 1% acid alcohol for a few seconds. After washing again in tap water, the sections were placed in eosin solution for 5 min and washed in tap water later on. After dehydration, the sections were covered using mowiol and analyzed further under a microscope.

3.6 Whole Mount *In situ* Hybridization on post-implantation mouse embryos

In situ Hybridization (ISH) is a powerful method used for detection of specific mRNA sequences in a whole mount or sections. It is based on the ability of a synthetic tagged RNA probe to hybridize the complementary strand of the mRNA of interest present in the tissue or cells (Roche). The sensitivity of the technique is sufficient to detect 10 to 20 copies of mRNA per cell.

3.6.1 RNA probes

The RNA probes are in vitro synthesized oligonucleotides complementary to the specific mRNA sequence of interest. The size of the probes varies between 20-40 base pairs and 1000 bp. In order to generate the RNA probes, I have cloned the complete LINA cDNA sequence into a pCS2+ vector between E*coR* I and Xho I restriction sites. In pCS2+ vector the LINA sequence was flanked by T7 promoter in the 3' position and Sp6 promoter in the 5' position. To synthesize the sense probe, the LINA plasmid was linearized with Not I which cuts at 346th site and to synthesize the antisense probe, the LINA plasmid was digested with Hind III which cuts at 28th site. The linearization was verified then by electrophoresis on an agarose gel and the linearized plasmid subsequently purified using the Qiagen purification kit. For both sense and anti-sense probe synthesis, 1µg of linearized plasmids was transcribed in vitro using the digoxigenin (DIG) RNA-labeling kit (Roche) and 20 units of Sp6 and T7 RNA polymerase respectively. DIG is a steroid isolated from the digitalis plant (Roche) and the DIG labeled probe can be detected with antibodies conjugated to alkaline phosphatase, which results in a blue precipitate when the enzyme is incubated in the presence of the substrate NBT/BCIP (Nitro-Blue Tetrazolium Chloride/5-bromo- 4-chloro- 3 idolyl-phosphate) (Roche). The entire transcription reaction took place in the presence of RNAse inhibitors, for 2 h at 37°C. Size and integrity of the DIG-labeled RNA probes were checked on an agarose gel. After purification on a G50 column (Qiagen), the DIG-labelled probes were brought to a final volume of 100 µl using freshly prepared pre-hybridization buffer. In order to have a high specificity and sensitivity in ISH, temperature of hybridization, formamide concentration, salt concentrations and pH can be varied. In my *in situ* experiments, I have used high stringency conditions, which means high hybridization temperatures (68°C), high formamide concentrations (50%) and low salt concentrations in both the hybridization solutions and post-hybridization washes.

3.6.2 Materials for hybridization

Pre-hybridization buffer for 5 ml: 2.5 ml demineralized formamide, 1.25 ml 20% SSC, 0.25 ml 20% SDS, 1 ml DEPC- H_2O, 25 µl Heparin

Solution post-hybridization wash 1 for 5 ml: 2.5 ml demineralized formamide, 1.25 ml 20% SSC, 0.25 ml 20% SDS, 1 ml DEPC- H_2O

Solution post-hybridization wash 2 for 5 ml: 2.5 ml demineralized formamide, 0.5 ml 20% SSC, 2 ml DEPC- H_2O

NTMT: 100 mM NaCl, 100 mM Tris, pH 9.5, 50 mM $MgCl_2$, 0.1% Tween

NBT stock solution: 75 mg/ml in 70% dimethylformamid

BCIP: 50 mg/ml in dimethylformamid

Heparin stock: 25 mg/ml

NTMT with Levamisole: 2 mM Levamisole in NTMT

0.1 M Glycine-HCl pH 2.2, 0.1 M Tris-HCl, pH 8.2

Sheep serum: inactivated for 1 h at 70°C, centrifuged at 4000 rpm, 4°C

Embryo powder: 12 - 14 day old embryos were homogenized in ice cold PBS-T with four times the amount of ice cold aceton and mixed well for 30 min on the ice. Finally the homogenized embryos were centrifuged for 10 min, at 1000 rpm and the pellet was collected and air-dried on the filter paper and kept at 4°C.

Blocking solution: 500 µl TBS-T was added to 3 mg embryo powder and incubated for 30 min at 68°C. The solution was then shortly kept on the ice for cooling, 5 µl sheep serum and 1 µl anti-digoxigenin antibody were added and incubated for 1 h at 4°C with rotation. Finally the solution was centrifuged for 10 min at 4000 rpm, 4°C.

3.6.3 Mouse whole mount *in situ* Hybridization

E9.25 mouse embryos and chemicals were provided by Dr. Ioan Ovidiu Sirbu from the Institute of Biochemistry and Molecular Biology at Ulm University and this ISH experiment was done by the collaboration with the institute of Biochemistry and Molecular Biology at Ulm University. Wild type mice were mated over night and the mating plugs were checked every morning. The day of the plug was considered day 0.5 post coitum (0.5 dpc). The pregnant females were killed by cervical dislocation in the morning of day 9 (9.25 dpc) and the embryos dissected in cold DEPC-treated PBS (pH 7.4) and further fixed overnight in PFA 4% in PBS at 4°C. Embryos were then dehydrated gradually using 25%, 50% and 75% methanol/PBS-T for 10 min each and finally kept in 100% methanol at -20°C for further use.

Embryos were taken out from -20°C and rehydrated using first 75% Methanol/PBS-T for 10 min and further 50%, 25% methanol/PBS-T 10 min each and finally washed twice with PBS-T for 10 min. Rehydrated embryos were next bleeched with 6% H_2O_2 in PBS-T for 1 h, which is thought to reduce the background staining due to inactivation of endogenous alkaline phosphatase and

washed again with PBS-T three times each for 10 min. Next the embryos were permeabilized. The permeabilization makes it possible that the probes reach the target within the embryos. Permeabilization was necessary because the probes had to reach deep inside the embryo, over fairly big distances. Three common reagents are commonly used to permeabilize tissues: HCl, detergents (Triton or SDS) and Proteinase K. I have used Proteinase K, an endopeptidase which is non-specific and attacks all peptide bonds. Proteinase K was prepared fresh in PBS-T (10 µg/10 ml) and embryos were treated for different time points depending on the age of the embryos, namely 15 min proteinase K treatment for E10, 10 min for E9.5, 5 min for E8.5. Incubation had to be carefully monitored because if the digestion proceeded too far, it could end up destroying most of the tissue or cell integrity. Proteinase K incubation was stopped exactly at the right time by incubating with glycin/PBS-T solution for 5 min and the embryos were washed twice with PBS-T. After permeabilization, embryos were immediately fixed in 0.2% glutaraldehyde, 4% PFA in PBS-T for 1 h at 4°C and afterwards washed with PBS-T. The fixed embryos were gradually brought into pre-hybridization buffer at RT and then pre-incubated at 68°C in pre-hybridization solution to allow for the unwinding of the RNA targets. After 1 h of pre-hybridization I added 10 µl DIG-labelled RNA probe and then incubated the treated embryos at 68°C overnight. Following hybridization, the embryos were washed to remove unbound probe or probe which has loosely bound to imperfectly matched sequences. Washing was carried out initially in stringent conditions similar to the hybridization ones and only the final washes was done in low stringency solutions. The embryos were thus incubated in pre-warmed pre-hybridization buffer for 30 min at 68°C and then washed three times for 30 min with post-hybridization solution 1 and 2, again at 68°C. Afterwards, the embryos were transferred into TBS-T and washed three times for 10 min each and finally blocked with 10% sheep serum in TBS-T for 1 h at RT. Before incubating with antibody, the neural tube of the embryos was opened to avoid the trapping of antibodies. Embryos were then incubated with anti-DIG AP-coupled antibody in 33% embryo blocking solution and 1% sheep serum in TBS-T, overnight at 4°C. The next day, the embryos were washed in TBS-T (3 x 10 min then 6 x 1 h) at RT. This extensive washing was critical for reducing the staining background. It depended on the size of the embryos and could last up to three days. When washing was considered satisfactory, the embryos were transferred to and equilibrated (3 x 10 min) in NTMT+2 mM Levamisole. The NTMT provides the right cofactors (Mg^{2+}; NaCl) and the right pH (9.5) for the optimum activity of alkaline phosphatase, while Levamisole is used

to block residual endogenous alkaline phosphatase and thus to reduce the background staining (Roche). The staining *per se* was initiated by adding 4 µl NBT, and 4 µl BCIP with further incubation of the embryos in the dark at RT. The progression of staining was checked every hour to avoid developing of the background. When estimated as properly developed, the staining was stopped by washing once with NTMT then with PBS-T pH 5.5 and the embryos were stored in PBS-T pH 5.5 at 4°C.

4 Results

4.1 Cloning and sequence analysis of LINA

It was recently shown that the regenerative switch of RGCs to a regenerative state, caused by optic nerve crush (ONC) or lens injury (LI), is associated with a change in gene expression (Fischer et al., 2004b). Less than one hundred from 16,000 genes show significant gene expression changes between regenerating and axotomized RGCs. Among those were i) known genes like gap 43, galanin, sprr1a which have been described previously to be associated with successful axonal regeneration in the peripheral nervous system, ii) characterized genes which so far have not been linked to axonal regeneration and iii) expressed sequence tags (ESTs) representing uncharacterized proteins so far not linked to axonal regeneration. In our lab we focused on genes that showed a similar gene expression pattern as typical genes associated with axonal regeneration, such as gap43 and sprr1a. Among these genes showing this expression pattern was an EST, which revealed a similarity to a so far uncharacterized mouse gene with the technical name [redacted](probe set ID: 1373485_at, Chip RAE230A). This gene showed a 1.9 fold increase after ONC and a 3.6 fold increase after additional LI compared with untreated controls (Table 2, Lee et al., 2006).

Table 2: Some of the gene expression changes between regenerating and axotomized RGCs on the microarrays (ONC: optic nerve crush, LI: lens injury, gap43: growth associated protein 43, sprr1a: small proline rich protein 1a). The numbers show the increase ratios of gene expression of each gene after ONC, ONC combined with LI (Lee et al., 2006).

	ONC	ONC + LI
gap43	1.6	2.3
sprr1a	3.7	10.0
Galanin	2.9	8.2
EST (LINA)	1.9	3.6

Using RT-PCR, the cDNA including the putative coding sequence of rat was generated and sequenced by Prof. Dr. Dietmar Fischer in our lab and additionally I generated and sequenced human [redacted] Rat [redacted] was named „**l**ens **i**njury induced factor with **n**eurite outgrowth promoting **a**ctivity" (LINA) in our lab. It consisted of 155 amino acids. Amino acid sequences of LINA and mouse [redacted] were identical and human [redacted] differed in five amino acids at the C-terminus of the protein (Figure 4-1).

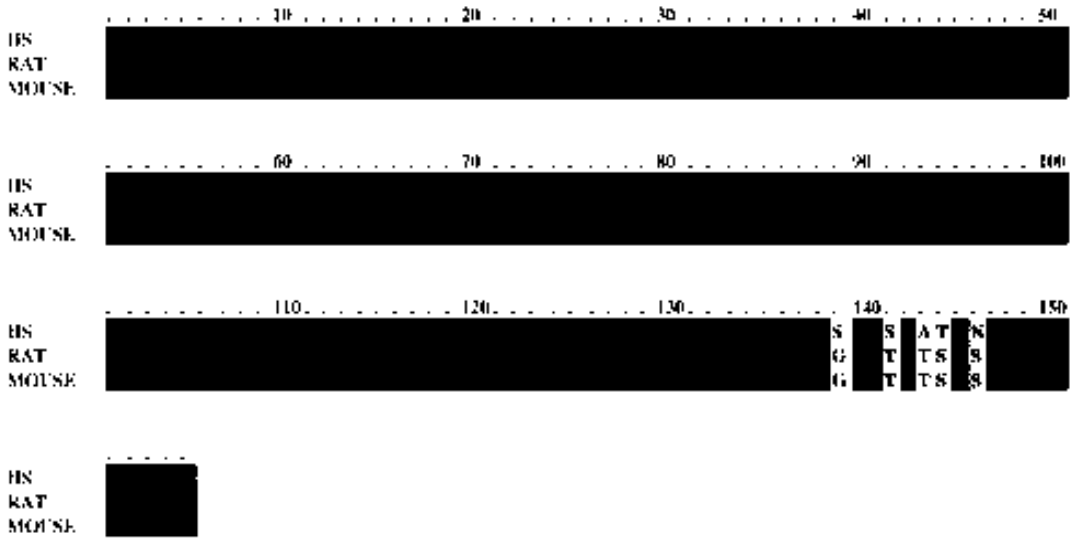

Figure 4-1: The alignment of the human, rat and mouse LINA proteins with PRALINE multiple alignment program

Amino acid sequence of rat LINA was screened and compared with human and mouse using the multiple sequence alignment program, PRALINE (http://zeus.cs.vu.nl/programs/pralinewww/). HS: Homo Sapiens.

On the RNA level LINA and mouse [redacted] showed a homology of 95.7% within the coding sequence. The RNA sequence homology between LINA and human [redacted] was 89.7% (Figure 4-2).

Figure 4-2: The alignment of the human, rat and mouse LINA RNA sequence with CLUSTAL W multiple sequence alignment program.

The RNA sequence of LINA was screened and compared with human and mouse using the multiple sequence alignment program, CLUSTAL W. HS: Homo Sapiens.

My sequence analysis indicated that LINA is a highly conserved protein. NCBI data bases (http://www.pubmed.de/data/nlm.link.html) predicted that the LINA/[redacted]gene consists of 6 exons, which are all located in the chromosome 8p12 region of the rat, mouse and human genome. In order to identify functional domains, I used the bioinformatic sequence analysis tool Prosite (http://expasy.org/prosite). This program predicted a RING finger domain ($C_3H_2C_3$ type) between amino acids 93 and 133 and a putative transmembrane domain between amino acids 36 and 59. Furthermore the analysis revealed a potential N-glycosylation site located at N20, two protein kinase C phosphorylation sites at T19 and S69, and one casein kinase II phosphorylation site at S29 as illustrated in Figure 4-3.

Figure 4-3: Schematic drawing of the LINA protein with functional domains, potential glycosylation and phosphorylation site as predicted by the analysis tool "PROSITE" in ExPASy (**Ex**pert **P**rotein **A**nalysis **Sy**stem).

TM: Transmembrane domain spanning amino acid residues 36 - 59, RF: RING finger domain spanning amino acid residues 93 - 133, N20: a potential *N*-glycosylation site at asparagine 20. T19, S69: a potential protein kinase C phosphorylation site at threonine 19, serine 69. S29: a potential casein kinase II phosphorylation site at serine 29.

After these genetic and proteomic analysis, I next investigated the functional effect of LINA in PC12 cell system.

4.2 Functional characterization of LINA

4.2.1 LINA promotes NGF-induced neurite outgrowth of PC12 cells

In order to assess a potential role of the LINA in neurite outgrowth, I initially used PC12 cells. PC12 cells differentiate and extend neurites in response to the nerve growth factor (NGF) that was added to the medium. I investigated whether LINA expression affects neurite outgrowth of PC12 cells. First the cDNA of LINA was cloned into a pAAV-IRES-hrGFP expression vector using the Eco*R* I and Xho I restriction sites and this expression vector was overexpressed in PC12 cells by a lipofectamine transfection. Overexpression of LINA itself did not affect neurite outgrowth in PC12 cells. However, when overexpressing cells were exposed to NGF, neurite outgrowth was increased about 2.5 fold compared to controls transfected with an empty control expressing vector after 3 days (Figure 4-4), suggesting that LINA has a neurite outgrowth promoting effect in PC12 cells exposed to NGF.

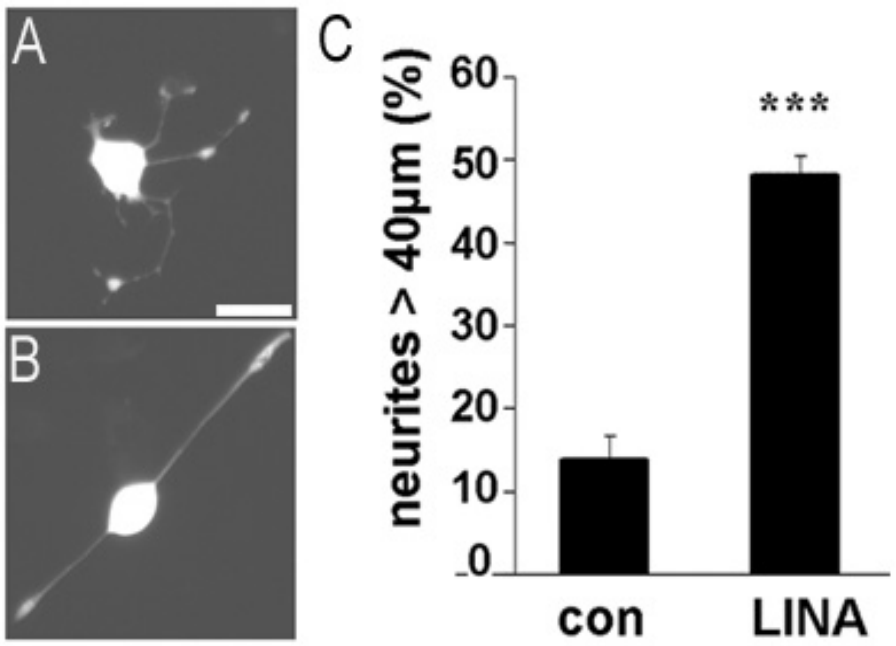

Figure 4-4: LINA promotes neurite outgrowth in PC12 cells with NGF

LINA was overexpressed in PC12 cells with NGF and the neurite outgrowth was measured after 3 days and compared with control groups. LINA overexpressing cells showed 2.5 fold longer neurite outgrowth than control groups (con). A: PC12 cell overexpressing a control empty plasmid, B: PC12 cells overexpressing LINA treated with NGF. C: Diagram shows the percentage of PC12 cells with neurites longer than 40 µm. Student´s t-test, n=4, ***p<0.001, scale bar: 20 µm.

Next, LINA was overexpressed in PC12 cells and cultured on myelin-coated dishes to investigate whether LINA overexpression can overcome the inhibitory effect of myelin. Myelin was isolated from the adult rat brain. After sterilization, myelin was coated on the plate according to protocol (shown in 3.1.7) and PC12 cells were then cultured on the myelin. LINA was next overexpressed in these PC12 cells treated with NGF. The outgrowth of neurites was compared with a control group transfected by an empty vector after 3 days. Generally, PC12 cells cultured on myelin-coated dishes showed a reduced neurite outgrowth compared to those on poly-L-lysine (PLL) because of the inhibitoric effect of myelin proteins. But LINA overexpressing cells exposed to NGF showed the same neurite outgrowth ratio on myelin like before compared to a control group, suggesting that LINA does not desensitize the growth cones towards myelin (Figure 4-5).

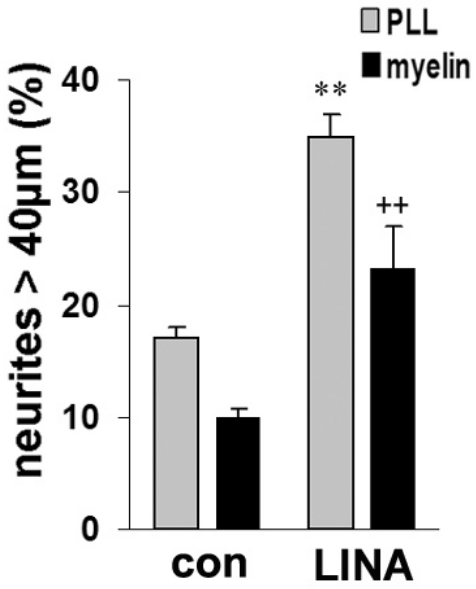

Figure 4-5: LINA does not desensitize the growth cones towards myelin

Neurite outgrowth effect of LINA in PC12 cells cultured on myelin-coated dishes (dark bars) was compared with those on poly-L-lysine (PLL) (light bars). Even on myelin, LINA overexpressing PC12 cells exposed to NGF showed about two fold longer neurite outgrowth compared to a control group (con) on myelin. Diagram shows the percentage of the neurites longer than 40 µm. Student´s t-test, n=4, ++p<0.01, **p<0.01.

4.2.2 LINA^{C93A} abrogates the neurite outgrowth effect of LINA in PC12 cells

The bioinformatic sequence analysis showed that LINA could contain the RING finger domain between 93 and 133 amino acids, which is often related with its functional effects. In order to test whether the RING finger domain of LINA can play a significant role of the functional effect of LINA, I created the RING finger-mutated LINA, called LINA^{C93A}, by substituting the 93th cysteine (C) with alanine (A) using a point mutation (C93A). With this LINA mutant, LINA^{C93A}, I investigated whether a point mutation in the first zinc finger of LINA may influence the neurite outgrowth effect of LINA in PC12 cells. I cloned the cDNA of LINA^{C93A} into a pAAV-IRES-hrGFP expression vector using the Eco*R* I and Xho I restriction sites and finally a control empty expression vector, LINA- and LINA^{C93A} expressing vectors were transfected and overexpressed in PC12 cells exposed to NGF. The longest neurite was measured after 3 days in each group and compared to each other.

The representative phenotypes of each group in PC12 cells are shown in Figure 4-6. The expression of LINA^{C93A} showed a dramatically reduced neurite outgrowth compared with LINA. Introducing this point mutation in the RING finger completely eliminated the neurite outgrowth promoting activity of LINA and thus significantly abrogated NGF induced neurite outgrowth compared to controls transfected with a control plasmid. This result suggested that the neurite outgrowth promoting effect of LINA is dependent on an intact RING finger domain.

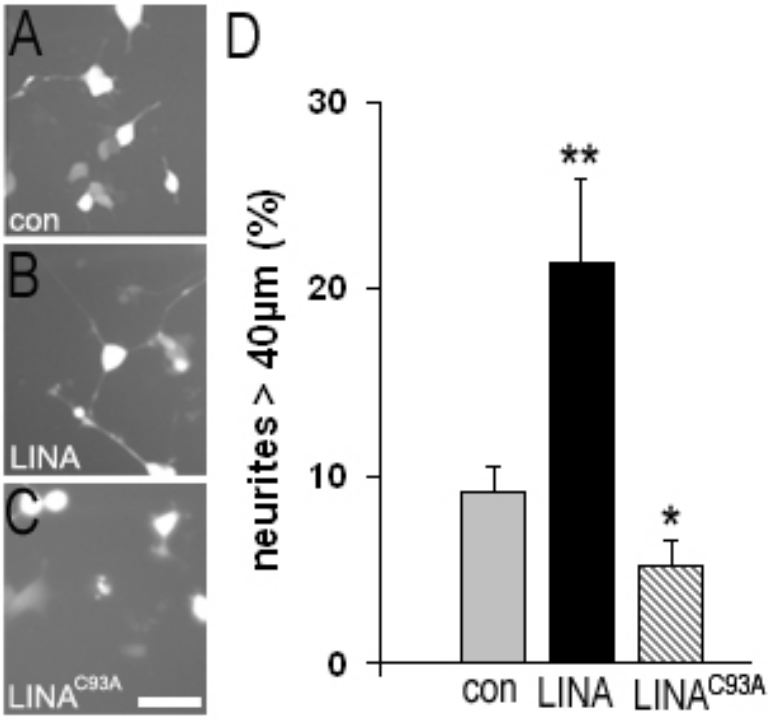

Figure 4-6: Functional phenotype of PC12 cells expressing control (con), LINA and LINA^{C93A}.

LINA and LINA^{C93A} were overexpressed in PC12 cells exposed to NGF including a control. After 3 days, the longest neurite was measured in each group and compared to each other. A: PC12 cells overexpressing a control (con) B: PC12 cells overexpressing LINA C: PC12 cells overexpressing LINA^{C93A} D: The diagram represents the percentage of the number of neurites longer than 25 µm. PC12 cells overexpressing LINA showed 2.5 fold longer neurite outgrowth than the control group and LINA^{C93A} reduced the outgrowth completely. Student´s t-test, n=4, **p<0.01, *p<0.1 scale bar: 20 µm.

In summary, I showed here that LINA has a neurite outgrowth promoting effect in PC12 cells when the cells are exposed to NGF and as a novel RING finger protein, the RING finger domain of LINA plays a significant role for this effect.

4.3 Biochemical characterization of LINA

4.3.1 LINA is a membrane associated protein

After a functional characterization of LINA, I next focused on the characterization of each hypothesized domain of LINA. According to the bioinformatic sequence analysis of LINA, LINA may contain a hydrophobic transmembrane domain between amino acid 36 and 59 (Figure 4-3). In order to verify this character of LINA, I generated a LINA mutant lacking this domain ($LINA^{60-155}$) using the forward primer lacking a hydrophic domain of LINA (2.11.1). As a template, I used the vector pAAV-IRES-hrGFP-LINA to amplify the coding sequence of $LINA^{60-155}$ using the PCR method.

The coding sequence of $LINA^{60-155}$ was cloned into a pAAV-IRES-hrGFP expression vector using the Eco*R* I and Xho I restriction sites. Using the accordant reverse primer containing the HA (hemagglutinin) expression sequence, LINA and $LINA^{60-155}$ were tagged with HA at the C-terminus, which is often used to detect the certain proteins by an anti-HA antibody. Additionally I used the HA-tagged Nogo Receptor (NgR) protein as a control for this experiment. Since the NgR represents a membrane bound protein, it served as a positive control. The NgR expression vector was kindly provided by Prof.Dr. Dietmar Fischer (Fischer et al., 2004a).

In order to yield sufficient amounts of exogenously expressed protein, HEK 293 cells were used for transfection with the expression vectors using the calcium phosphate transfection method (3.1.4). After 1 day of expression, protein lysates of each group were separated into membranous and cytosolic fractions using a sucrose density ultracentrifugation (3.4.7). The proteins of each fraction were evaluated by western blot analysis using an anti-HA antibody to detect the HA-tagged LINA and NgR proteins. As indicated in Figure 4-7, the NgR and LINA proteins were almost exclusively found in membranous fraction and showed only low amounts in the cytosolic fraction. In contrast, the $LINA^{60-155}$ protein was almost completely detected in the cytosolic fraction. These data support the hypothesis that LINA is a membrane bound protein and that the hydrophobic domain between amino acid residues 36 – 59 might represent a transmembrane domain.

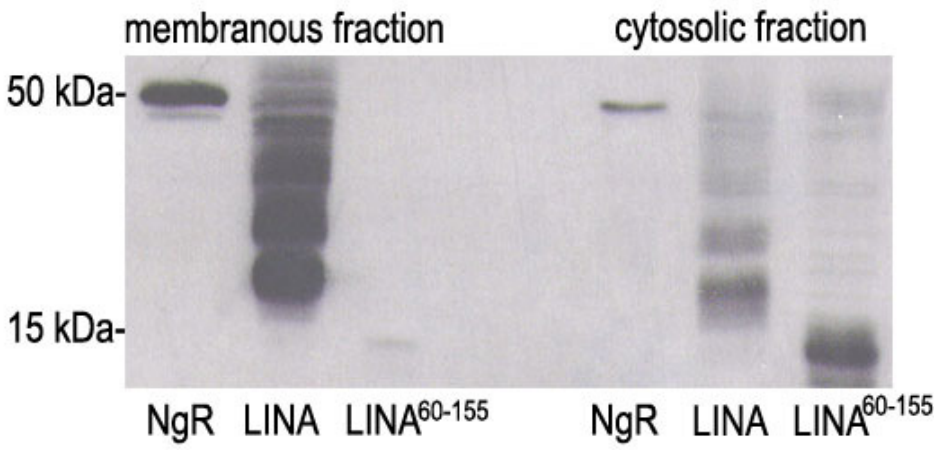

Figure 4-7: Membrane fragmentation of LINA and LINA$^{60-155}$

Nogo Receptor protein (NgR) as a positive control for a membrane bound protein, LINA, and a mutant form of LINA lacking a hydrophobic transmembrane domain (LINA$^{60-155}$) were overexpressed in HEK293 cells to obtain protein lysates. All proteins were HA-tagged at the C-terminus which was then detected by an anti-HA antibody in the western blot analysis. Western blots were repeated at least three times to confirm results.

4.3.2 LINA has a glycosylation site at N20

I observed from the western blot analysis that exogenously expressed HA-tagged-LINA ran in gels as two bands at 19 kDa as a monomer of LINA and at 23 kDa as a posttranslationally modified LINA under denaturating conditions (Figure 4-8, lane 1).

To verify whether this upper band resulted from the posttranslational glycosylation, I incubated first the exogenously expressed HA-tagged-LINA protein with *N*-glycosidase, PNGaseF (Sigma). I observed that incubation with glycosidase eliminated this upper band, verifying that this band resulted from the glycosylation of LINA (Figure 4-8, lane 2).

To test whether this glycosylation occurs at the potential glycosylation site N20 according to the bioinformatics sequence analysis (Figure 4-3), I first introduced a point mutation. The 20th amino acid asparagine (N20) was substituted with glutamine (Q) by using a mutagenesis kit (Strategene). I named this new LINA mutant, LINA^{N20Q}, which contains no more potential *N*-glycosylation site. I cloned the coding sequence of LINA^{N20Q} into a pAAV-IRES-hrGFP expressing vector and added a HA-tag to the C-terminus using the accordant reverse primer for detection by an anti-HA antibody. The point mutation was verified by sequencing. To

measure the effects of the point mutation, I transfected this expression vector containing the cDNA of LINA^{N20Q} into HEK293 cells to yield enough amount of exogenously expressed protein. This protein lysate was evaluated by western blot analysis using an anti-HA antibody.

I observed the elimination of the upper band from LINA^{N20Q} (Figure 4-8, lane 3), verifying that LINA is glycosylated at N20 and that exogenously overexpressed LINA ran as glycosylated and unglycosylated forms in the gel.

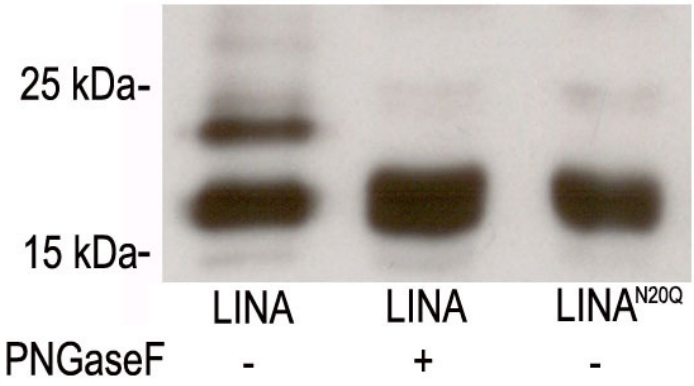

Figure 4-8: *N*-Glycosylation of LINA at N20

HA-tagged LINA was overexpressed in HEK293 cells and evaluated by western blot analysis using an anti-HA antibody. The first lane represents LINA, which is not treated with *N*-glycosidase PNGaseF showing two bands at 19 kDa and 23 kDa. The second lane represents LINA protein treated with *N*-glycosidase PNGaseF showing no upper band. Through the treatment with PNGaseF, the glycosylated form of LINA was eliminated. The third lane represents LINA^{N20Q}, in which the 20th asparagine (N) was substituted with glutamine (Q) by a point mutation. The point mutation abolished the upper band at 23 kDa, meaning that the glycosylation site of LINA was eliminated by a mutation. HA-tag was added to all proteins at the C-terminus and detected by an anti-HA antibody. Western blots were repeated at least three times to confirm results.

The fact that LINA is glycosylated at the N-terminus and most likely possesses a TM domain suggests that the RING finger was located in the cytoplasm since glycosylations normally occur in the lumen of the endoplasmatic reticulum (Alberts et al., 2001).

4.3.3 LINA forms a ternary complex

During the characterization of the structural domain of LINA with western blot analysis, I observed that under mild SDS (sodium dodecyl sulphate) conditions

LINA ran in gels as one band at 50kDa (data not shown). This observation pointed to the possibility that LINA might form an aggregate by a self assembling, which has been often reported as a biochemical character of RING finger protein (Kentsis et al., 2002).

To test this hypothesis, I performed a co-immunoprecipitation (Co-IP) approach (3.4.6). Here, I generated a LINA-FLAG fusion protein as well as a LINA-HA fusion protein. FLAG-tag was introduced at the C-terminus of LINA by substituting the stop codon with an Xho I restriction site using a PCR-based approach. The PCR fragment was then cloned into pAAV-IRES-hrGFP, which yielded in-frame constructs expressing FLAG-tagged LINA using the Eco*R* I and Xho I restriction sites.

HEK293 cells were co-transfected with both expression vectors LINA-HA and LINA-FLAG. The protein lysates were then incubated with the agarose beads coupled with an anti-HA antibody for Co-IP. The HA-tagged LINA protein binds specifically to the anti-HA-antibody and can finally be precipitated separately. If LINA self assembles, the FLAG-tagged LINA protein can bind with the HA-tagged LINA protein and it can be precipitated together with the HA-tagged LINA protein selectively and detected in eluates by western blot analysis using an anti-FLAG antibody. As a control for a membrane bound protein, both HA- and FLAG-tagged Nogo Receptor (NgR) protein were also overexpressed in HEK293 cells together with each FLAG- and HA-tagged LINA protein to exclude any unspecific binding of proteins.

Before Co-IP, the whole protein lysates were first tested by anti-HA and anti-FLAG antibodies in western blot analysis in order to confirm that both tagged proteins were successfully expressed in the cells (Figure 4-9, A).

After Co-IP, the eluates were detected in western blot with both anti-HA- and anti-FLAG-antibodies (Figure 4-9, B). I investigated at first that Co-IP with an anti-HA-antibody was successfully done. As a control, the HA-tagged NgR and the HA-tagged LINA were separately overexpressed in HEK293 cells (Figure 4-9, A, lane 1, 2 at HA detection) and precipitated by anti-HA antibody (Figure 4-9, B, lane 1, 2 at HA detection). The absence of detection with anti-FLAG antibody in eluate showed that Co-IP with anti-HA antibody was specific (Figure 4-9, B, lane 1, 2 at FLAG detection). Whereas, the anti-FLAG antibody detected FLAG-tagged LINA in the eluate where the HA-and FLAG-tagged LINA were co-expressed (Figure 4-9, B, lane 3 at FLAG detection), showing that LINA-FLAG was co-precipitated with LINA-HA.

This suggests that LINA self assembles (Figure 4-9, B, lane 3). In comparison to this, the FLAG-tagged LINA protein was not detected in the eluate co-expressed together with the HA-tagged NgR protein and vice versa, confirming that the self assembling of LINA was specific (Figure 4-9, B, lane 4, 5).

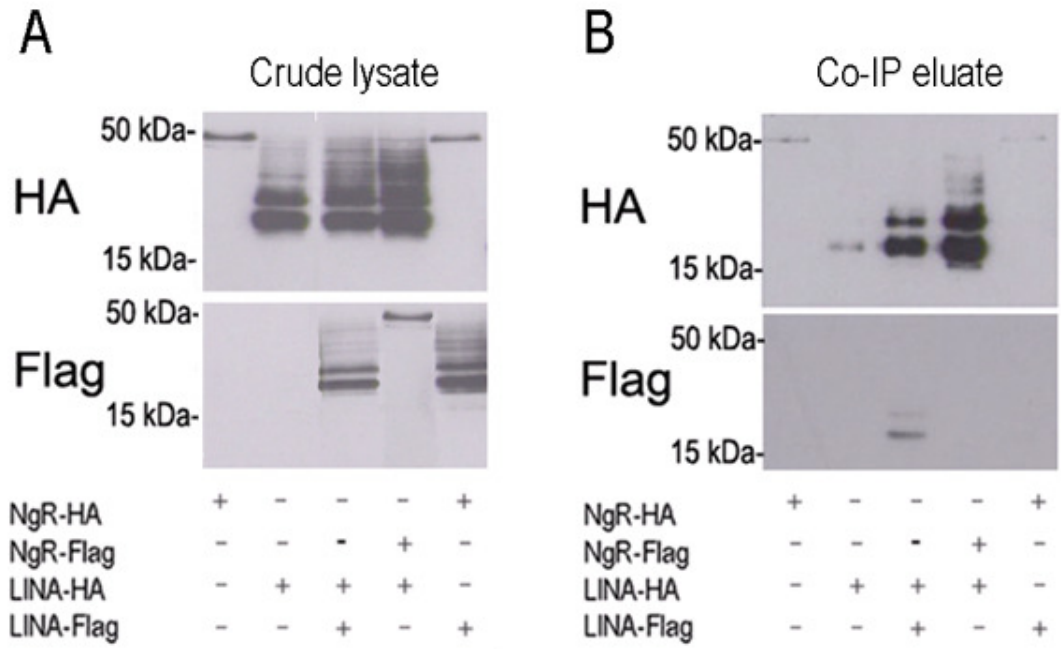

Figure 4-9: Co-immunoprecipitation showing the self assembling of LINA protein

A: Western blot analysis of crude lysate showed the successful overexpression of each protein before Co-IP. B: The HA-tagged NgR and HA-tagged LINA were separately overexpressed in HEK293 cells and precipitated by anti-HA antibody as a control (B, lane 1, 2). The HA- and the FLAG-tagged LINA were co-expressed in HEK293 cells and precipitated by anti-HA antibody (B, lane 3). The FLAG-tagged NgR and HA-tagged LINA were co-expressed in HEK293 cells and precipitated by anti-HA antibody (B, lane 4) and vice versa (B, lane 5). Western blots were repeated at least three times to confirm results.

Which domain of LINA may be responsible for this self assembling? In order to identify the structural domain underlying self assembling, three different LINA variants were first designed; 1) $LINA^{60\text{-}155}$, which has no transmembrane domain, 2) $LINA^{IgK}$, in which the whole N-terminal sequence of LINA is substituted with an Ig-Kappa signal sequence, and 3) LINA-GFP (green fluorescence protein) fusion protein (a schematic drawing of these LINA variants is illustrated in Figure 4-12).

LINA$^{60-155}$ and LINA^{IgK} were HA-tagged at the C-terminus using the accordant reverse primer and as a template the vector pAAV-IRES-hrGFP-LINA was used by PCR method. Finally a coding sequence of each was cloned into the expression vector pAAV-IRES-hrGFP using the Eco*R* I and Xho I restriction sites. The cloning was verified successfully by sequencing analysis and each of these variants was co-expressed in HEK293 cells together with the FLAG-tagged LINA^{WT} protein. The LINA-GFP construct (shown in 3.3.2), which has a GFP as a marker at the C-terminus was also overexpressed in HEK293 cells together with the HA-tagged LINA^{WT} protein.

Before Co-IP, the whole protein lysates were first tested by anti-HA (Figure 4-10, A, first three lanes), -FLAG (Figure 4-10, A, lane 4, 5), and -GFP antibodies (Figure 4-10, A, lane 6) in western blot analysis in order to confirm that both tagged proteins were successfully expressed in the cells and the protein lysates were co-immunoprecipitated by anti-HA antibody (Figure 4-10, B).

Co-IP was done in each group and each eluate was detected by anti-HA, anti-FLAG, and anti-GFP antibodies. The HA-tagged proteins were bound by the agarose beads coupled to the anti-HA antibody and successfully precipitated with detection by the anti-HA antibody in the eluates (Figure 4-10, B, first three lanes). The FLAG- tagged LINA^{WT} protein was detected also in both eluates, showing that LINA can bind with two LINA variants, LINA$^{60-155}$ and LINA^{IgK} (Figure 4-10, B, lane 4, 5). This suggests that the whole N-terminal sequence of LINA does not influence the self assembling of the LINA protein. Next, LINA-GFP fusion protein was also detected in the eluate by the anti-GFP antibody (Figure 4-10, B, lane 6), showing that LINA can also bind to the LINA-GFP fusion protein, which suggested that there was no steric hindrance of the C-terminus from the GFP protein for the self assembling of the LINA protein, although the GFP protein itself is bigger than LINA. From this result, I concluded that LINA could self assemble with amino acid sequences spanning from position 60 to 155.

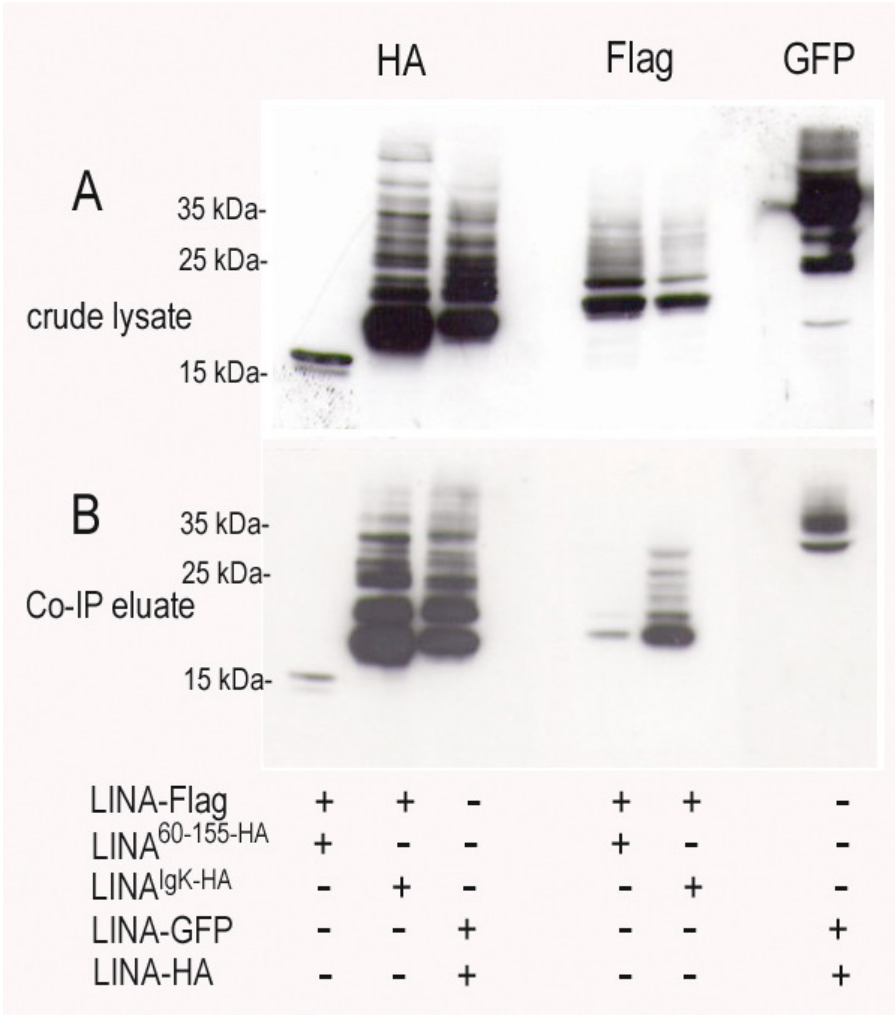

Figure 4-10: The amino acids spanning position 60 to 155 are responsible for the self assembling of LINA.

A: Cell crude lysates were first tested by western blot analysis with three different antibodies to confirm the expression of both tagged proteins before Co-IP. B: All HA-tagged LINA variants were detected in the eluates by the anti-HA antibody, confirming that Co-IP with the anti-HA antibody was successful (B, first three lanes). The FLAG-tagged LINA was detected by the anti-FLAG antibody in both eluates co-precipitated with the HA-tagged $LINA^{60-155}$ and $LINA^{Igk}$ (B, lane 4, 5). LINA-GFP fusion protein was detectable by the anti-GFP antibody in the eluate co-precipitated with the HA-tagged $LINA^{WT}$ (B, lane 6). Western blots were repeated at least three times to confirm results.

Furthermore, it was next investigated whether LINA forms a ternary complex using a cross linking experiment. The principle of a cross linking experiment is that using ethylene glycolbis (EGS, succinimidylsuccinate), ϵ- amine of lysine in the protein can react with N-hydroxysuccinimide ester at pH 7-9 and form covalent amide bonds. When two or more proteins have specific interaction, those interac-

tions can be investigated using this cross linking reagent, EGS, which can capture protein-protein complexes by a covalent binding. The cross linking reagent, EGS was kindly provided by Prof. Dr. R. Marienfeld (the institute of Physiological chemistry at Ulm University).

I used the HA-tagged LINA$^{60-155}$, because I showed previously that LINA needs the domain spanning amino acids 60 to 155 for its self assembling. The HA-tagged LINA$^{60-155}$ was overexpressed in HEK293 cells to obtain the protein lysate. The whole protein lysates were then incubated with EGS at the final concentration of 2.5 mM on the ice for 2 h and further treated according to protocol (shown in 3.4.5). The protein sample was next detected by a western blot analysis using an anti-HA antibody.

As a control, I used the protein lysate of the HA-tagged LINA$^{60-155}$ without the cross linking reagent EGS. As shown in Figure 4-11, the cross-linked lysate showed two bands more than the control lysate. One band was approximately 36 kDa, suggesting a ternary complex of LINA since monomer LINA$^{60-155}$ has a weight of around 13 kDa, and the other, 80 kDa, a high molecular complex which was bound with the HA-tagged LINA$^{60-155}$ protein.

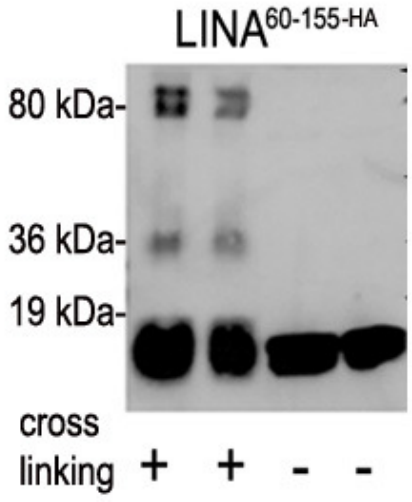

Figure 4-11: Cross linking experiment confirms that LINA forms a ternary complex

The HA-tagged LINA$^{60-155}$ was overexpressed in HEK293 cells and the protein lysate next treated, one for a control, without a cross linking (tested twice in lane 3, 4), the other for a cross linking (tested twice in lane 1, 2). Each protein lysate was analyzed by the anti-HA antibody in western blotting. In comparison to the control (lane 3, 4), two more bands were detected in the cross linked protein, approximately at 36 kDa and 80 kDa (lane 1, 2). It was repeated at least three times to confirm results.

4.3.4 LINA forms a ternary complex with its RING finger domain

Since now I showed that LINA as a membrane bound protein, can self assemble and forms a ternary complex with its amino acids spanning 60 to 155, which include the RING finger domain (amino acids 93-133), C-terminal domain (amino acids 133-155), and the rest uncharacterized domain encompassing the amino acids 60 to 92.

My next question was which structural domain in LINA plays a critical role for forming the ternary complex? In order to identify the exact region required for building the ternary complex, I performed progressive depletions of the LINA. All the deletion mutants of LINA are schematically illustrated as follows.

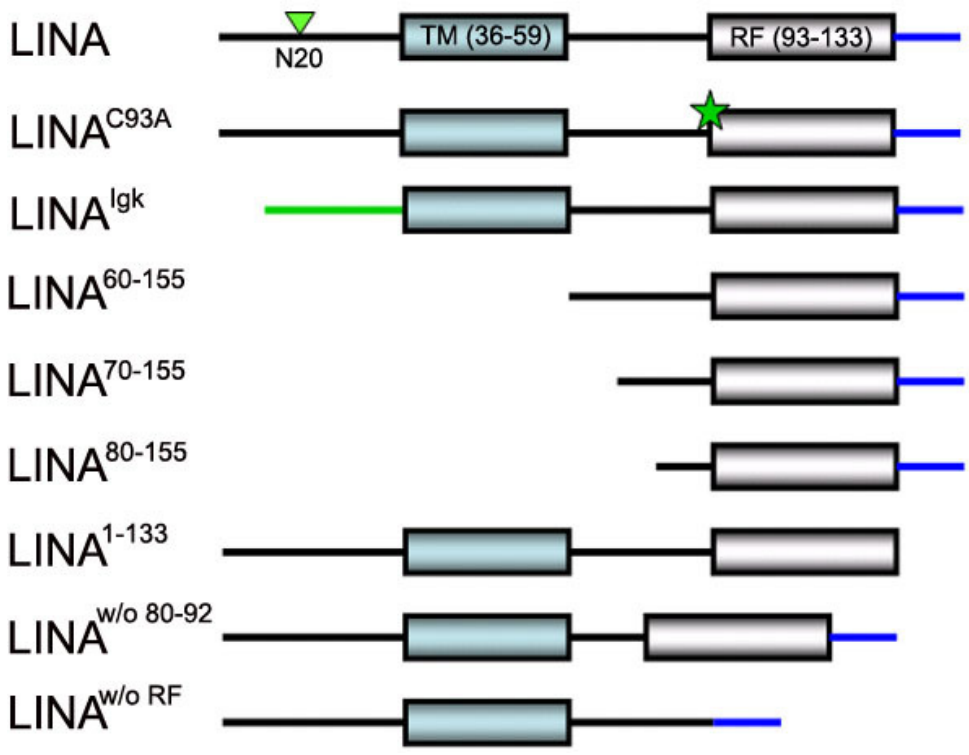

Figure 4-12: Schematic drawing of different LINA variants

TM: Transmembrane domain, RF: RING finger, lgk: Ig-kappa signal sequence (green line), N20: 20th amino acid, asparagine, LINA^{C93A}: LINA substituted cysteine (C) at position 93 with alanine (A), LINA^{lgk}: LINA substituted the N-terminus with IgK, LINA$^{60-155}$: amino acids from 1st - 59th depleted LINA, LINA$^{70-155}$: amino acids from 1st – 69th depleted LINA, LINA$^{80-155}$: amino acids from 1st - 79th depleted LINA, LINA$^{1-133}$: amino acids from 134th - 155th depleted LINA (blue line), LINA$^{w/o\ 80-92}$: LINA without amino acid residues 80 - 92, LINA$^{w/o\ RF}$: LINA without RING finger domain.

I created five LINA variants: 1) by depleting either 60^{th}-69^{th} or 60^{th}-79^{th} amino acids from $LINA^{60-155}$, two different LINA variants, $LINA^{70-155}$ and $LINA^{80-155}$ were generated to investigate the characteristic of the region between the transmembrane and RING finger domain, 2) by depleting the amino acid residues 80^{th}-92^{th} from $LINA^{WT}$, $LINA^{w/o\ 80-92}$ was created (shown in 3.3.5) , 3) by depleting the C-terminus (134^{th}-155^{th}) of $LINA^{WT}$, $LINA^{1-133}$ was generated to investigate whether the C-terminus of LINA is responsible for a complex formation, 4) by depleting the whole RING finger domain of LINA (shown in 3.3.5), $LINA^{w/o\ RF}$ was generated to investigate the role of the whole RING finger domain for a complex formation.
Each depleted cDNA of LINA was amplified by PCR using the accordant primers containing the domain depletion sequences (shown in 2.11.1). The pAAV-IRES-hrGFP-$LINA^{WT}$ was used as a template. The coding sequence of each variants were then cloned into pAAV-IRES-hrGFP expression vector using Eco*R* I and Xho I restriction sites. All expression constructs were tagged with FLAG-tag at the C-terminus by substituting the stop codon with an Xho I restriction site using a PCR-based approach. All constructs were verified by sequencing.
Each variant was then co-expressed in HEK293 cells together with the HA-tagged $LINA^{60-155}$ to obtain the protein lysate. The whole protein lysate was first tested by anti-HA and anti-FLAG antibodies to confirm that both proteins in each group were successfully overexpressed in cells. Finally proteins in each groups were co-immunoprecipitated by the anti-HA antibody and each eluate was detected with anti-HA and anti-FLAG antibodies in western blot analysis.

As shown in Figure 4-13, first the HA-tagged $LINA^{60-155}$ was detected with anti-HA antibody in all eluates, suggesting that Co-IP was successfully achieved. Interestingly, I detected all FLAG-tagged LINA variants in the eluates except for the $LINA^{w/o\ RF}$protein, indicating that $LINA^{w/o\ RF}$protein did not bind with $LINA^{60-155}$ (Figure 4-13, lane 6 of Co-IP eluate, at FLAG detection). I detected the FLAG-tagged $LINA^{C93A}$ in the eluate, suggesting that the whole RING finger domain is involved in a ternary complex formation. This is in good agreement with a study reporting that RING finger domains often have a strong tendency to aggregate (Kentsis et al., 2002).

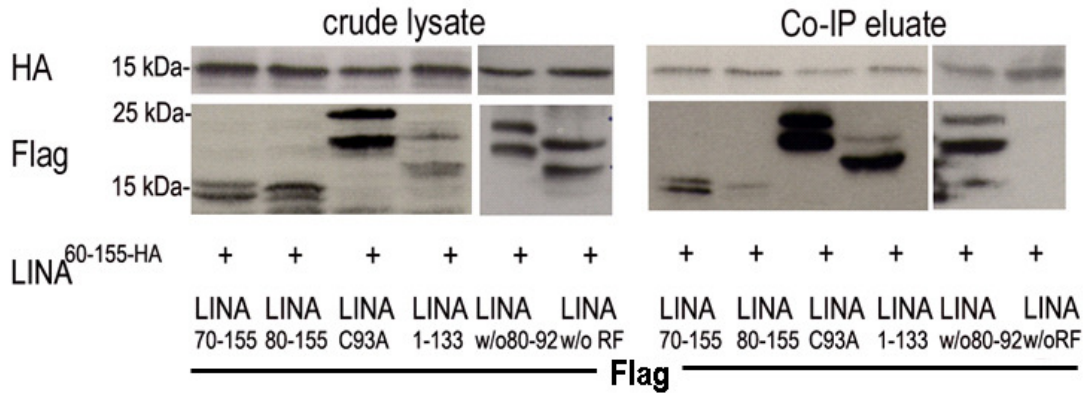

Figure 4-13: The RING finger domain is required for a ternary complex formation.

Six different FLAG-tagged LINA variants, LINA$^{70-155}$, LINA$^{80-155}$, LINA^{C93A}, LINA$^{1-133}$, LINA$^{w/o\ 80-92}$, and LINA$^{w/o\ RF}$ were co-expressed in HEK293 cells together with the HA-tagged LINA$^{60-155}$. All protein samples were obtained and tested first before Co-IP in western blot to confirm the expression of both proteins (crude lysate). After Co-IP, all eluates were detected by anti-HA and anti-FLAG antibodies in western blotting (Co-IP eluate). Detection by the anti-HA antibody in the eluates showed the successful Co-IP. Using the anti-FLAG antibody, only LINA$^{w/o\ RF}$ protein was not detected in the eluate (last lane in Co-IP eluate), confirming that the RING finger domain is required for this complex formation. Western blots were repeated at least twice to confirm results.

In summary, using the variable cloning methods and biochemical analysis, I characterized here that LINA, a novel RING finger protein, is a membrane bound protein, has an *N*-glycosylation site at 20th amino acid and forms a ternary complex with its RING finger domain.

4.4 Subcellular localization of exogenous LINA

Since the identification of the subcellular localization of a protein can provide insights into its possible functional roles, I investigated next the cellular localization of LINA in PC12 cells, where the LINA showed the neurite outgrowth effect exposed to NGF.

LINA contains no special sequence motifs that indicate its subcellular localization, such as, a signal peptide or a nuclear localization signal. Therefore, to examine its subcellular localization, I generated fusion proteins in which enhanced green fluorescence protein (GFP) or enhanced red fluorescence protein (RFP) was fused to the C-terminus of LINA (shown in 3.3.2).

In order to determine the intracellular compartment where LINA is located, PC12 cells overexpressing LINA-GFP were stained with organelle specific markers.

First, I investigated the localization of LINA in the trans-Golgi network (TGN), since the TGN is the region where proteins are sorted and transported to their own destinations (Lodish et al., 2004). The mouse anti-TGN38 antibody (provided by Dr. Knippschild, Ulm University), which is specific for the TGN, was used for the investigation. TGN38 is known as one of the few known resident integral membrane proteins of the TGN. Since it cycles constitutively between the TGN and the plasma membrane, it is reported that TGN38 is suitable for the identification of post-Golgi trafficking motifs (Roquemore and Banting, 1998). For the staining, the PC12 cells were first transfected with LINA-GFP expression vector exposed to NGF. After 1 day, the LINA expressing cells were then fixed by 4% paraformaldehyde (PFA) and finally incubated with the mouse anti-TGN38 antibody (dilution 1:50) for overnight to investigate the co-localization of both proteins. The mouse anti-TGN38 antibody was finally detected by the fluorescent secondary antibody, Alexa Fluor® goat Anti-Mouse 594 and the co-localization was documented using fluorescence microscopy. The staining showed that the LINA-GFP was enriched in the perinuclear region and partially co-localized with TGN38 (Figre 4-14, A).

Since the expression pattern of LINA-GFP fusion protein in PC12 cells shows a typical vesicle protein pattern and at least three different types of vesicles are sorted in the TGN to their own compartments including exocytotic vesicles, secretory vesicles and lysosomal vesicles (Lodish et al., 2004), I investigated next the localization of LINA in lysosomes in order to see whether LINA can be processed from the TGN to lysosomal vesicles. It is also reported by Mader et al. (2007) that some RING finger proteins are localized in lysosomes. Therefore, I stained PC12 cells overexpressing LINA-GFP with lysotracker (Invitrogen), a red lysosome specific marker. 50 nM lysotracker was used to stain the living cell in the medium and the cells were incubated for 30 min. Staining with lysotracker was stopped by replacing with fresh medium and the co-localization was documented using fluorescence microscopy. However, LINA-GFP did not show any co-localization with lysosomes (Figure 4-14, B).

I then analyzed the localization of LINA in peroxisomes. It is known that peroxisomes contain membrane proteins which have functions for importing proteins into the organelles (Lodish et al., 2004). Thus, it was interesting to investigate the localization of LINA as a vesicle protein also in peroxisomes to test the co-localization. I used the SKL-GFP fusion protein (provided by Dr. Franz Oswald, Institute of Internal Medicine 1 at Ulm University) to analyze the localization of LINA in peroxisomes. SKL is three peptides (serine-lysine-leucine),

specific signal peptide indicator for peroxisomal localization (Reumann, 2004) and this carboxyl-terminal sequence SKL has been shown to direct proteins to the peroxisomes of mammalian cells *in vivo* (Wolins and Donaldson, 1997). Since a SKL-expressing vector was provided as a green fluorescent GFP fusion expression vector, I used a red fluorescent LINA fusion protein expression vector, LINA-RFP together with SKL-GFP for the co-transfection in PC12 cells. After co-transfection with both expressing vectors in PC12 cells, the cells were differentiated by NGF and after 1 day, the cells were fixed by 4% PFA and the co-localization was then analyzed using fluorescence microscopy. LINA did not show any co-localization with peroxisome (Figure 4-14, C).

The punctate staining pattern of LINA, however, suggested that LINA might be associated with some vesicular compartments. Therefore, I investigated next the co-localization of LINA with one of the endosomal vesicle membrane proteins, beta-site amyloid precursor protein (APP) cleaving enzyme 1 (BACE1). BACE1 is a member of aspartic proteases, which contains an N-terminal catalytic domain, a 17-residue transmembrane domain and a short C-terminal cytoplasmic tail (Vassar et al, 1999). In cells, BACE1 is expressed initially as a preproprotein, and is then processed to its mature form in the Golgi apparatus (Bennet et al, 2000). The cellular localization of BACE1 is not exactly known yet but it is localized in the ER and Golgi or endosome compartment where APP is processed. The BACE1-GFP fusion protein expression vector was provided by Dr. C. von Arnim (Institute of Neurology at Ulm University). The BACE1-GFP and the LINA-RFP protein were co-expressed in PC12 cells differentiated by NGF and after 1 day, the co-localization was observed using the fluorescence confocal scan microscopy (with help of Mrs. Glaschick, Institute of Biophysics at Ulm University). LINA showed partial co-localization with BACE1 (Figure 4-14, D), suggesting that LINA might be involved in secretory vesicles in cells.

These results demonstrated that in PC12 cell system the overexpressed LINA is partially localized in TGN and in the endosomal vesicle compartment, suggesting that it may participate in a secretory pathway.

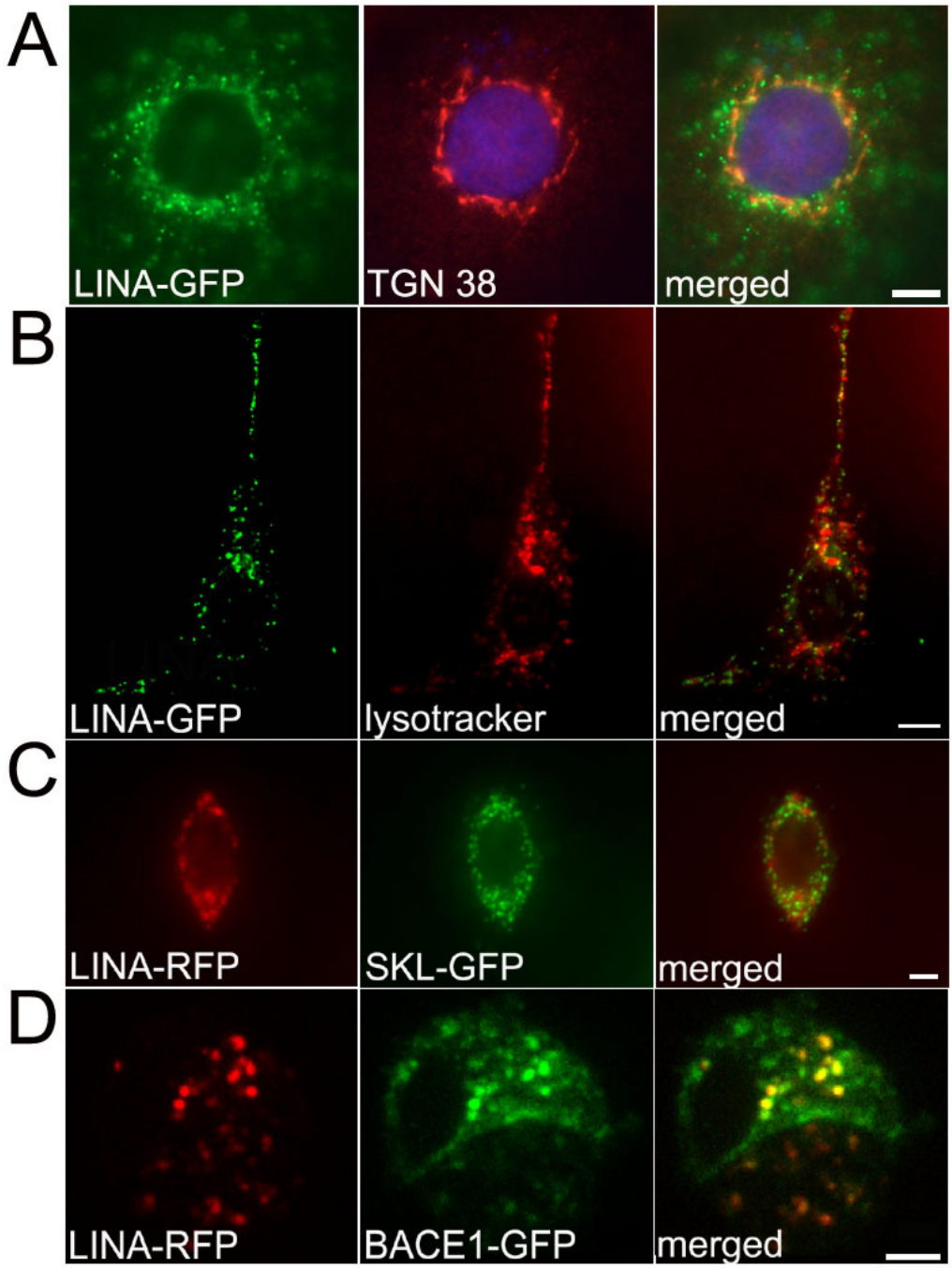

Figure 4-14: Characterization of subcellular localization of LINA with different cellular markers

A: LINA-GFP fusion protein was expressed in PC12 cells and stained by the specific antibody against protein TGN38. Blue shows the DAPI staining of cell nucleus. LINA showed a partial co-localization with TGN38. B: LINA-GFP overexpressing PC12 cells were stained with a red lyso-tracker, showing no localization in lysosomes. C: LINA-RFP and SKL-GFP were co-expressed in PC12 cells, showing no co-localization in peroxisomes. D: LINA-RFP and BACE1-GFP were co-expressed in PC12 cells, showing a partial co-localization, suggesting that LINA might be involved in a secretory pathway. This picture was taken by a confocal laser microscopy. Scale bars: 1µm. These staining were repeated at least three times to confirm results.

4.5 Investigation of endogenous LINA expression

4.5.1 Verification of anti-LINA antibody

Since I detected the exogenously expressed LINA with different tags, it was necessary to generate anti-LINA antibody to detect endogenous expression of the LINA protein. With anti-LINA antibody, it can be investigated that either expression, or upregulation, or localization pattern of this protein in different tissues on the endogenously expressed protein levels.

In order to generate an anti-LINA antibody, two different strategies were used. First, the specific LINA antibody was generated by company Invitrogen against a synthetic peptide sequence, NKPIAGPTETSQS, corresponding to the sequence of the LINA protein between residues 134 to 146 at the C-terminus of LINA. After immunization of this peptide epitope into rabbit, the polyclonal anti-peptide serum was taken after 6 weeks. The serum was first tested by immunocytochemistry. As control, preserum which was taken from the rabbit before the immunization, was also tested to compare the specific effect of the polyclonal serum. For immunocyto- and -histochemistry, it was necessary to exclude the unspecific factors of the polyclonal serum to obtain the accurate staining and it was the reason to further perform the affinity chromatography purification using a column linked with the synthetic peptide sequence, NKPIAGPTETSQS (3.4.9).

The titer of each fractions of the affinity purified rabbit anti-LINA antibody was next tested and the affinity purified rabbit anti-LINA antibody fraction 2 was finally used for immunocyto- and -histochemistry to detect the LINA protein at the dilution of 1:50. In order to verify the specificity of this purified rabbit anti-LINA antibody for staining, LINA-GFP fusion protein was first overexpressed in HEK293 cells (Figure 4-15, A). I used here the HEK 293 cell system for immunocytochemistry, since comparing to PC12 cells originated from rat, HEK293 cells are originated from human and little expression of LINA gene was detectable in this cell system according to the result of RT-PCR in our lab (data not shown). 1 day after the transfection, the cells were fixed by 4% PFA and incubated with this purified rabbit anti-LINA antibody for overnight. This purified rabbit anti-LINA antibody was next detected by the fluorescent secondary antibody, Alexa Fluor® goat Anti-Rabbit 594. The staining was documented using a fluorescence microscopy. As shown in Figure 4-15, the purified rabbit anti-LINA antibody recognized correctly the LINA-GFP positive cells, not the LINA-GFP negative cells which were stained only by DAPI, suggesting that the affinity purified rabbit anti-LINA antibody is specific in HEK293 cell system.

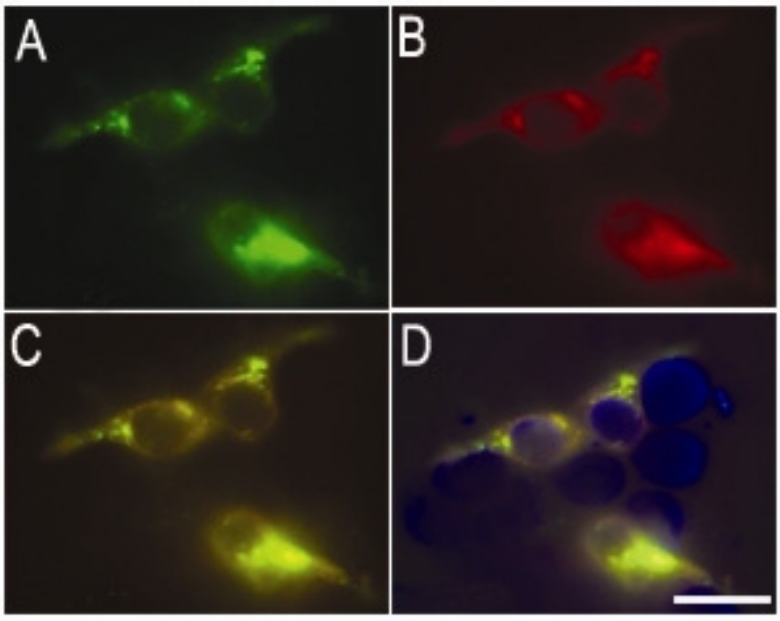

Figure 4-15: Specificity of the affinity purified rabbit anti-LINA antibody by immunocytochemistry in HEK293 cell system

Affinity purified rabbit anti-LINA antibody was used for immunocytochemistry (dilution 1:50). A: HEK293 cells overexpressing LINA-GFP showed the typical vesicular pattern, B: same cells detected by the affinity purified rabbit anti-LINA antibody, C: merged image, D: merged image with nuclear DAPI staining. Only LINA-GFP expressing cells showed a positive staining with anti-LINA antibody. Only DAPI-staining positive cells are LINA-untransfected cells, confirming the specifity of the affinity purified rabbit anti-LINA antibody. Scale bar: 10 µm. These stainings were repeated at least three times to confirm results.

Second, the specific LINA antibody was generated against a LINA-GST (Glutathione-S-transferase) fusion protein. GST-fusion protein is commonly used for generating the specific antibody, since it is possible to yield a huge amount of protein of interest in *E.coli* with GST-fusion system. Either a part of protein of interest, or the whole protein can be expressed with GST-tag in *E.coli* and this recombinant protein can be purified against the GST-tag using the GST-affinity column (shown in 3.4.8). This purified GST-fusion protein of interest is used as an immunogen for generating the specific antibody. The advantage of the GST-fusion protein provides variable epitopes from some peptides to the whole protein for the immunization and finally it allows to obtain a specific antibody recognizing the protein of interest.

LINA possesses a hydrophobic transmembrane domain which often forms an inclusion body and finally disturbs successful expression and purification of the recombinant protein in *E.coli* (Smith et al., 1988; Saluta et al., 1998). For this rea-

son, I cloned the cDNA of LINA$^{60-155}$ lacking the transmembrane domain into the GST-expression vector, pGEX-4T-1 using the Eco*R* I and Xho I restriction sites. The best condition for the induction and expression of the recombinant protein was first optimized (shown in 3.4.8.1) and finally the LINA$^{60-155}$-GST fusion protein was successfully overexpressed in *E.coli*-BL21 induced by IPTG. The LINA$^{60-155}$-GST protein was then purified by using a glutathione sepharose column (shown in 3.4.8.2). The purity of the protein was confirmed by the coomasie blue staining and finally used for immunization by company PINEDA (Berlin, Germany).

One serum taken 90 days after immunization in a guinea pig showed positive staining in the western blot. This serum was further used for western blot analysis together with the polyclonal rabbit anti-LINA antibody at the dilution of 1:1000. Figure 4-16 showed the verification of rabbit polyclonal anti-LINA antibody by western blot analysis.

HA-tagged LINA was overexpressed in HEK293 cells and the whole protein lysates were obtained and further analyzed by western blot analysis. As a negative-control, untransfected HEK293 cells protein lysates were also obtained and analyzed same like LINA overexpressed HEK293 cells protein lysates. First both protein lysates, control protein lysate and LINA overexpressed protein lysate were detected with the polyclonal rabbit serum anti-LINA antibody.

Detection the protein in untransfected control HEK293 cells showed one single unspecific band which is slightly bigger than LINA protein (Figure 4-16, lane 1). Whereas, the polyclonal rabbit serum anti-LINA antibody detected successfully both a glycosylated and an unglycosylated form of the HA-tagged overexpressed LINA in HEK293 cells very specifically (Figure 4-16, lane 2). At the same time, as a positive control, the same HA-tagged LINA overexpressed protein lysate was detected by anti-HA-antibody, which can recognize all HA-tagged proteins in cell lysate. This detection showed the same result as that by the polyclonal rabbit serum anti-LINA antibody in western blot analysis (Figure 4-16, lane 3).

This suggested that the polyclonal rabbit serum anti-LINA antibody can recognize and detect the LINA protein overexpressed in HEK293 cells in western blot analysis, although it could be arguable that this serum could recognize the unspecific band slightly bigger than LINA in HEK293 cell system.

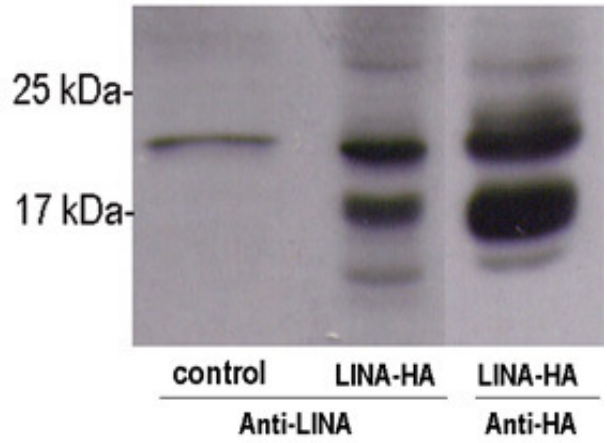

Figure 4-16: Verification of the polyclonal rabbit serum anti-LINA antibody by western blot analysis

Lane 1: As a negative control, untransfected HEK293 cell protein lysates analyzed by the polyclonal rabbit serum anti-LINA antibody, showing an unspecific single band. Lane 2: Overexpressed HA-tagged LINA detected by the polyclonal rabbit serum anti-LINA antibody, recognizing both a glycosylated and an unglycosylated LINA. Lane 3: as a positive control, overexpressed HA-tagged LINA detected by the anti-HA antibody. Anti-HA antibody recognized both HA-tagged glycosylated and unglycosylated LINA as same bands by the polyclonal rabbit serum anti-LINA antibody, suggesting that the polyclonal rabbit serum anti-LINA antibody detects LINA exogenously expressed in HEK293 cells. Western blots were repeated at least three times to confirm results.

4.5.2 Endogenous LINA expression in cultured primary RGCs and hippocampal neurons

Using the affinity purified rabbit anti-LINA antibody, I first investigated the endogenous expression of LINA in dissociated RGCs, since the dissociated RGCs in culture enabled me to focus on the expression of LINA in isolated RGCs, not in glial cells, in a more accurate way. I isolated the retinas and prepared mixed retinal cultures (shown in 3.1.5). 3 day-old-cultured RGCs were fixed by 4% PFA and incubated with the purified rabbit anti-LINA and anti-ßIII tubulin antibodies for overnight. The latter exclusively detects RGCs and allows their clear identification. The purified rabbit anti-LINA antibody was detected further by the fluorescent secondary antibody Alexa Fluor® goat Anti-Rabbit 594 and the anti-ßIII tubulin antibody by the Alexa Fluor® goat Anti-mouse 488.
A significant LINA expression was prominent in the cell body and axons of regenerating RGCs (Figure 4-17, A and C).

Since the embryonic hippocampal neural culture is an established model system to study neurite development (Turson et al., 2005), next it was interesting to in-

vestigate the LINA expression in primary hippocampal neurons of rat embryos (E19) using the purified anti-LINA antibody. Hippocampal neurons first extend several undifferentiated neurites in culture and then one of these neurites grows rapidly to become the axon, whereas the other neurites develop into dendrites (Turson et al., 2005). Since axon and dendrites of hippocampal neurons are well developed between day 14 and day 21 in culture, I stained the 14 day-old-neurons. This embryonic hippocampal neural culture is well established in the institute of Anatomy and Cellbiology at Ulm University and this cell culture was done with collaboration. The 14 day-old neurons in culture were first fixed with 4% PFA and incubated with both purified anti-LINA antibody and anti-ßIII tubulin antibody for overnight at 4°C. These two antibodies were then detected by each Alexa Fluor® goat Anti-Rabbit 594 and Alexa Fluor® goat Anti-mouse 488 using a fluorescence microscopy.

This result showed that LINA was widely expressed punctually in the cell body, some accumulation in the TGN region, axon and dendrites, showing a similar localization pattern as exogenously expressed LINA (Figure 4-17, B and D).

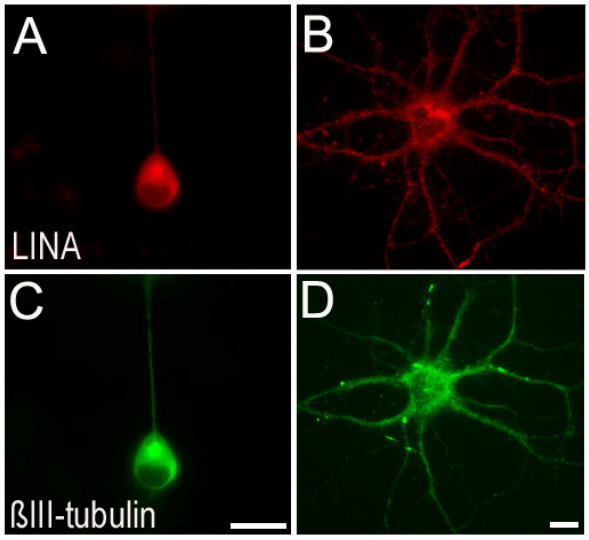

Figure 4-17: Endogenously expressed LINA in cultured primary RGCs and hippocampal neurons

Dissociated retinal cells were fixed after 3 days in culture and stained by the affinity purified rabbit anti-LINA antibody (A) and the anti-ßIII tubulin antibody (C). 14 day-old-cultured dissociated embryonic (E19) hippocampal neurons were stained by the anti-LINA (B) and the anti-ßIII tubulin antibody (D). Scale bars: 10 µm. These stainings were repeated at least three times to confirm results.

4.5.3 Subcellular localization of endogenous LINA in Hippocampal neurons

I showed before that LINA partially co-localized with BACE1 protein in PC12 cells, suggesting that LINA might be involved in secretory vesicles in PC12 cell system (Figure 4-14, D). Furthermore, I found that LINA was also expressed in hippocampal neurons as punctual forms (Figure 4-17, B), speculating the role of LINA in synaptic vesicles. Therefore, it was interesting to investigate the localization of LINA in hippocampal neuron system to characterize LINA in synaptic vesicles. In order to investigate the LINA expression pattern in synapse in detail, I co-stained the hippocampal neurons with anti-LINA antibody and the anti-ProSAP2 antibody. ProSAP2 (Proline-rich synapse-associated protein 2) is a protein of postsynaptic density which is located direct behind the postsynaptic membrane (Böckers et al., 2004; Ziff EB, 1997) and it is often used to investigate the identification of postsynaptic proteins. Anti-ProSAP2 antibody was provided by Prof. Dr. Tobias Böckers, Institute of Anatomy and Cellbiology at Ulm University.

The 21 day-old-cultured hippocampal neurons were fixed first by 4% PFA and incubated with the purified rabbit anti-LINA antibody and mouse anti-ProSAP2 antibody for overnight at 4°C. These two antibodies were then detected by each fluorescent secondary antibodies, Alexa Fluor® goat Anti-Rabbit 488 and Alexa Fluor® goat Anti-mouse 594 and documented by using a fluorescence microscopy. Figure 4-18 showed the co-staining of the purified anti-LINA antibody (Figure 4-18, A) and the anti-ProSAP2 antibody (Figure 4-18, B) in 21 day-old-cultured hippocampal neurons.

As shown in Figure 4-18, I observed the partial co-localization of both proteins in hippocampal neurons, speculating the role of LINA related with proteins in postsynaptic density. The partial co-localization of both proteins in dendritic synapses of hippocampal neurons was detailly documented with a higher magnification (Figure 4-18, D).

It is known that proteins in postsynaptic density are involved in anchoring and trafficking the postsynaptic receptors and modulate the activity of receptors (Klauck and Scott, 1995; Kennedy MB, 1993). They play an essential role for a synaptic signaling (Ziff EB, 1997). It has been reported that ProSAP2 is found in the rat brain, for example cerebellum, cortex and hippocampal area and involved in dendrite formation in the development (Böckers et al., 2004). The fact that LINA showed the partial co-localization with ProSAP2 in primary hippocampal neurons and ProSAP2 is found in the rat brain, especially in cerebellum, cortex

and hippocampal area gave me the next question to investigate the LINA expression in the rat brain.

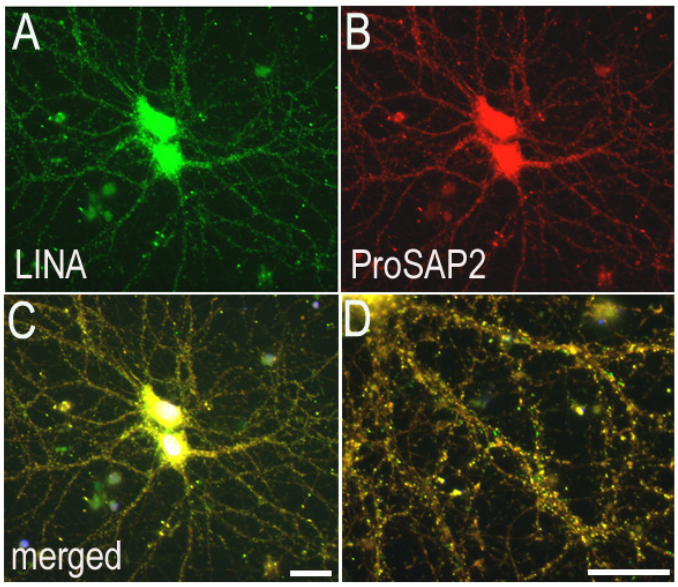

Figure 4-18: LINA and ProSAP2 are partially co-localized in primary hippocampal neurons

21 day-old hippocampus cells in culture were fixed and co-stained by the affinity purified rabbit anti-LINA antibody (A) and the anti-ProSAP2 antibody (B). C: merged image. D: Higher magnification of synapses. LINA is partially co-localized with ProSAP2, Scale bars: 20 µm. These stainings were repeated at least three times to confirm results.

4.5.4 Investigation of endogenous LINA expression in the rat brain

Since the brain is a center of the CNS and composed of a complex of neurons, it was interesting to investigate the endogenous expression of LINA in the brain to screen the expression of LINA in different neurons in the CNS. Thus, I screened next the endogenous LINA expression in the rat brain including cerebellum, cortex, and hippocampus using an affinity purified rabbit anti-LINA antibody. The adult rat was perfused with PBS and fixed with 4% PFA. The brain was post-fixed by 4% PFA and 30% sucrose solution further for overnight at 4℃ and finally embedded in Tissue-Tek. Frozen sections were cut on a cryostat and finally incubated by the purified rabbit anti-LINA antibody for screening the expression of LINA and the anti-ßIII tubulin antibody for detecting different neurons and these two antibodies were detected finally by each fluorescent secondary antibodies, Alexa Fluor® goat Anti-Rabbit 594 and Alexa Fluor® goat Anti-mouse 488 and documented by using a fluorescence microscopy.

LINA was markedly expressed in Purkinje cells in the cerebellum (Figure 4-19). The overview of cerebellum was first documented by Haematoxylin and eosin (HE) staining (Figure 4-19, A and B) and the positive stained Prukinje cells in the cerebellum were next documented with a higher magnification (Figure 4-19, C, D and E). LINA expressions were accumulated in the TGN region, and also in cell bodies and dendrites of Purkinje cells (Figure 4-19, C).

It has been characterized that Purkinje cells have a large perikaryon with one long axon, which conducts the impulse to the outside of the cerebellum and large dendritic arbors, where a number of synapses are present (Trepel, 1999; Patestas and Gartner, 2006). It is also reported that the postsynaptic density in their dendritic spines consists of very fine filaments with globular proteins (Landis et al., 1987). Some proteins, such as receptors for glutamate, are reported as associated proteins with postsynaptic densities in Purkinje cells (Fagg and Matus, 1984). Functional role of LINA underlying this expression pattern in dendrites in Purkinje cells should be further elucidated but the abundant expression of LINA in dendrites in Purkinje cells supposed that LINA may have a function for the postsynaptic regulatory machinery.

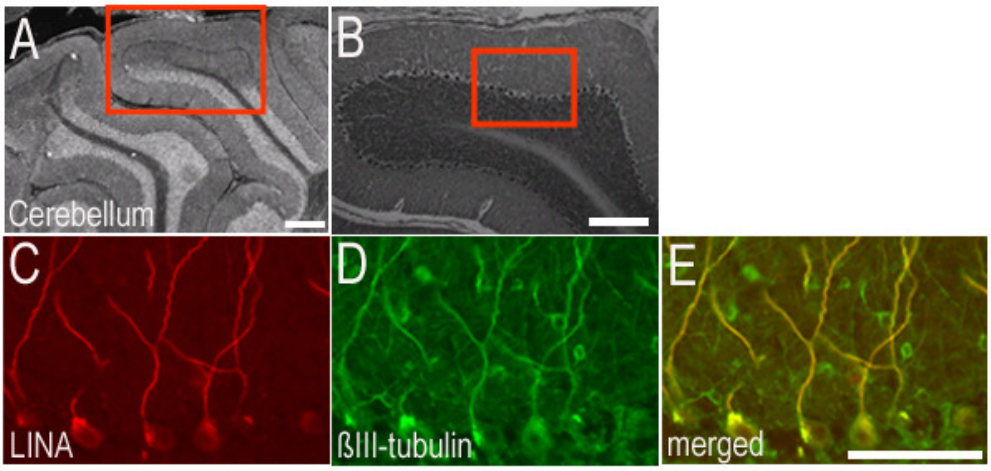

Figure 4-19: LINA is expressed in Purkinje cells in the cerebellum of the rat brain

LINA expression in Purkinje cells in the cerebellum stained by the affinity purified rabbit anti-LINA antibody (sagittal sections of the rat brain). A, B: HE staining showed the overview of the cerebellum. The red boxed regions are shown at the higher magnification in C, D, and E. C: LINA expression in Purkinje cells stained by the anti-LINA antibody. D: anti-ßIII tubulin staining of C. E: merged image. Scale bars: 50 µm. These stainings were repeated at least three times to confirm results.

LINA expression was also detected in pyramidal neurons in the cortex of the rat brain (Figure 4-20). The cortex of the rat was stained with the purified rabbit anti-

LINA antibody and anti-ßIII tubulin antibody as same procedures. The overview of the stained cortex was first documented (Figure 4-20, A, B and C). The higher magnification showed more exactly the positive LINA-expressing pyramidal neurons in the cortex (Figure 4-20, D and G).

Pyramidal neurons are known as main neurons of the cortex. It has been characterized that they have a triangularly shaped cell body, a single axon, a single apical dendrite and multiple basal dendrites (Lüllmann-Rauch, 2002; Patestas and Gartner, 2006). As major excitatory neurons in the cortex, they release glutamate as neurotransmitter and transmit signals to other parts of the CNS (Patestas and Gartner, 2006). From this staining, I investigated that LINA is found also in pyramidal cells, especially in cell bodies and dendrites, a similar staining pattern as in Purkinje cells of the cerebellum.

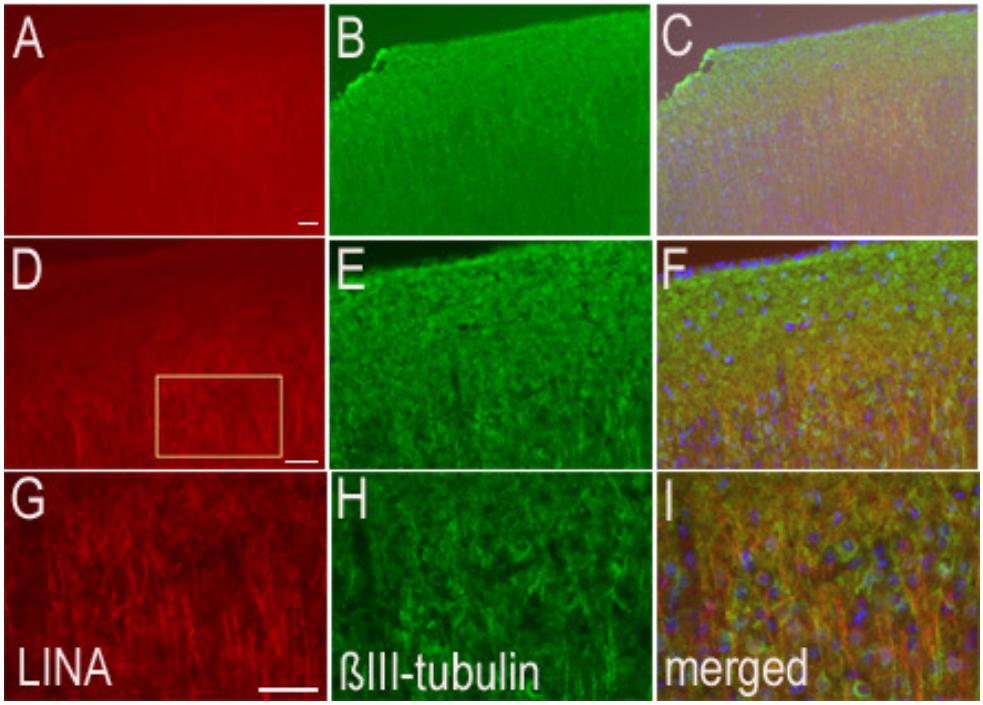

Figure 4-20: LINA is expressed in the cortex of the rat brain

LINA expression was observed in the cortex (sagittal sections of the rat brain). A, D, G: LINA expression in pyramidal cells stained by the affinity purified rabbit anti-LINA antibody with different magnifications. B, E, H: Same pictures as in A, D, G stained by the anti-ßIII tubulin antibody. C, F, I: merged images with blue DAPI staining. LINA is expressed markedly in cell bodies and dendrites of pyramidal cells. The boxed region was focused for higher magnifications. Scale bars: 50 µm. These stainings were repeated at least three times to confirm results.

Afterwards, I observed that LINA was markedly expressed in the hippocampus, in particular in the dentate gyrus (Figure 4-21). The dentate gyrus is a part of the hippocampus and it is known to have the ability for neurogenesis in adult humans (Cameron and Mckay, 2001). The overview of the hippocampus was first documented with a HE staining (Figure 4-21, A) and the dentate gyrus region was focused with a higher magnification to investigate the expression of LINA. The neurons in the dentate gyrus were significantly stained by the purifed rabbit anti-LINA antibody (Figure 4-21, B, C and D). The granule cells, basket cells and pyramidal cells are the main cell types in the dentate gyrus. From the localization and cell morphology, the cells showing strongly LINA positive were defined as basket cells, which are known to have an inhibitory activity on pyramidal cells of the hippocampus (Figure 4-21, D).

This result was consistent with the result of Figure 4-17, B and Figure 4-18, confirming that LINA is highly expressed in the hippocampus, especially in the dentate gyrus in the rat.

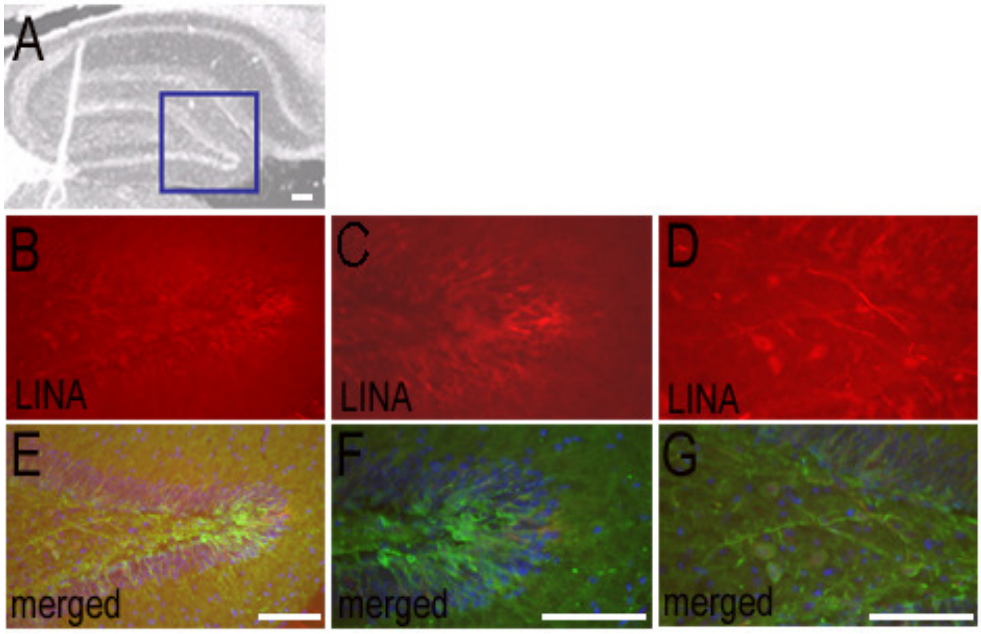

Figure 4-21: Investigation of endogenous LINA expression in the dentate gyrus of the rat brain

LINA expression was investigated in the hippocampus (sagittal sections of the rat brain). A: HE staining showed the overview of the hippocampus in the rat brain. B, C, D: higher magnification of the boxed region in A. LINA expression in basket cells and pyramidal cells stained by the affinity purified rabbit anti-LINA antibody. E, F, G: merged images of the purified anti-LINA and the anti-ßIII tubulin antibodies staining. Scale bars: 50 µm. These stainings were repeated at least three times to confirm results.

In summary, from this screening of LINA expression, LINA is found in the rat brain, for example cerebellum, cortex and hippocampal area, suggesting that LINA may play a significant role in the central nervous system.

4.5.5 Upregulation of LINA expression in PC 12 cells after NGF treatment

The PC12 cell line is often used for the investigation of neuronal differentiation. Since PC12 cells usually stop dividing and undergo differentiation when they are treated with nerve growth factor (NGF), and LINA overexpression promotes the neurite outgrowth in PC 12 cells exposed to NGF (Figure 4-4), it was interesting to investigate the change of endogenous LINA expression in PC12 cells depending on the NGF treatment. Thus, I compared the change of the endogenous LINA expression in PC12 cells depending on the NGF treatment using the anti-LINA antibody.

The PC12 cells were divided into two groups, one without NGF, the other with NGF treatment. The cells were then incubated for 3 days and finally fixed with 4% PFA and incubated by the affinity purified rabbit anti-LINA antibody. The anti-LINA antibody was finally detected by the fluorescent secondary antibody Alexa Fluor® goat Anti-Rabbit 594.

The PC12 cells which were treated with NGF stopped dividing and had undergone differentiating (Figure 4-22, B) compared with the cells untreated with NGF (Figure 4-22, A). The PC12 cells exposed to NGF showed the upregulation of endogenous LINA expression (Figure 4-22, B) compared to those without NGF treatment (Figure 4-22, A). The LINA protein was detected in the cell body and also in neurites in PC12 cells.

I next investigated this upregulation by western blot analysis. PC12 cells were divided into two groups same as above and cultured for 3 days. Finally the cells were harvested and the whole proteins were obtained from each group. These protein samples were loaded on the gel for western blot analysis and finally detected by the polyclonal serum anti-LINA antibody, producing the result that endogenous LINA expression was upregulated by NGF treatment in PC12 cells (Figure 4-22, C). The signal of ß-actin verified that the same amounts of protein were loaded per lane.

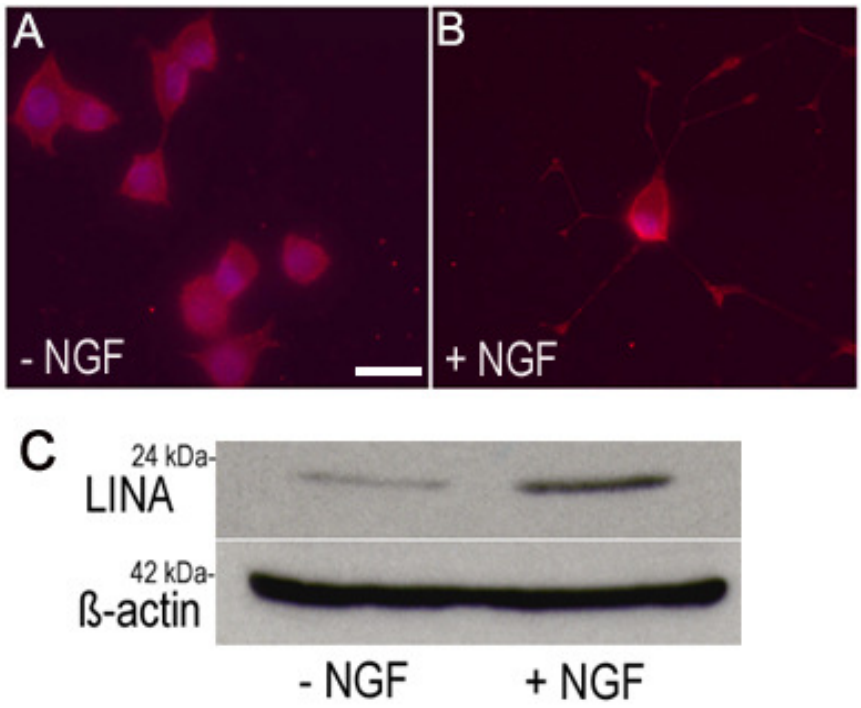

Figure 4-22: Upregulation of endogenous LINA expression with NGF treatment in PC12 cells

NGF-untreated PC12 cells (A) and NGF-treated PC12 cells (B) were stained with the affinity purified rabbit anti-LINA antibody. The cell nucleus was stained with DAPI. C: Western blot analysis: Upregulation of LINA expression was detected by the polyclonal rabbit serum anti-LINA antibody in the NGF-treated PC12 cells compared with untreated control, confirming the result of immunocytochemistry. Bands of ß-actin verify that the same amounts of protein were loaded per lane. Scale bar: 20 µm. These experiments were repeated at least twice to confirm results.

4.5.6 Upregulation of LINA expression after optic nerve crush (ONC) and lens injury (LI) in retina

I have previously shown that the LINA gene was one of the upregulated EST genes in purified RGCs treated by ONC only and ONC+LI. Therefore, I investigated the whole retina by immunohistochemistry using the affinity purified rabbit anti-LINA antibody to confirm this upregulation of LINA expression on the protein level.

Rats were subjected to different surgical procedures, ONC, LI and ONC+LI. Lens injury (LI) was used to induce inflammatory reactions for the regeneration of RGCs to activate the intrinsic growth state of neurons. These surgical procedures were done by Prof. Dr. Dietmar Fischer. After 5 days, rats were perfused by PBS and 4% PFA. Eyes were post-fixed and then finally embedded to prepare cryosections. Retinal cryosections were incubated by the affinity purified rabbit anti-

LINA and mouse anti-ßIII-tubulin antibodies for overnight at 4℃ and these two antibodies were finally detected by each fluorescent secondary antibody Alexa Fluor® goat Anti-Rabbit 594 and Alexa Fluor® goat Anti-mouse 488.

For the investigation of upregulated LINA expression on the protein level, I chose day 5 after operations, since Fischer et al. (2004b) showed that RGCs switch into the active regenerating state at this time point. In the RGCs layer (GCL), I observed the strong LINA positive RGCs after ONC+LI (Figure 4-23, D) compared with controls (Figure 4-23, A). In retina that received only ONC, a few RGCs showed also positive staining of LINA (Figure 4-23, B). The retina after LI showed a pronounced LINA staining in RGCs (Figure 4-23, C) and also in the inner plexiform layer (IPL) where the dendrites of RGCs exist, indicating that LI might induce the activation of LINA in dendrites. The anti-ßIII tubulin antibody (Tuj1) stained the RGCs layer specifically (Figure 4-23, E-H). The cell nucleus was stained by DAPI (Figure 4-23, I-L) and the merged pictures of each group were shown in Figure 4-23, M-P.

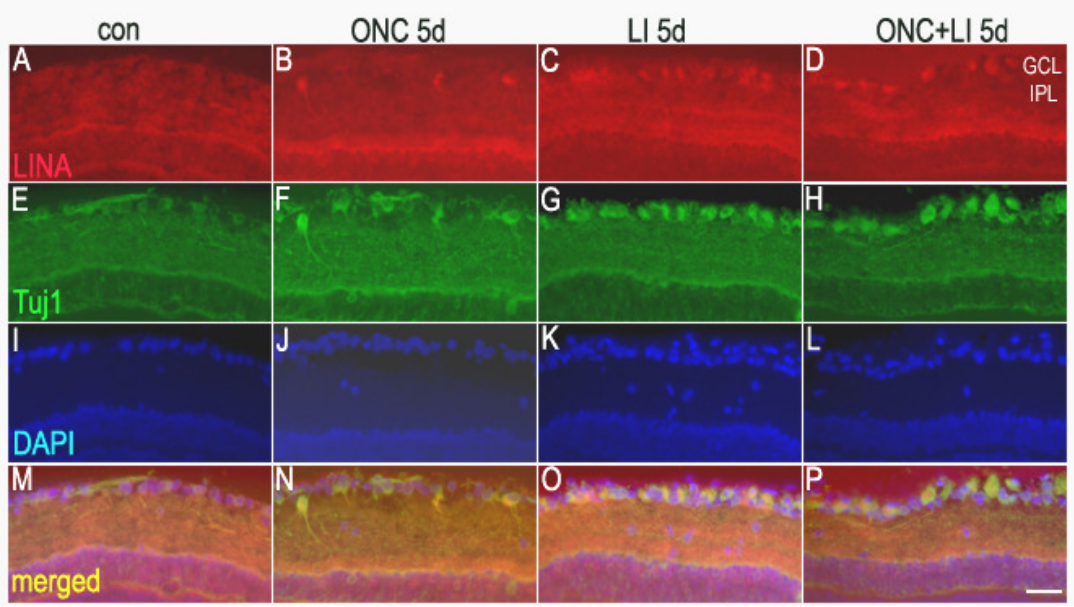

Figure 4-23: Upregulation of LINA in retina after ONC+LI and LI

A, E, I, M: Untreated control retina section showing negative staining of LINA in RGCs layer (GCL). B, F, J, N: 5 days after optic nerve crush (ONC). C, G, K, O: 5 days after lens injury (LI). RGCs layer showed an upregulation of LINA expression including the inner plexiform layer (IPL). D, H, L, P: 5 days after ONC+LI. Regenerating RGCs showed an upregulation of LINA expression. The cell nucleus was stained by DAPI. Scale bar: 30 µm. These stainings were repeated at least three times to confirm results.

The upregulation of the LINA protein in retinas after ONC+LI was also detected by the western blot analysis (Figure 4-24). Rats were subjected to different surgical procedure, such as ONC, LI, and ONC+LI as above. After 5 days, the operated rats were killed and the retina from eyes was isolated. The whole proteins isolated from each retina were loaded on the gel for western blot analysis and detected by the polyclonal rabbit serum anti-LINA antibody. Since the whole retina, not single RGCs, was used for the detection, only a slight increase of LINA expression was detected in western blot analysis treated with LI and ONC+LI when compared with control. As a positive control, I used the LINA protein overexpressed from HEK293 cells to detect the same size protein in retinal protein lysates. Interestingly, endogenous LINA was detected only in its glycosylated form by the polyclonal rabbit serum anti-LINA antibody, whereas exogenously expressed LINA was detected as both in unglycosylated- and glycosylated forms by the polyclonal rabbit serum anti-LINA antibody. Bands of ß-actin verified that the same amounts of protein were loaded per lane.

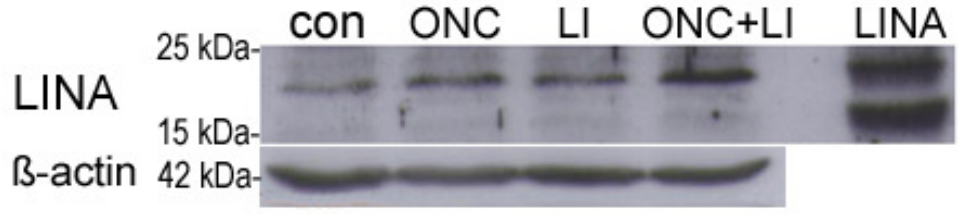

Figure 4-24: Upregulation of LINA in retina after ONC+LI

Upregulation of LINA after ONC+LI measured by western blot analysis. The total protein of retinas was obtained from differently treated retinas 5 days after surgery. Western blot analysis showed the slight upregulation of the LINA protein in retina protein lysate treated with ONC+LI compared with other groups. Bands of ß-actin verified same amounts of protein per lane. This western blot was done using the polyclonal rabbit serum anti-LINA antibody and repeated at least three times to confirm results.

In summary, I investigated the expression pattern of endogenous LINA with two different anti-LINA antibodies using the immunocyto- and –histochemical method and western blot analysis. After verifying the specificity of anti-LINA antibodies, I detected that the expression pattern of endogenous LINA showed as a punctuate form, located in cell body, dendrites and axon, found mainly in the CNS, such as cerebellum, cortex and hippocampus. Additionally LINA showed a partial co-

localization with ProSAP2, indicating the possible role of LINA in synapse. PC12 cells differentiated with NGF showed also the upregulation of LINA and through the LI and ONC+LI, endogenous LINA expression was also upregulated in retina of rat, confirming the upregulation of LINA gene expression by ONC+LI (Table 2), suggesting that LINA may be somehow involved in the inflammatory reaction for the regeneration of RGCs.

4.6 Investigation of LINA expression on mRNA level

After investigating the expression pattern of LINA on protein level using the anti-LINA antibodies, I investigated next the LINA expression on mRNA level to confirm the expression pattern of LINA in another aspect.

To determine the LINA expression on mRNA level, I investigated the LINA expression in the mouse embryo using the *in situ* hybridization (ISH) approach. Since mouse embryos represent a powerful model system for gene discovery and understanding of gene function for development and LINA has the same sequence with mouse [redacted] it was more useful to use the mouse as a model system for responding to the issues considering the expression of LINA on mRNA level.

9.25 day post coitum (dpc) mouse embryos were used, kindly provided by Dr. Ovidiu Sirbu in the institute of Biochemistry at Ulm University and prepared according to protocol (shown 3.6). In order to generate the LINA mRNA probe for ISH, the whole LINA cDNA was cloned into a pCS2+ expression vector flanked by SP6 (5´) and T7 (3´) promoters and further retro-transcribed using T7 polymerase in the presence of DIG-labelled nucleotides. Sense RNA control probes were similarly transcribed in the presence of DIG-labelled nucleotides using SP6 polymerase. The probes were then purified on agarose columns and integrity of the probes verified by electrophoresis on agarose gels. E9.25 old mouse embryos were used as experimental samples, since at this stage eye development in the mouse embryo is well under way, starting at 8 dpc. After dehydration and rehydration in successive methanol/PBS, embryos were permeated using proteinase K, refixed in PFA/Glutaraldehyde and hybridized overnight at 68°C. Incubation overnight at 4°C with an alkaline-phosphatase linked antibody and further incubation in NBT/BCIP produced a strong hybridization signal for LINA mRNA in the forebrain, optic cup, branchial arches and pharynx, otic vesicles and all the somites (Figure 4-25, A, B). These signals were considered to be specific, since the labelled sense probe did not give any specific signals under the same hybridization and washing conditions (Figure 4-25, C).

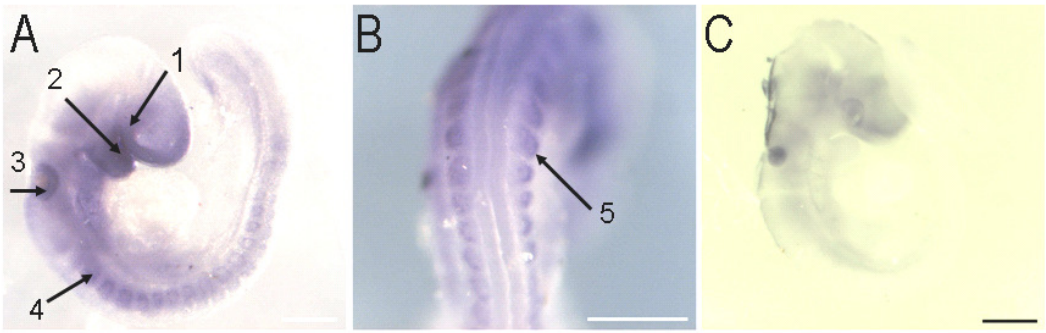

Figure 4-25: Whole mount mouse embryo stained by *in situ* hybridization (ISH)

Whole mount ISH with antisense (A, B) and sense LINA probes (C) on 9.25 dpc mouse embryos; lateral view (A, C) and dorsal view (B). 1: eye; 2: first branchial arch; 3: otic vesicle; 4, 5: somites. Scale bars: 1 mm. These experiments were repeated at least three times to confirm results.

The expression of LINA in the optic cup, head mesoderm, and forebrain in embryos showed a similar expression pattern as the result of immunocyto- and -histochemistry. But it was interesting that LINA was also expressed in somites of embryos, which will be developed into dermis, skeletal muscle, and vertebrae.
In summary, LINA mRNA was detected in eye in mouse embryo including branchial arch, otic vesicle, and somites. This result indicated that LINA is expressed also in the embryos rising further questions of interesting role of LINA gene in the development.

5 Discussion

5.1 LINA ([redacted]a new RING finger protein

Injury to the CNS results in very limited regeneration of axons and this axonal injury causes many complex reactions involving nerve cells and glial cells. Fischer et al. (2004b) showed that rat RGCs enter into a robust regenerative state 4 days after axotomy and lens injury (LI). They found that this regenerative switch is associated with a dramatic change in gene expression and less than one hundred genes revealed significant expression changes between regenerating and axotomized RGCs from 16,000 genes represented on the microarrays.
My work described the initial characterization of a gene of rat, named LINA in our lab for the first time, which is upregulated by axonal injury and LI. LINA consists of 155 amino acids and contains a characteristic sequence motif known as the RING-H2 finger motif and a hydrophobic transmembrane domain. The gene coding LINA is a homology of a gene known in mouse as [redacted]and located in chromosome 8, p12 in rat, mouse and human. The amino acid sequence of rat LINA showed 100% identity with mouse [redacted]and only 5 amino acids difference to human [redacted]On the RNA level rat and mouse [redacted]showed a homology of 95.7% within the coding sequence. Whereas, the RNA sequence homology between rat and human [redacted]was 89.7%. I also found the LINA protein sequence in other species from the sequence database bank, for example, horse, cattle, fugu, chicken, dog, duckbill, opossum, rhesus monkey, xenopus tropica and zebrafish (data not shown). The sequence analysis showed that the transmembrane domain to RING finger domain is highly conserved in each species, demonstrating that LINA is one of the proteins which contain a highly conserved domain.

Through the characterization of its hydrophobic transmembrane domain, I showed that LINA is likely a membrane associated protein. Membrane proteins often possess a signal sequence at the N-terminal end (von Heijne, 1983). The bioinformatic protein analysis predicted that LINA may have a signal sequence or signal anchor spanning the amino acids 1 to 19 at its N-terminus. The signal sequence orients to which cell compartment the proteins finally have to move. It is usually composed of about 15 – 60 amino acids and often cleaved off from the protein (Alberts et al., 2001). There are concrete amino acid sequences as a signal sequence for a nucleus (for example, PPKKKRKV), an ER (for example,

KDEL), mitochondrial matrix (for example, MLSLRQSIRFFKPATRTLCSSRYLL) and peroxisome (for example, SKL) as a target (Alberts et al., 2001). Therefore, I compared the N-terminal sequence of the LINA protein with all known signal sequences, but no similarity was found. However, when I fused a HA-tag at the N-terminus end of the LINA protein, I detected this HA-tagged LINA protein neither by western blot analysis nor by immunocytochemistry, suggesting that LINA might have a so far unknown signal sequence at the N-terminus, which is cleaved off by the signal peptidase after integration of the transmembrane domain in the double lipid membrane layer.

I further characterized LINA to have an asparagine-linked glycosylation (*N*-glycosylation) site at the 20th amino acid, where the process of addition of saccharides occurs. The *N*-glycosylation is a highly conserved protein post-translational modification reaction that occurs in the synthesis of membrane and secreted proteins in all eukaryotes (Silberstein and Gilmore, 1996). From western blot analysis, the HA-tagged LINA protein was detected at 19 kDa as a monomer by an anti-HA antibody. However, this overexpressed HA-tagged LINA protein additionally ran at 23 kDa, indicating that this additional band could result from a post-translational modification of the LINA protein. The bioinformatic protein analysis suggested that LINA has one predicted *N*-glycosylation site at the 20th amino acid with a tripeptide sequence pattern, Asn-X-Ser, where X could be any amino acid except proline. LINA contains a tripeptide, Asn-Lys-Ser sequence pattern. For *N*-glycosylation, the oligosaccharide chain is linked to the NH_2 terminal of the asparagine side chain (Welply et al., 1983). Treatment with a glycosidase (PNGaseF) and a point mutation at the 20th amino acid (N20Q) by substituting the asparagine (N) with glutamine (Q) confirmed finally that LINA is glycosylated at its N20. Usually the polysaccharide chains attached to the target proteins have a variety of functions in cells (Dennis et al., 1999; Yan and Lennarz, 2005; Rudd et al, 2001; Crocker and Feizi, 1996). For example, some proteins do not fold correctly unless they are glycosylated first (Yan and Lennarz, 2005). Polysaccharide linked to proteins allows stability on some secreted glycoproteins and also glycosylation may play a role in cell-cell adhesion (Rudd et al, 2001; Crocker and Feizi, 1996). Watson et al. (1999) characterized the glycosylation of the NGF receptor tyrosine kinase receptor A (TrkA). TrkA contains four potential *N*-glycosylation sites which are highly conserved and nine additional sites which are less conserved (Watson et al., 1999). Through the mutations of both conserved and variable other sites, they showed this unglycosylated TrkA failed to localize to the cell surface and finally could not promote neuronal differentiation in PC12

cells. However, glycosylation itself does not seem to be always necessary for the correct transport of the protein. Studies that block the glycosylation show that normal proteins are still produced and this blocking does not seem to interfere severely with the viability of the cells. Tansky et al. (2007) showed that although they blocked the *N*-glycosylation sites on the neurokinin 1 receptor by inducing a mutation, all mutant receptors were able to bind to their substance with similar affinities and internalize, when compared with a wild type receptor. Therefore, I also investigated whether the glycosylation of LINA was necessary for its neurite outgrowth promoting effects in PC12 cells. $LINA^{N20Q}$ lacking the *N*-glycosylation site showed a similar function for the neurite outgrowth in PC12 cells, when compared with wild type LINA ($LINA^{WT}$), demonstrating that the glycosylation of LINA does not play a crucial role for its neurite outgrowth function in PC12 cells.

Protein *N*-glycosylation has been known as a highly conserved metabolic process and reported its cellular functions in secretion, cytoskeletal organization, proliferation and apoptosis. But the functional consequences of *N*-glycosylation in each protein differ from subtle to significant (Kukuruzinska and Lennon, 1998). Probably, the glycosylation of LINA has a subtle effect for its neurite outgrowth function.

In addition to these biochemical charaterizations of LINA demonstrated above, I found that LINA can self-assemble and form a ternary complex by its RING finger domain *in vitro*. The destabilization of the first zinc binding site did not abolish the ability to self-assemble and the whole RING finger domain of LINA might function as the binding domain. It is known that the RING finger domain has diverse functions (Li and Seth, 2004; Wooff et al., 2004; Meroni and Diez-Roux, 2005; Pan et al., 2005), but some studies described that the RING finger domain functions biochemically for a complex formation (Wooff et al., 2004; Pan et al., 2005; Peng et al, 2000; Kentsis et al., 2002). For example, Peng et al. (2000) showed that the RING finger domain of transcriptional intermediary factor 1 beta (TIFß) is required for the formation of a homohexameric complex, which is finally associated with DNA binding and transcriptional repression. Furthermore, Kentsis et al. (2002) showed that purified arenaviral protein Z self-assembles in a RING finger domain-dependent manner, suggesting that such a self assembly is a general property of RING domains for biochemical processes in cells.

Here I observed that the RING finger domain of LINA is required for the formation of a ternary complex, however, the role of this compex formation of LINA remains to be determined in the future to understand the mechanism underlying its function.

5.2 What could be the signaling mechanism underlying the neurite outgrowth promoting effects of LINA?

The functional characterization of LINA in this study showed that LINA has a neurite outgrowth promoting effect in PC12 cells exposed to NGF. LINA overexpressing PC12 cells showed a 2.5 fold stronger neurite outgrowth 3 days after NGF treatment compared with untreated controls. Furthermore, this neurite outgrowth effect did not desentisize the growth cones against the inhibitory effects of myelin. Additionally, I showed that the neurite outgrowth promoting effects of LINA required an intact RING finger domain. Among many different LINA mutants, I observed in the PC12 cell assay that $LINA^{C93A}$, which has a point mutation in the first zinc finger, functioned as a dominant negative variant of LINA. A point mutation in the first zinc finger induced the entire functional abrogation of LINA, suggesting that the RING finger domain of LINA is significantly involved in its functional role.

Regarding the NGF dependence of LINA promoting neurite outgrowth, a role of NGF should be discussed as possible postulations for the signaling mechanism underlying neurite outgrowth promoting effect of LINA related with mediating the neuritogenesis and elongation of neurites. NGF is well known for its ability to stimulate the formation of neurites in neuronal cell lines (Negishi and Katoh, 2002; Tarsa and Balkowiec, 2008) and the NGF treatment of PC12 cells causes a decrease in active Rho and its effector Rho-kinase downstream of Rac activation, which results in neuritogenesis and mediating the neurite promoting effects (Nishiki et al., 1990; Aoki et al., 2004). Nusser et al. (2002) showed that NGF treatment rapidly translocates RhoA from the plasma membrane to the cytosol and simultaneously decreases RhoA affinity to its target Rho-associated kinase (ROCK), a key mediator of neurite outgrowth. However they showed also that this effect was transient. During the elongation phase of neuronal differentiation, 2 days after NGF treatment, RhoA was relocated to the plasma membrane and its activation state returned to the control level. This shows that NGF somehow inactivated RhoA-ROCK signaling during the initiation phase of neuronal differentiation. I observed the highest neurite outgrowth promoting effect of LINA in PC12 cells at least 3 days after NGF treatment. Furthermore, non-presented data indicate no significant difference of neurite outgrowth between LINA groups and control groups 2 days after NGF treatment. It is thus possible that LINA may function as a mediator for permanent translocation of RhoA compensating for the transient NGF effect and finally decreases RhoA affinity to ROCK.

TrkA and $p75^{NTR}$ are cell surface receptors for NGF (Chao et al., 1998). Binding of NGF to TrkA induces internalization of the receptor into signaling vesicles, which mediates NGF differentiation (Zhang et al., 2000). Hondermarck et al. (1992) showed that dipeptide inhibitors of the ubiquitin pathway blocked NGF-induced differentiation of PC12 cells, suggesting that TrkA might function in an ubiquitin-dependent manner. Some studies showed that ubiquitination is involved in neurite outgrowth of PC12 cells mediated by NGF (Obin et al. 1999; Kavakebi et al. 2005). The diverse proteins are involved in ubiquitination and many recent observations suggest that the RING finger protein plays a prominent role in the ubiquitination reaction as an E3 ligase (Freemont, 2000; Joazeiro and Weissman, 2000; Fang et al., 2000; Honda and Yasuda, 2000; Meroni and Diez-Roux, 2005). Some RING finger proteins have been reported for its functional role related in the neurite outgrowth and axon regeneration promoting effect (El-Husseini and Vincent, 1999; Olsson et al., 1999; Araki et al., 2001; van Diepen et al., 2005; Tursun et al., 2005). For example, Araki et al. (2001) identified the new RING finger protein Nin283 whose gene expression was upregulated after nerve injury in Schwann cells and El-Husseini and Vincent (1999) identified a novel RING finger protein, BERP, a specific partner for the tail domain of myosin V. Neurodap1, a novel RING-H2 motif protein is downregulated by facial nerve axotomy (Nakayama et al., 1995), RNF6, as an E3 ubiquitin ligase regulates the growth cone actin dynamics (Tursun et al., 2005), and a novel RING finger protein, MIR interacts with the cytoskeleton and regulates cell motility in PC12 cells (Olsson et al., 1999). As a novel RING finger protein, I speculated that LINA might also be involved in ubiquitination.

Ubiquitin (Ub) is composed of a highly conserved 76 amino acids sequence and is involved in variable cellular processes. Ubiquitination of proteins requires the cascade action of three enzymes; ubiquitin activating enzyme (E1), which forms a high energy thioester bond with ATP, the ubiquitin conjugating enzyme (E2), which transfers the activated ubiquitin to the active site cysteine, and the ubiquitin ligase (E3), which is responsible for specific substrate recognition and facilitates the transfer of Ub from E2 to the target protein (Laney and Hochstrasser, 1999; Freemont, 2000). Monoubiquitination and polyubiquitination have been reported as important signals for the internalization of membrane proteins (Haglund et al., 2003a; Haglund et al., 2003b). Geetha et al. (2005) showed that the NGF receptor, TrkA, could be regulated by ubiquitination and this ubiquitination led to the internalization of TrkA. They showed that TrkA forms a multimeric complex and TNF receptor-associated factor 6 (TRAF6) ubiquitinates TrkA at lysine 485

(K485) as E3 ligase. Interestingly, there remained a possibiltiy that K485 might be targeted by another E3 ligase as well. Additionally, it has been shown that the site K485 within the TrkA receptor is necessary for further TrkA-induced signaling with mitogen activated protein kinase (MAPK), extracelluar signal related protein kinase 5 (Erk5) and active human protein kinase (Akt), which connects to NGF-regulated expression of specific genes for survival and differentiation (Geetha et al., 2005). The diverse proteins are known to be regulated by ubiquitination, however, until recently relatively few E3s were known (Joazeiro and Weissman, 2000). As a novel RING finger protein, it should be elucidated in the future whether LINA might be involved in the ubiquitination reaction as an E3 ligase for the NGF-dependent neurite outgrowth in PC12 cells.

I next generated the expression plasmids carrying either LINA or LINA^{C93A} for adeno-associated virus system (AAVs), which were used further for investigation of the fuctional effect of LINA *in vivo*. Viral transfection of RGCs represents a powerful tool in investigation the role of gene products in axon regeneration (Grant et al., 1997; Martin et al., 2002; Martin et al., 2003; Dinoculescu et al., 2005; Leaver et al., 2006) and in our lab, we observed further this functional effect of LINA and LINA^{C93A} using a gene therapeutic approach based on adeno-associated virus system in RGCs of rats. The non-presented data indicated that overexpression of LINA promotes axon regeneration and LINA^{C93A} abrogates this effect also *in vivo*.

The analysis of the subcellular localization of LINA yielded some insights into its signaling mechanism. In PC12 cell system, exogenously expressed LINA showed a partial co-localization with the trans-Golgi network (TGN) marker TGN38 and it was further detected in the cell body and neurites showing a punctate staining pattern. LINA did not co-localize with lysosomes or peroxisomes. LINA partially co-localized with BACE1-GFP-fusion protein, indicating that LINA may be located in endosomal vesicle compartment of a secretory pathway. To test this hypothesis I performed life cell imaging, which showed rapidly moving vesicles within the cells, providing further evidence that LINA is mainly localized in vesicles.

Recently, Lussier et al. (2008) have reported a new RING finger protein, RNF24, which interacts with transient receptor potential cation channel superfamily 6 (TRPC6) in the Golgi apparatus. They found that the RNF24, as a membrane protein, is localized in the Golgi apparatus showing a punctate staining pattern, consistent with the localization of LINA. Interestingly, the RNF24 has a high sequence homology with the LINA including a transmembrane region and a $C_3H_2C_3$ type RING finger domain. In their study, Lussier et al. (2008) showed that the

overexpression of RNF24 promoted the subcellular redistribution of TRPC6, suggesting that RNF24 as a new TRPC6 interacting protein affects the intracellular trafficking of the TRPC6 without influencing its activity. It has been reported also that they did not detect any change in the ubiquitination of TRPC6 following the overexpression of RNF24, suggesting that in their system, RNF24 is not involved in the ubiquitination as an E3 ligase which is often considered as a function of the RING finger protein.

Besides, some other RING finger proteins have been also reported related in its function and the subcellular localization. A novel RING finger protein BERP, which was found by El-Husseini and Vincent (1999), is expressed in a punctuate pattern in the neurites and growth cones of PC12 cells and another RING finger protein Nin283 is located in the endosome compartment involved in ubiquitin-mediated protein modification (Araki et al., 2001).

With further various endosomal vesicle approaches, it should be elucidated in the future in detail in which endosomal compartment is LINA exactly located. In order to answer this question further and to understand more about the signaling mechanism of LINA underlying its functional effect, it had been significantly considered and tried to find and verify the interacting protein of LINA. For this purpose I used the yeast two hybrid method and immunoprecipitation, but no positive candidates were found in those systems I used (data not shown).

From the investigation of LINA expression using the affinity purified anti-LINA antibody, I found that LINA is highly expressed in the retina, cortex, cerebellum and hippocampus and it is also induced by nerve growth factor in PC12 cells. Endogenous LINA in PC12 cells, cultured RGCs and embryonic hippocampal neurons showed a granular staining pattern with a pronounced accumulation in the TGN region, especially expressed in the cell bodies and regenerating axons in cultured RGCs.

These results from the antibody staining are well co-related with the result of the screening of LINA mRNA level in different tissues with RT-PCR in our lab (data not shown) and also the result of the investigation of LINA mRNA in mouse embryos.

In particular, I observed partial co-localization of LINA with a postsynaptic protein ProSAP2 in embryonic hippocampal neuron. Differently from the PC12 cell system, the hippocampal neuron system provided the possibility to investigate the localization and the promising role of LINA in dendritic synapses of neurons. It has been reported that ProSAP2 is preferentially expressed in the cerebral cortex and the cerebellum and it is involved in the postsynaptic density of excitatory

synapses and in the dendrite formation (Bonaglia et al., 2001; Böckers et al., 2004). The postsynaptic density is a cluster which consists of cytoskeletal and regulatory proteins located direct behind to the postsynaptic membrane (Ziff EB, 1997) and many proteins in the postsynaptic density are known that they are involved in anchoring and trafficking the postsynaptic receptors (Klauck and Scott, 1995; Kennedy MB, 1993). Some of these proteins make a contact the cytoplasmic domains of ion channels in the postsynaptic membrane to regulate the intracellular ionic fluxes (Hsueh et al., 1997). The facts that LINA showed a high homology with RNF24, which interacts with the cation channel receptor protein TRPC6, as discussed above, and that LINA showed a partial co-localization with the postsynaptic protein ProSAP2 in hippocampal neurons supposed that LINA might play a role in the postsynaptic region, such as modulating the activity of neurotransmitter receptors or signal transduction machinery.

Besides those speculations, however, I cannot exclude the possibility that the purifed antibody could still detect some unspecific proteins except LINA in different cell- and tissue systems, since it has been reported and discussed that some purchasable or custom-made antibodies show often unexpected cross-linking effects with other proteins (Hauk et al., 2008). Therefore, although the expressing pattern of endogenous LINA detected by purified anti-LINA antibody shows the accordance with those of exogenously overexpressed LINA and mRNA of LINA, it could be still possible that purified anti-LINA antibody could recognize not only LINA protein but also some other unspecific proteins and react differently in different cell systems.

In parallel with the immunocyto- and –histochemistry investigation of LINA expression using the affinity purified anti-LINA antibody, I investigated the different expression pattern of LINA in western blot analysis using polyclonal rabbit serum anti-LINA antibody. Since the serum detected the LINA protein overexpressed in HEK293 cells in western blot analysis (Figure 4-16), I used this serum for further approaches without any further purification. Anyhow it can be arguable that this serum can have an unspecific effect for detecting the endogenous expressed LINA, since the serum recognized an unspecific protein in HEK293 cells slightly bigger than LINA. But the result of detection of endogenous LINA expression in retina treated different surgical operations with this serum in western blot analysis (Figure 4-24) was consistent with that of immunostaining of retina (Figure 4-23). Although this detected protein shows the same size with the overexpressed LINA which was used as a positive control, the additional experiment to block the anti-

body with LINA protein should be performed further in order to exclude any arguments of unspecificity of serum.

In summary, I characterized a new RING finger protein, LINA, which was one of the genes, whose expression was upregulated in purified RGCs treated by ONC and ONC + LI. The characterization included many aspects. First I analyzed the genetic sequence of LINA and compared with other species. As a biochemical characterization using the immunoprecipitation and cross-linking method, I showed that LINA as a membrane associated glycoprotein formed a ternary complex with its RING finger domain. Additionally formation of a ternary complex of LINA was investigated also by a gel filtration method (data not shown). From the investigation of mRNA and protein expression, I showed that LINA was mainly expressed in retina and the rat brain such as cortex, cerebellum, hippocampus. Additionally I characterized the subcellular localization of LINA, suggesting that LINA might be involved in secretory vesicles in PC12 cell system and also might have a promising role in postsynaptic vesicles in hippocampal neuron system. In particular, I showed that LINA expression was strongly increased in differentiating PC12 cells after NGF treatment and the overexpression of LINA in PC12 cells enhanced the neurite outgrowth exposed to NGF and the RING finger domain plays a significant role for this function.

It is thus promising to develop the new strategies to improve the recovery after CNS injuries with LINA. CNS injuries result in an exposure of damaged axons to inhibitory substrates and finally the damaged axons fail to reinnervate former targets. Many experimental strategies were performed to overcome this inhibitory signaling and to enhance axonal regeneration. Since peripheral nerves lack major inhibitory molecules present in the CNS myelin, the sciatic nerve graft model was used to study a regenerative response of RGCs (Thanos et al., 1997). Lingor et al. (2008) used the combinatorial treatment with CNTF and ROCK inhibitor in addition to the transplantation of sciatic nerve to the optic nerve stump. They activated the intrinsic survival pathway via CNTF treatment and simultaneously attenuated growth inhibitory signaling cascade using ROCK inhibitor to obtain the additive effects for regeneration. Schwann cells are also known to promote axon elongation after injury by secreting F-Spondin, a developmental protein (Burstyn-Cohen et al., 1998). Thus, Schwann cell transplantation into the damaged CNS was often tested for the better treating demyelinating disorders and spinal cord injuries (Kamada et al., 2005; Kohama et al., 2001; Bachelin et al., 2005). There are some recent studies aimed of axonal regeneration for spinal cord injuries using the transplantation of neural stem cells and precursor cells (Murakami et

al., 2004; Okano et al., 2007a; Okano et al., 2007b). Some molecular therapies blocking the axon regeneration inhibitors were used for the functional recovery after nervous system injuries and diseases (Tsai et al., 2002; Lenzlinger et al., 2005; Yang et al., 2006; Logan et al., 2006; Freund et al., 2007; Hu et al., 2007; Cao et al., 2008; Yang and Schnaar, 2008). Since LINA is essentially involved in the axonal regeneration, it must be promising to develop the combinatorial approach with LINA overexpression and other substances, such as, CNTF, C3, or axon regeneration inhibitors for enhanced axon regeneration after CNS injuries.

6 References

Adams JM, Cory S (1998)
The Bcl-2 protein family: arbiters of cell survival. Science 281:1322-1326.

Adams JM, Cory S (2001)
Life-or-death decisions by the Bcl-2 protein family. Trends Biochem Sci 26:61-66.

Alberts B, Bray D, Johnson A, Lewis J, Raff M, Roberts K, Walter P (2001)
Molekularbiologie der Zelle, VCH, Weinheim,1986

Aoki K, Nakamura T, Matsuda M (2004)
Spatio-temporal regulation of Rac1 and Cdc42 activity during nerve growth factor-induced neurite outgrowth in PC12 cells. J Biol Chem 279:713-719.

Araki T, Nagarajan R, Milbrandt J (2001)
Identification of genes induced in peripheral nerve after injury. Expression profiling and novel gene discovery. J Biol Chem 276:34131-34141.

Arber S, Barbayannis FA, Hanser H, Schneider C, Stanyon CA, Bernard O, Caroni P (1998)
Regulation of actin dynamics through phosphorylation of cofilin by LIM-kinase. Nature 393:805-809.

Bachelin C, Lachapelle F, Girard C, Moissonnier P, Serguera-Lagache C, Mallet J, Fontaine D, Chojnowski A, Le Guern E, Nait-Oumesmar B, Baron-Van Evercooren A (2005)
Efficient myelin repair in the macaque spinal cord by autologous grafts of Schwann cells. Brain 128:540-549.

Baer R, Ludwig T (2002)
The BRCA1/BARD1 heterodimer, a tumor suppressor complex with ubiquitin E3 ligase activity. Curr Opin Genet Dev 12:86-91.

Bamburg JR (1999)
Proteins of the ADF/cofilin family: essential regulators of actin dynamics. Annu Rev Cell Dev Biol 15:185-230.

Bennett BD, Denis P, Haniu M, Teplow DB, Kahn S, Louis JC, Citron M, Vassar R (2000)

A furin-like convertase mediates propeptide cleavage of BACE, the Alzheimer's beta -secretase. J Biol Chem 275:37712-37717.

Benson MD, Romero MI, Lush ME, Lu QR, Henkemeyer M, Parada LF (2005) Ephrin-B3 is a myelin-based inhibitor of neurite outgrowth. Proc Natl Acad Sci U S A 102:10694-10699

Berkelaar M, Clarke DB, Wang YC, Bray GM, Aguayo AJ (1994)
Axotomy results in delayed death and apoptosis of retinal ganglion cells in adult rats. J Neurosci 14:4368-4374.

Berry M, Carlile J, Hunter A (1996)
Peripheral nerve explants grafted into the vitreous body of the eye promote the regeneration of retinal ganglion cell axons severed in the optic nerve. J Neurocytol 25:147-170.

Bishop AL, Hall A (2000)
Rho GTPases and their effector proteins. Biochem J 348 Pt 2:241-255.

Bito H, Furuyashiki T, Ishihara H, Shibasaki Y, Ohashi K, Mizuno K, Maekawa M, Ishizaki T, Narumiya S (2000)
A critical role for a Rho-associated kinase, p160ROCK, in determining axon outgrowth in mammalian CNS neurons. Neuron 26:431-441.

Bockers TM, Segger-Junius M, Iglauer P, Bockmann J, Gundelfinger ED, Kreutz MR, Richter D, Kindler S, Kreienkamp HJ (2004)
Differential expression and dendritic transcript localization of Shank family members: identification of a dendritic targeting element in the 3' untranslated region of Shank1 mRNA. Mol Cell Neurosci 26:182-190.

Bonaglia MC, Giorda R, Borgatti R, Felisari G, Gagliardi C, Selicorni A, Zuffardi O (2001)
Disruption of the ProSAP2 gene in a t(12;22)(q24.1;q13.3) is associated with the 22q13.3 deletion syndrome. Am J Hum Genet 69:261-268.

Borden KL, Freemont PS (1996)
The RING finger domain: a recent example of a sequence-structure family. Curr Opin Struct Biol 6:395-401.

Bunge RP, Puckett WR, Hiester ED (1997)
Observations on the pathology of several types of human spinal cord injury, with emphasis on the astrocyte response to penetrating injuries. Adv Neurol 72:305-315.

Burstyn-Cohen T, Frumkin A, Xu YT, Scherer SS, Klar A (1998)
Accumulation of F-spondin in injured peripheral nerve promotes the outgrowth of sensory axons. J Neurosci 18:8875-8885.

Bush TG, Puvanachandra N, Horner CH, Polito A, Ostenfeld T, Svendsen CN, Mucke L, Johnson MH, Sofroniew MV (1999)
Leukocyte infiltration, neuronal degeneration, and neurite outgrowth after ablation of scar-forming, reactive astrocytes in adult transgenic mice. Neuron 23:297-308.

Cai D, Shen Y, De Bellard M, Tang S, Filbin MT (1999)
Prior exposure to neurotrophins blocks inhibition of axonal regeneration by MAG and myelin via a cAMP-dependent mechanism. Neuron 22:89-101.

Cameron HA, McKay RD (2001)
Adult neurogenesis produces a large pool of new granule cells in the dentate gyrus. J Comp Neurol 435:406-417.

Cao Y, Shumsky JS, Sabol MA, Kushner RA, Strittmatter S, Hamers FP, Lee DH, Rabacchi SA, Murray M (2008)
Nogo-66 receptor antagonist peptide (NEP1-40) administration promotes functional recovery and axonal growth after lateral funiculus injury in the adult rat. Neurorehabil Neural Repair 22:262-278.

Caroni P, Schwab ME (1993)
Oligodendrocyte- and myelin-associated inhibitors of neurite growth in the adult nervous system. Adv Neurol 61:175-179.

Chao M, Casaccia-Bonnefil P, Carter B, Chittka A, Kong H, Yoon SO (1998)
Neurotrophin receptors: mediators of life and death. Brain Res Brain Res Rev 26:295-301.

Chaudhry N, Filbin MT (2007)
Myelin-associated inhibitory signaling and strategies to overcome inhibition. J Cereb Blood Flow Metab 27:1096-1107.

Chen DF, Jhaveri S, Schneider GE (1995)
Intrinsic changes in developing retinal neurons result in regenerative failure of their axons. Proc Natl Acad Sci U S A 92:7287-7291.

Chen DF, Schneider GE, Martinou JC, Tonegawa S (1997)
Bcl-2 promotes regeneration of severed axons in mammalian CNS. Nature 385:434-439.

Chen MS, Huber AB, van der Haar ME, Frank M, Schnell L, Spillmann AA, Christ F, Schwab ME (2000)
Nogo-A is a myelin-associated neurite outgrowth inhibitor and an antigen for monoclonal antibody IN-1. Nature 403:434-439.

Crocker PR, Feizi T (1996)
Carbohydrate recognition systems: functional triads in cell-cell interactions. Curr Opin Struct Biol 6:679-691.

DeBellard ME, Tang S, Mukhopadhyay G, Shen YJ, Filbin MT (1996)
Myelin-associated glycoprotein inhibits axonal regeneration from a variety of neurons via interaction with a sialoglycoprotein. Mol Cell Neurosci 7:89-101.

Dennis JW, Granovsky M, Warren CE (1999)
Protein glycosylation in development and disease. Bioessays 21:412-421.

Dickson BJ (2001)
Rho GTPases in growth cone guidance. Curr Opin Neurobiol 11:103-110.

Dinculescu A, Glushakova L, Min SH, Hauswirth WW (2005)
Adeno-associated virus-vectored gene therapy for retinal disease. Hum Gene Ther. 16(6):649-663.

Dodd DA, Niederoest B, Bloechlinger S, Dupuis L, Loeffler JP, Schwab ME (2005)
Nogo-A, -B, and -C are found on the cell surface and interact together in many different cell types. J Biol Chem 280:12494-12502.

Domeniconi M, Cao Z, Spencer T, Sivasankaran R, Wang K, Nikulina E, Kimura N, Cai H, Deng K, Gao Y, He Z, Filbin M (2002)
Myelin-associated glycoprotein interacts with the Nogo66 receptor to inhibit neurite outgrowth. Neuron 35:283-290.

El-Husseini AE, Vincent SR (1999)
Cloning and characterization of a novel RING finger protein that interacts with class V myosins. J Biol Chem 274:19771-19777.

Fagg GE, Matus A (1984)
Selective association of N-methyl aspartate and quisqualate types of L-glutamate receptor with brain postsynaptic densities. Proc Natl Acad Sci U S A 81:6876-6880.

Fang S, Jensen JP, Ludwig RL, Vousden KH, Weissman AM (2000)

Mdm2 is a RING finger-dependent ubiquitin protein ligase for itself and p53. J Biol Chem 275:8945-8951.

Fawcett JW, Asher RA (1999)
The glial scar and central nervous system repair. Brain Res Bull 49:377-391.

Finkbeiner S, Tavazoie SF, Maloratsky A, Jacobs KM, Harris KM, Greenberg ME (1997)
CREB: a major mediator of neuronal neurotrophin responses. Neuron 19:1031-1047.

Fischer D, Pavlidis M, Thanos S (2000)
Cataractogenic lens injury prevents traumatic ganglion cell death and promotes axonal regeneration both in vivo and in culture. Invest Ophthalmol Vis Sci 41:3943-3954.

Fischer D, Heiduschka P, Thanos S (2001)
Lens-injury-stimulated axonal regeneration throughout the optic pathway of adult rats. Exp Neurol 172:257-272.

Fischer D, He Z, Benowitz LI (2004a)
Counteracting the Nogo receptor enhances optic nerve regeneration if retinal ganglion cells are in an active growth state. J Neurosci 24:1646-1651.

Fischer D, Petkova V, Thanos S, Benowitz LI (2004b)
Switching mature retinal ganglion cells to a robust growth state in vivo: gene expression and synergy with RhoA inactivation. J Neurosci 24:8726-8740.

Fischer D, Hauk TG, Muller A, Thanos S (2008)
Crystallins of the beta/gamma-superfamily mimic the effects of lens injury and promote axon regeneration. Mol Cell Neurosci 37:471-479.

Fitch MT, Doller C, Combs CK, Landreth GE, Silver J (1999)
Cellular and molecular mechanisms of glial scarring and progressive cavitation: in vivo and in vitro analysis of inflammation-induced secondary injury after CNS trauma. J Neurosci 19:8182-8198.

Fournier AE, GrandPre T, Strittmatter SM (2001)
Identification of a receptor mediating Nogo-66 inhibition of axonal regeneration. Nature 409:341-346.

Freemont PS (1993)
The RING finger. A novel protein sequence motif related to the zinc finger. Ann N Y Acad Sci 684:174-192.

Freemont PS (2000)
RING for destruction? Curr Biol 10:R84-87.

Freund P, Wannier T, Schmidlin E, Bloch J, Mir A, Schwab ME, Rouiller EM (2007)
Anti-Nogo-A antibody treatment enhances sprouting of corticospinal axons rostral to a unilateral cervical spinal cord lesion in adult macaque monkey. J Comp Neurol 502:644-659.

Geetha T, Jiang J, Wooten MW (2005)
Lysine 63 polyubiquitination of the nerve growth factor receptor TrkA directs internalization and signaling. Mol Cell 20:301-312.

Gmachl M, Gieffers C, Podtelejnikov AV, Mann M, Peters JM (2000)
The RING-H2 finger protein APC11 and the E2 enzyme UBC4 are sufficient to ubiquitinate substrates of the anaphase-promoting complex. Proc Natl Acad Sci U S A 97:8973-8978.

GrandPre T, Nakamura F, Vartanian T, Strittmatter SM (2000)
Identification of the Nogo inhibitor of axon regeneration as a Reticulon protein. Nature 403:439-444.

Grandpre T, Strittmatter SM (2001)
Nogo: a molecular determinant of axonal growth and regeneration. Neuroscientist 7:377-386.

Grant CA, Ponnazhagan S, Wang XS, Srivastava A, Li T (1997)
Evaluation of recombinant adeno-associated virus as a gene transfer vector for the retina. Curr Eye Res 16:949-56.

Greene LA, Tischler AS (1976)
Establishment of a noradrenergic clonal line of rat adrenal pheochromocytoma cells which respond to nerve growth factor. Proc Natl Acad Sci U S A 73:2424-2428.

Haglund K, Di Fiore PP, Dikic I (2003a)
Distinct monoubiquitin signals in receptor endocytosis. Trends Biochem Sci 28:598-603.

Haglund K, Sigismund S, Polo S, Szymkiewicz I, Di Fiore PP, Dikic I (2003b)
Multiple monoubiquitination of RTKs is sufficient for their endocytosis and degradation. Nat Cell Biol 5:461-466.

Harvey AR, Hu Y, Leaver SG, Mellough CB, Park K, Verhaagen J, Plant GW, Cui Q (2006)
Gene therapy and transplantation in CNS repair: the visual system. Prog Retin Eye Res 25:449-489.

Hattori C, Asai M, Oma Y, Kino Y, Sasagawa N, Saido TC, Maruyama K, Ishiura S (2002)
BACE1 interacts with nicastrin. Biochem Biophys Res Commun 293:1228-1232.

Hauk TG, Muller A, Lee J, Schwendener R, Fischer D (2008)
Neuroprotective and axon growth promoting effects of intraocular inflammation do not depend on oncomodulin or the presence of large numbers of activated macrophages. Exp Neurol 209:469-482.

Hershko A, Ciechanover A (1998)
The ubiquitin system. Annu Rev Biochem 67:425-479.

Hick C, Hick A (2002)
Kurzlehrbuch Physiologie. Urban & Fischer.

Holm K, Isacson O (1999)
Factors intrinsic to the neuron can induce and maintain its ability to promote axonal outgrowth: a role for BCL2? Trends Neurosci 22:269-273.

Honda R, Yasuda H (2000)
Activity of MDM2, a ubiquitin ligase, toward p53 or itself is dependent on the RING finger domain of the ligase. Oncogene 19:1473-1476.

Hondermarck H, Sy J, Bradshaw RA, Arfin SM (1992)
Dipeptide inhibitors of ubiquitin-mediated protein turnover prevent growth factor-induced neurite outgrowth in rat pheochromocytoma PC12 cells. Biochem Biophys Res Commun 189:280-288.

Hu Y, Cui Q, Harvey AR (2007)
Interactive effects of C3, cyclic AMP and ciliary neurotrophic factor on adult retinal ganglion cell survival and axonal regeneration. Mol Cell Neurosci 34:88-98.

Huang JK, Phillips GR, Roth AD, Pedraza L, Shan W, Belkaid W, Mi S, Fex-Svenningsen A, Florens L, Yates JR, 3rd, Colman DR (2005)
Glial membranes at the node of Ranvier prevent neurite outgrowth. Science 310:1813-1817.

Hsueh YP, Kim E, Sheng M (1997)

Disulfide-linked head-to-head multimerization in the mechanism of ion channel clustering by PSD-95. Neuron 18:803-814.

Inatani M (2005)
Molecular mechanisms of optic axon guidance. Naturwissenschaften 92:549-561.

Ishizaki T, Uehata M, Tamechika I, Keel J, Nonomura K, Maekawa M, Narumiya S (2000)
Pharmacological properties of Y-27632, a specific inhibitor of rho-associated kinases. Mol Pharmacol 57:976-983.

Jessen KR, Brennan A, Morgan L, Mirsky R, Kent A, Hashimoto Y, Gavrilovic J (1994)
The Schwann cell precursor and its fate: a study of cell death and differentiation during gliogenesis in rat embryonic nerves. Neuron 12:509-527.

Jessen KR, Mirsky R (2005)
The origin and development of glial cells in peripheral nerves. Nat Rev Neurosci 6:671-682.

Joazeiro CA, Weissman AM (2000)
RING finger proteins: mediators of ubiquitin ligase activity. Cell 102:549-552.

Jordan M, Wurm F (2004)
Transfection of adherent and suspended cells by calcium phosphate. Methods 33:136-143.

Kamada T, Koda M, Dezawa M, Yoshinaga K, Hashimoto M, Koshizuka S, Nishio Y, Moriya H, Yamazaki M (2005)
Transplantation of bone marrow stromal cell-derived Schwann cells promotes axonal regeneration and functional recovery after complete transection of adult rat spinal cord. J Neuropathol Exp Neurol 64:37-45.

Kavakebi P, Hausott B, Tomasino A, Ingorokva S, Klimaschewski L (2005)
The N-end rule ubiquitin-conjugating enzyme, HR6B, is up-regulated by nerve growth factor and required for neurite outgrowth. Mol Cell Neurosci 29:559-568.

Kennedy MB (1993)
The postsynaptic density. Curr Opin Neurobiol 3:732-737.

Kentsis A, Gordon RE, Borden KL (2002)
Self-assembly properties of a model RING domain. Proc Natl Acad Sci U S A 99:667-672.

Klauck TM, Scott JD (1995)
The postsynaptic density: a subcellular anchor for signal transduction enzymes. Cell Signal 7:747-757.

Kohama I, Lankford KL, Preiningerova J, White FA, Vollmer TL, Kocsis JD (2001)
Transplantation of cryopreserved adult human Schwann cells enhances axonal conduction in demyelinated spinal cord. J Neurosci 21:944-950.

Kolb H, Fernandez E, Nelson R (2007)
The organization of the retina and visual system, National Library of Medicine (USA), NCBI

Kukuruzinska MA, Lennon K (1998)
Protein N-glycosylation: molecular genetics and functional significance. Crit Rev Oral Biol Med 9:415-448.

Landis DM, Weinstein LA, Reese TS (1987)
Substructure in the postsynaptic density of Purkinje cell dendritic spines revealed by rapid freezing and etching. Synapse 1:552-558.

Laney JD, Hochstrasser M (1999)
Substrate targeting in the ubiquitin system. Cell 97:427-430.

Leaver SG, Cui Q, Plant GW, Arulpragasam A, Hisheh S, Verhaagen J, Harvey AR (2006)
AAV-mediated expression of CNTF promotes long-term survival and regeneration of adult rat retinal ganglion cells. Gene Ther 13:1328-1341.

Lee J, Hauk TG, Nonnenmacher L, Böckers TM, Benowitz LI, Fischer D (2006)
Characterization of LINA a new axonal regeneration promoting factor. 36th The society for Neuroscience.

Lenzlinger PM, Shimizu S, Marklund N, Thompson HJ, Schwab ME, Saatman KE, Hoover RC, Bareyre FM, Motta M, Luginbuhl A, Pape R, Clouse AK, Morganti-Kossmann C, McIntosh TK (2005)
Delayed inhibition of Nogo-A does not alter injury-induced axonal sprouting but enhances recovery of cognitive function following experimental traumatic brain injury in rats. Neuroscience 134:1047-1056.

Leon S, Yin Y, Nguyen J, Irwin N, Benowitz LI (2000)
Lens injury stimulates axon regeneration in the mature rat optic nerve. J Neurosci 20:4615-4626.

Li H, Seth A (2004)
An RNF11: Smurf2 complex mediates ubiquitination of the AMSH protein. Oncogene 23:1801-1808.

Liebl DJ, Morris CJ, Henkemeyer M, Parada LF (2003)
mRNA expression of ephrins and Eph receptor tyrosine kinases in the neonatal and adult mouse central nervous system. J Neurosci Res 71:7-22.

Lingor P, Tonges L, Pieper N, Bermel C, Barski E, Planchamp V, Bahr M (2008)
ROCK inhibition and CNTF interact on intrinsic signalling pathways and differentially regulate survival and regeneration in retinal ganglion cells. Brain 131:250-263.

Liu BP, Fournier A, GrandPre T, Strittmatter SM (2002)
Myelin-associated glycoprotein as a functional ligand for the Nogo-66 receptor. Science 297:1190-1193.

Lodish et al. (2004)
Molecular cell biology. 5th edition. W.H. Freeman and company. P0-7167-4366-3

Logan A, Ahmed Z, Baird A, Gonzalez AM, Berry M (2006)
Neurotrophic factor synergy is required for neuronal survival and disinhibited axon regeneration after CNS injury. Brain 129:490-502.

Lottspeich F, Zorbas H (1998)
Bioanalytik, Spektrum akademischer Verlag 688-690.

Luo L (2000)
Rho GTPases in neuronal morphogenesis. Nat Rev Neurosci 1:173-180.

Lüllmann-Rauch R (2002)
Histologie, Thieme 488-508.

Lussier MP, Lepage PK, Bousquet SM, Boulay G (2008)
RNF24, a new TRPC interacting protein, causes the intracellular retention of TRPC. Cell Calcium 43:432-443.

Mader S (2007)
Biology, 9th ed. McGraw Hill, New York.

Maekawa M, Ishizaki T, Boku S, Watanabe N, Fujita A, Iwamatsu A, Obinata T, Ohashi K, Mizuno K, Narumiya S (1999)
Signaling from Rho to the actin cytoskeleton through protein kinases ROCK and LIM-kinase. Science 285:895-898.

Martin KR, Klein RL, Quigley HA (2002)
Gene delivery to the eye using adeno-associated viral vectors. Methods 28:267-275.

Martin KR, Quigley HA, Zack DJ, Levkovitch-Verbin H, Kielczewski J, Valenta D, Baumrind L, Pease ME, Klein RL, Hauswirth WW (2003)
Gene therapy with brain-derived neurotrophic factor as a protection: retinal ganglion cells in a rat glaucoma model. Invest Ophthalmol Vis Sci. 44:4357-4365.

McKerracher L, David S, Jackson DL, Kottis V, Dunn RJ, Braun PE (1994)
Identification of myelin-associated glycoprotein as a major myelin-derived inhibitor of neurite growth. Neuron 13:805-811.

Meroni G, Diez-Roux G (2005)
TRIM/RBCC, a novel class of 'single protein RING finger' E3 ubiquitin ligases. Bioessays 27:1147-1157.

Merry DE, Veis DJ, Hickey WF, Korsmeyer SJ (1994)
bcl-2 protein expression is widespread in the developing nervous system and retained in the adult PNS. Development 120:301-311.

Mi S, Lee X, Shao Z, Thill G, Ji B, Relton J, Levesque M, Allaire N, Perrin S, Sands B, Crowell T, Cate RL, McCoy JM, Pepinsky RB (2004)
LINGO-1 is a component of the Nogo-66 receptor/p75 signaling complex. Nat Neurosci 7:221-228.

Moreau-Fauvarque C, Kumanogoh A, Camand E, Jaillard C, Barbin G, Boquet I, Love C, Jones EY, Kikutani H, Lubetzki C, Dusart I, Chedotal A (2003)
The transmembrane semaphorin Sema4D/CD100, an inhibitor of axonal growth, is expressed on oligodendrocytes and upregulated after CNS lesion. J Neurosci 23:9229-9239.

Mukhopadhyay G, Doherty P, Walsh FS, Crocker PR, Filbin MT (1994)
A novel role for myelin-associated glycoprotein as an inhibitor of axonal regeneration. Neuron 13:757-767.

Muller A, Hauk TG, Fischer D (2007)
Astrocyte-derived CNTF switches mature RGCs to a regenerative state following inflammatory stimulation. Brain 130:3308-3320.

Murakami K, Kanno H, Yamamoto I, Saito T (2004)
Lavendustin A enhances axon elongation in VHL gene-transfected neural stem cells. Neuroreport 15:611-614.

Nakayama M, Miyake T, Gahara Y, Ohara O, Kitamura T (1995)
A novel RING-H2 motif protein downregulated by axotomy: its characteristic localization at the postsynaptic density of axosomatic synapse. J Neurosci 15:5238-5248.

Negishi M, Katoh H (2002)
Rho family GTPases as key regulators for neuronal network formation. J Biochem 132:157-166.

Niederost B, Oertle T, Fritsche J, McKinney RA, Bandtlow CE (2002)
Nogo-A and myelin-associated glycoprotein mediate neurite growth inhibition by antagonistic regulation of RhoA and Rac1. J Neurosci 22:10368-10376.

Nishiki T, Narumiya S, Morii N, Yamamoto M, Fujiwara M, Kamata Y, Sakaguchi G, Kozaki S (1990)
ADP-ribosylation of the rho/rac proteins induces growth inhibition, neurite outgrowth and acetylcholine esterase in cultured PC-12 cells. Biochem Biophys Res Commun 167:265-272.

Nusser N, Gosmanova E, Zheng Y, Tigyi G (2002)
Nerve growth factor signals through TrkA, phosphatidylinositol 3-kinase, and Rac1 to inactivate RhoA during the initiation of neuronal differentiation of PC12 cells. J Biol Chem 277:35840-35846.

Obin M, Mesco E, Gong X, Haas AL, Joseph J, Taylor A (1999)
Neurite outgrowth in PC12 cells. Distinguishing the roles of ubiquitylation and ubiquitin-dependent proteolysis. J Biol Chem 274:11789-11795.

Ogawa M, Mizugishi K, Ishiguro A, Koyabu Y, Imai Y, Takahashi R, Mikoshiba K, Aruga J (2008)
Rines/RNF180, a novel RING finger gene-encoded product, is a membrane-bound ubiquitin ligase. Genes Cells 13:397-409.

Okano H, Sakaguchi M, Ohki K, Suzuki N, Sawamoto K (2007a)
Regeneration of the central nervous system using endogenous repair mechanisms. J Neurochem 102:1459-1465.

Okano H, Kaneko S, Okada S, Iwanami A, Nakamura M, Toyama Y (2007b)
Regeneration-based therapies for spinal cord injuries. Neurochem Int 51:68-73.

Olsson PA, Korhonen L, Mercer EA, Lindholm D (1999)
MIR is a novel ERM-like protein that interacts with myosin regulatory light chain and inhibits neurite outgrowth. J Biol Chem 274:36288-36292.

Pan J, Goodheart M, Chuma S, Nakatsuji N, Page DC, Wang PJ (2005)
RNF17, a component of the mammalian germ cell nuage, is essential for spermiogenesis. Development 132:4029-4039.

Park JB, Yiu G, Kaneko S, Wang J, Chang J, He XL, Garcia KC, He Z (2005)
A TNF receptor family member, TROY, is a coreceptor with Nogo receptor in mediating the inhibitory activity of myelin inhibitors. Neuron 45:345-351.

Patestas MA, Gartner LP (2006)
A textbook of neuroanatomy. Blackwell publishing.

Peng H, Begg GE, Schultz DC, Friedman JR, Jensen DE, Speicher DW, Rauscher FJ, 3rd (2000)
Reconstitution of the KRAB-KAP-1 repressor complex: a model system for defining the molecular anatomy of RING-B box-coiled-coil domain-mediated protein-protein interactions. J Mol Biol 295:1139-1162.

Perry VH, Henderson Z, Linden R (1983)
Postnatal changes in retinal ganglion cell and optic axon populations in the pigmented rat. J Comp Neurol 219:356-368.

Qiu J, Cai D, Filbin MT (2000)
Glial inhibition of nerve regeneration in the mature mammalian CNS. Glia 29:166-174.

Reumann S (2004)
Specification of the peroxisome targeting signals type 1 and type 2 of plant peroxisomes by bioinformatics analyses. Plant Physiol 135:783-800.

Robinson JS, Graham TR, Emr SD (1991)
A putative zinc finger protein, Saccharomyces cerevisiae Vps18p, affects late Golgi functions required for vacuolar protein sorting and efficient alpha-factor prohormone maturation. Mol Cell Biol 11:5813-5824.

Roquemore EP, Banting G (1998)
Efficient trafficking of TGN38 from the endosome to the trans-Golgi network requires a free hydroxyl group at position 331 in the cytosolic domain. Mol Biol Cell 9:2125-2144.

Rudd PM, Elliott T, Cresswell P, Wilson IA, Dwek RA (2001)
Glycosylation and the immune system. Science 291:2370-2376.

Saluta M, Bell PA (1998)
Troubleshooting GST fusion protein expression in E.coli. Life Science News. Amersham Pharmacia Biotech.

Schachner M, Bartsch U (2000)
Multiple functions of the myelin-associated glycoprotein MAG (siglec-4a) in formation and maintenance of myelin. Glia 29:154-165.

Scheffner M, Nuber U, Huibregtse JM (1995)
Protein ubiquitination involving an E1-E2-E3 enzyme ubiquitin thioester cascade. Nature 373:81-83.

Schnell L, Fearn S, Klassen H, Schwab ME, Perry VH (1999)
Acute inflammatory responses to mechanical lesions in the CNS: differences between brain and spinal cord. Eur J Neurosci 11:3648-3658.

Schwab ME, Caroni P (1988)
Oligodendrocytes and CNS myelin are nonpermissive substrates for neurite growth and fibroblast spreading in vitro. J Neurosci 8:2381-2393.

Schwab ME, Kapfhammer JP, Bandtlow CE (1993)
Inhibitors of neurite growth. Annu Rev Neurosci 16:565-595.

Schwab ME (2004)
Nogo and axon regeneration. Curr Opin Neurobiol 14:118-124.

Schwabe JW, Klug A (1994)
Zinc mining for protein domains. Nat Struct Biol 1:345-349.

Schwarz SE, Rosa JL, Scheffner M (1998)
Characterization of human hect domain family members and their interaction with UbcH5 and UbcH7. J Biol Chem 273:12148-12154.

Silberstein S, Gilmore R (1996)
Biochemistry, molecular biology, and genetics of the oligosaccharyltransferase. Faseb J 10:849-858.

Silver J, Miller JH (2004)
Regeneration beyond the glial scar. Nat Rev Neurosci 5:146-156.

Smith DB, Johnson KS (1988)
Single-step purification of polypeptides expressed in Escherichia coli as fusions with glutathione S-transferase. Gene 67:31-40.

Stichel CC, Muller HW (1998)
The CNS lesion scar: new vistas on an old regeneration barrier. Cell Tissue Res 294:1-9.

Tansky MF, Pothoulakis C, Leeman SE (2007)
Functional consequences of alteration of N-linked glycosylation sites on the neurokinin 1 receptor. Proc Natl Acad Sci U S A 104:10691-10696.

Tarsa L, Balkowiec A (2008)
Nerve growth factor regulates synaptophysin expression in developing trigeminal ganglion neurons in vitro. Neuropeptides.

Thanos S, Naskar R, Heiduschka P (1997)
Regenerating ganglion cell axons in the adult rat establish retinofugal topography and restore visual function. Exp Brain Res 114:483-491.

Teng FY, Tang BL (2006)
Axonal regeneration in adult CNS neurons--signaling molecules and pathways. J Neurochem 96:1501-1508.

Trepel M (1999)
Neuroanatomie Struktur und Funktion. Urban & Fischer.

Tsai SY, Chiu PY, Yang CP, Lee YH (2002)
Synergistic effects of corticosterone and kainic acid on neurite outgrowth in axotomized dorsal root ganglion. Neuroscience 114:55-67.

Tursun B, Schluter A, Peters MA, Viehweger B, Ostendorff HP, Soosairajah J, Drung A, Bossenz M, Johnsen SA, Schweizer M, Bernard O, Bach I (2005)
The ubiquitin ligase Rnf6 regulates local LIM kinase 1 levels in axonal growth cones. Genes Dev 19:2307-2319.

Vassar R, Bennett BD, Babu-Khan S, Kahn S, Mendiaz EA, Denis P, Teplow DB, Ross S, Amarante P, Loeloff R, Luo Y, Fisher S, Fuller J, Edenson S, Lile J, Jarosinski MA, Biere AL, Curran E, Burgess T, Louis JC, Collins F, Treanor J, Rogers G, Citron M (1999)
Beta-secretase cleavage of Alzheimer's amyloid precursor protein by the transmembrane aspartic protease BACE. Science 286:735-741.

van Diepen MT, Spencer GE, van Minnen J, Gouwenberg Y, Bouwman J, Smit AB, van Kesteren RE (2005)
The molluscan RING-finger protein L-TRIM is essential for neuronal outgrowth. Mol Cell Neurosci 29:74-81.

von Heijne G (1983)
Patterns of amino acids near signal-sequence cleavage sites. Eur J Biochem 133:17-21.

Wang KC, Kim JA, Sivasankaran R, Segal R, He Z (2002a)
P75 interacts with the Nogo receptor as a co-receptor for Nogo, MAG and OMgp. Nature 420:74-78.

Wang KC, Koprivica V, Kim JA, Sivasankaran R, Guo Y, Neve RL, He Z (2002b)
Oligodendrocyte-myelin glycoprotein is a Nogo receptor ligand that inhibits neurite outgrowth. Nature 417:941-944.

Watson FL, Porcionatto MA, Bhattacharyya A, Stiles CD, Segal RA (1999)
TrkA glycosylation regulates receptor localization and activity. J Neurobiol 39:323-336.

Watson FL, Heerssen HM, Bhattacharyya A, Klesse L, Lin MZ, Segal RA (2001)
Neurotrophins use the Erk5 pathway to mediate a retrograde survival response. Nat Neurosci 4:981-988.

Welply JK, Shenbagamurthi P, Lennarz WJ, Naider F (1983)
Substrate recognition by oligosaccharyltransferase. Studies on glycosylation of modified Asn-X-Thr/Ser tripeptides. J Biol Chem 258:11856-11863.

Wolins NE, Donaldson RP (1997)
Binding of the peroxisomal targeting sequence SKL is specified by a low-affinity site in castor bean glyoxysomal membranes. A domain next to the SKL binds to a high-affinity site. Plant Physiol 113:943-949.

Wong ST, Henley JR, Kanning KC, Huang KH, Bothwell M, Poo MM (2002)
A p75(NTR) and Nogo receptor complex mediates repulsive signaling by myelin-associated glycoprotein. Nat Neurosci 5:1302-1308.

Wooff J, Pastushok L, Hanna M, Fu Y, Xiao W (2004)
The TRAF6 RING finger domain mediates physical interaction with Ubc13. FEBS Lett 566:229-233.

Yan A, Lennarz WJ (2005)
Unraveling the mechanism of protein N-glycosylation. J Biol Chem 280:3121-3124.

Yang E, Zha J, Jockel J, Boise LH, Thompson CB, Korsmeyer SJ (1995)
Bad, a heterodimeric partner for Bcl-XL and Bcl-2, displaces Bax and promotes cell death. Cell 80:285-291.

Yang LJ, Lorenzini I, Vajn K, Mountney A, Schramm LP, Schnaar RL (2006) Sialidase enhances spinal axon outgrowth in vivo. Proc Natl Acad Sci U S A 103:11057-11062.

Yang LJ, Schnaar RL (2008)
Axon regeneration inhibitors. Neurol Res 30:1047-1052

Yasukawa H, Hoshijima M, Gu Y, Nakamura T, Pradervand S, Hanada T, Hanakawa Y, Yoshimura A, Ross J, Jr., Chien KR (2001)
Suppressor of cytokine signaling-3 is a biomechanical stress-inducible gene that suppresses gp130-mediated cardiac myocyte hypertrophy and survival pathways. J Clin Invest 108:1459-1467.

Yin Y, Cui Q, Li Y, Irwin N, Fischer D, Harvey AR, Benowitz LI (2003)
Macrophage-derived factors stimulate optic nerve regeneration. J Neurosci 23:2284-2293.

Yin Y, Henzl MT, Lorber B, Nakazawa T, Thomas TT, Jiang F, Langer R, Benowitz LI (2006)
Oncomodulin is a macrophage-derived signal for axon regeneration in retinal ganglion cells. Nat Neurosci 9:843-852.

Yiu G, He Z (2003)
Signaling mechanisms of the myelin inhibitors of axon regeneration. Curr Opin Neurobiol 13:545-551.

Yiu G, He Z (2006)
Glial inhibition of CNS axon regeneration. Nat Rev Neurosci 7:617-627.

Zhang Y, Moheban DB, Conway BR, Bhattacharyya A, Segal RA (2000)
Cell surface Trk receptors mediate NGF-induced survival while internalized receptors regulate NGF-induced differentiation. J Neurosci 20:5671-5678.

Ziff EB (1997)
Enlightening the postsynaptic density. Neuron 19:1163-1174.

http://thalamus.wustl.edu/course/eyeret.html

http://instruct.uwo.ca/anatomy/530/retina.jpg

http://www.pubmed.de/data/nlm.link.html

http://expasy.org/prosite

http://zeus.cs.vu.nl/programs/pralinewww

7 Appendices

Nucleotide sequence of LINA

[redacted]

Amino acid sequence of LINA

[redacted]

RING finger

N-Glycosylation site

Transmembrane domain

Vector pAAV-IRES-hrGFP

left inverted terminal repeat 1–141
CMV promoter 150–812
β-globin intron 820–1312
multiple cloning site 1392–1420
3× FLAG tag 1421–1492
internal ribosome entry site 1528–2114
hrGFP ORF 2112–2828
hGH polyA 2886–3364
right inverted terminal repeat 3404–3544
f1 origin 3636–3942
ampicillin resistance (*bla*) ORF 4461–5318
pUC origin 5469–6136

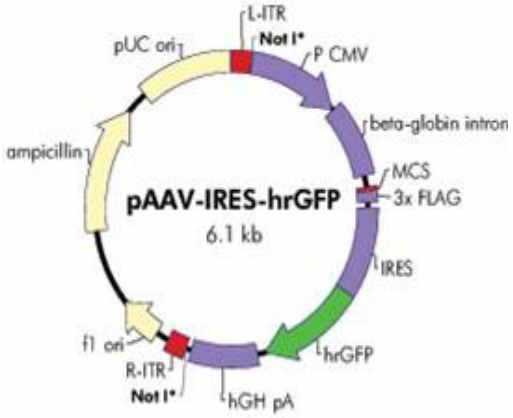

*Non-unique sites used to release the expression cassette

pAAV-IRES-hrGFP Multiple Cloning Site Region
(sequence shown 1392–1432)

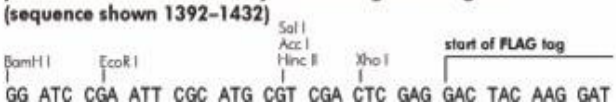

Vector pcDNA3.1/V5-His-TOPO

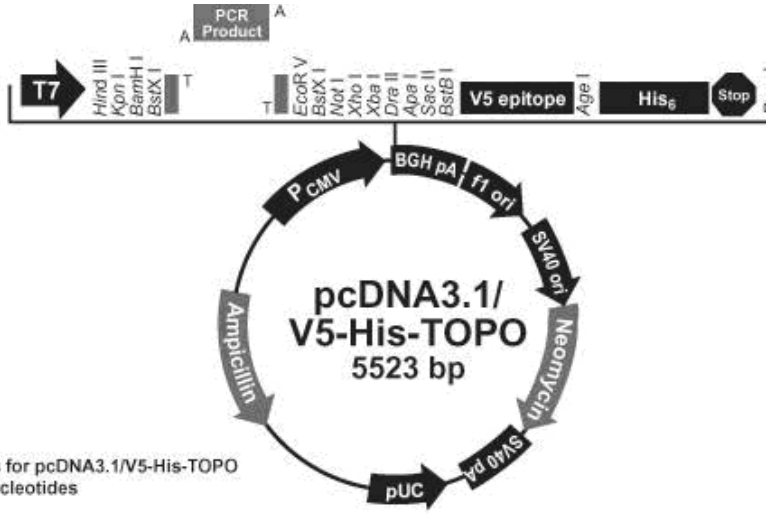

Comments for pcDNA3.1/V5-His-TOPO
5523 nucleotides

CMV promoter: bases 209-863
T7 promoter/priming site: bases 863-882
Multiple cloning site: bases 902-1019
TOPO® Cloning site: 953-954
V5 epitope: bases 1020-1061
Polyhistidine tag: bases 1071-1088
BGH reverse priming site: bases 1111-1128
BGH polyadenylation signal: bases 1110-1324
f1 origin of replication: bases 1387-1800
SV40 promoter and origin: bases 1865-2190
Neomycin resistance gene: bases 2226-3020
SV40 polyadenylation signal: bases 3039-3277
pUC origin: bases 3709-4382

Vector pcDNA3-RBP2N-mCherry

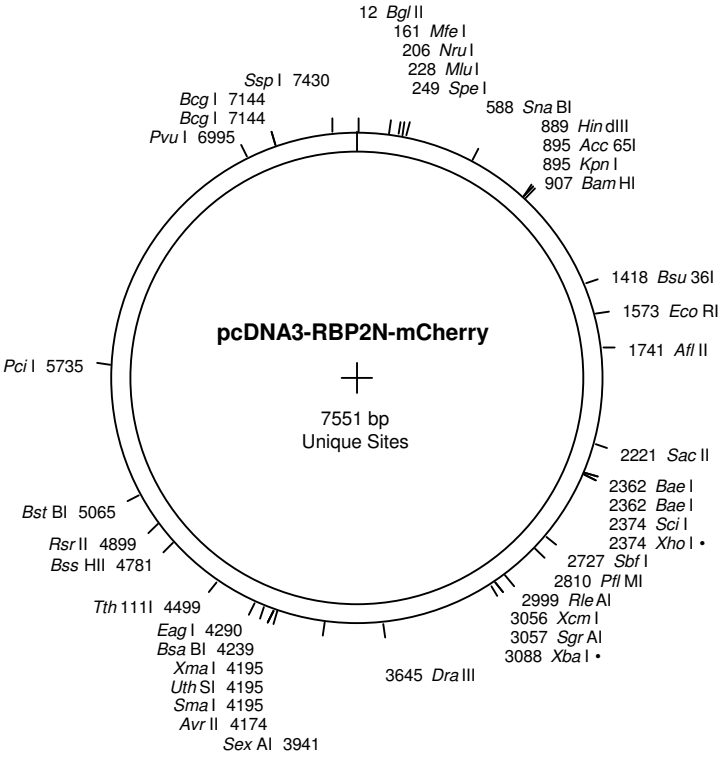

Vector pEGFP-N2

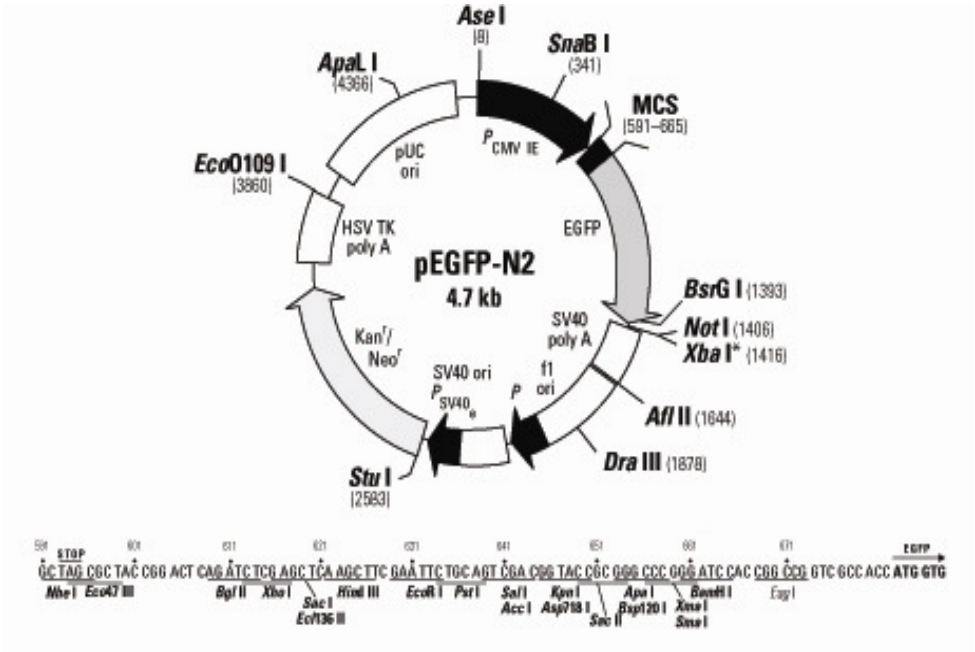

Vector pGEX-4T-1

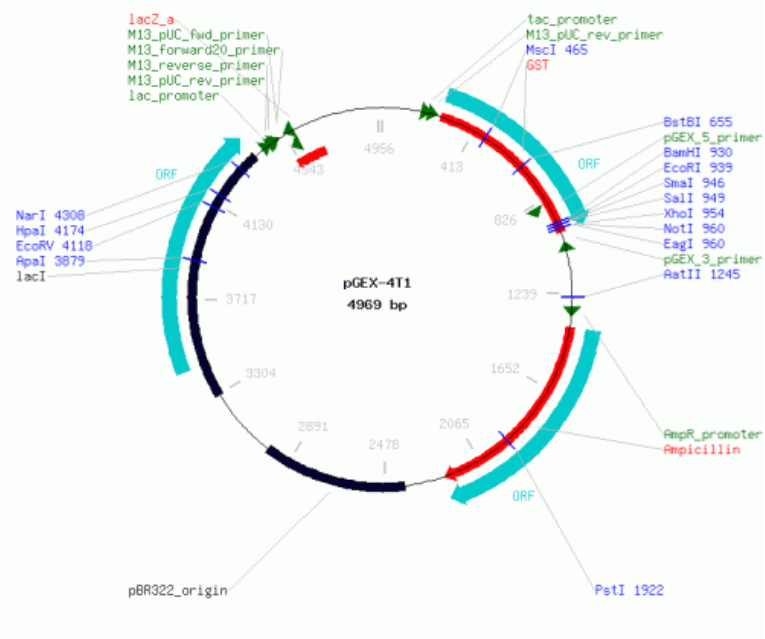

Vector pCS2+

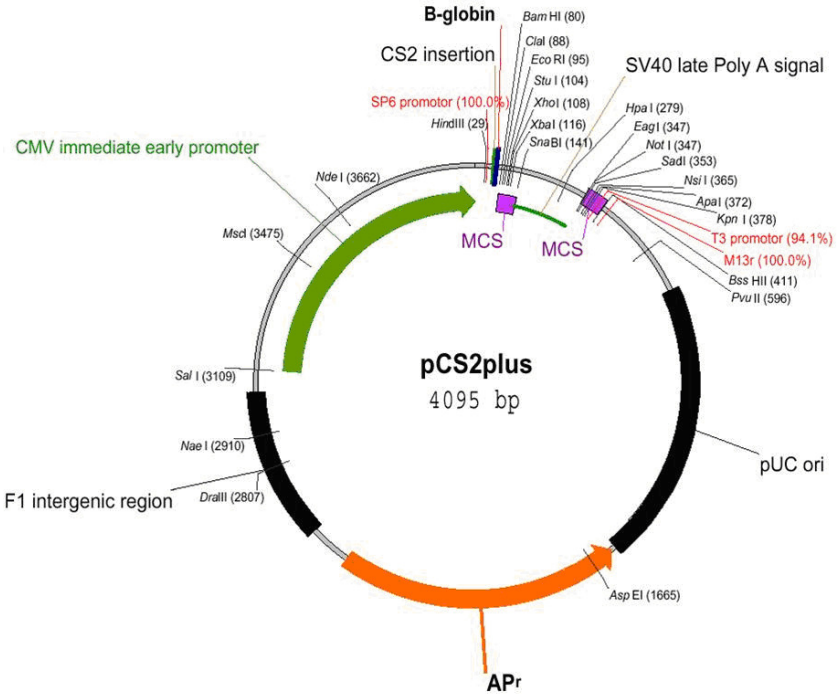

Acknowledgement

First of all, I am grateful to Prof. Dr. Dietmar Fischer for a great and interesting project for my Ph.D thesis and help and advices which he offered me all the time. I have obtained lots of experience in biochemistry and molecular biology and more important, great knowledges in the neurology field in his lab. This work would never have been possible without his help.

I would like to sincerely thank Prof. Dr. Harald Wolf from the Institute of Neurobiology for accepting me as his doctoral student and for his generous advices and supports when I had difficulties. At the same time, I would like to thank PD. Dr. Wolfgang Stein from the Institute of Neurobiology, as my second examiner, for his constructive corrections and many great advices. I am sincerely grateful to him for his great help.

I am thankful to PD. Dr. Franz Oswald, Institute of Internal Medicine 1, for graciously sharing his excellent insight and expertise to introduce me to the field of live imaging, and many experimental advices and discussions throughout this study. At the same time I wish to express my sincere gratitude to Dr. Ioan Ovidiu Sirbu from the Institute of Biochemistry and Molecular biology for his excellent support and advices for *in situ* hybridization and his helpful correction of my work. Then I would like to thank Dr. Ralf Marienfeld from the Institute of Physiological Chemistry for the initial idea and successful result of cross linking experiment. Specially I wish to thank Prof. Dr. Tobias Böckers and his Ph.D students Andreas Grabbrucker and Anna Dolnik from the Institute of Anatomy and Cell Biology for the amazing collaborations and supports with many experimental materials. I wish to thank Ph.D student Silvia Glaschik from the Institute of Biophysics for her great help with confocal microscopy. In addition, special thanks to Dr. Knippshild for his generous supply of an antibody TGN38 and Dr. C.von Arnim for kindly providing the BACE1-GFP plasmid. I would like to thank Ph.D student, Karin Dotzauer from the Institute of Neurobiology for her excellent correction of my work. Sincerely I would like to thank all Lab members, Thomas Hauk, Adrienne Mueller, Miriam Faender, Lisa Nonnenmacher and Natascha Andreadaki for help and support for my work. I am also grateful to my parents and brothers. They gave me always a new motivation to go further.

I have to give special thanks to my husband from my heart for supporting and encouraging me at every moment.

List of Publications

Hauk TG, Muller A, **Lee J**, Schwendener R, Fischer D (2008) Neuroprotective and axon growth promoting effects of intraocular inflammation do not depend on oncomodulin or the presence of large numbers of activated macrophages. Exp Neurol 209:469-482.

Abstracts/Symposium:

J. Lee[1], T.G. Hauk[1], L. Nonnenmacher, T.M. Böckers, LI. Benowitz, D. Fischer
Characterization of LINA a new axonal regeneration promoting factor.
36th The society for Neuroscience, 14.10. – 18.10.2006
[1] First author

D. Fischer, T.G. Hauk, **J. Lee**, R. Schwendener
Neuroprotective and growth promoting effects of a lens injury on retinal ganglion cells are not mediated by activated macrophages.
7th Göttingen Meeting of the German Neuroscience Society, 29.03. – 01.04.2007

J. Lee, T.G. Hauk, L. Nonnenmacher, T.M. Böckers, F. Oswald, D. Fischer
LINA, a RING-finger protein promoting axonal outgrowth and inhibiting cell proliferation
6th Forum of European Neuroscience, 12.07. –16.07.2008

A. Müller, **J. Lee**, T.G. Hauk, D. Fischer
CNTF stimulates axonal regeneration of mature RGCs and exhibits neuroprotective effects via different signaling pathways
6th Forum of European Neuroscience, 12.07. –16.07.2008

Erklärung

Hiermit erkläre ich, dass ich die vorliegende Arbeit selbständig verfasst und keine anderen als die angegebenen Quellen und Hilfsmittel benutzt habe. Die Arbeit wurde noch keiner Prüfungsbehörde vorgelegt und auch nicht veröffentlicht.

Ulm, den,....